UNIVERSIDADE DE LISBOA
FACULDADE DE CIÊNCIAS
DEPARTAMENTO DE BIOLOGIA ANIMAL

FUNCTIONAL MAPPING OF HUMAN BRAIN NETWORKS WITH HIGH TEMPORAL AND SPATIAL RESOLUTION METHODS

Alberto João Rodrigues Leal

DOUTORAMENTO EM BIOLOGIA
(Fisiologia e Bioquimica)

2008

UNIVERSIDADE DE LISBOA
FACULDADE DE CIÊNCIAS
DEPARTAMENTO DE BIOLOGIA ANIMAL

FUNCTIONAL MAPPING OF HUMAN BRAIN NETWORKS WITH HIGH TEMPORAL AND SPATIAL RESOLUTION METHODS

Alberto João Rodrigues Leal

Tese orientada pelos Prof. Doutores Paulo Fonseca, José Feijó e Jan de Munck

DOUTORAMENTO EM BIOLOGIA
(Fisiologia e Bioquimica)

2008

RESUMO

As limitações de ordem ética à investigação no homem impedem a aplicação dos métodos experimentais largamente usados em outros campos da fisiologia ao estudo da dinâmica cerebral humana. Os maiores avanços nesta área resultaram do estudo, por métodos não invasivos, das alterações associadas a lesões estruturais do cérebro em diversas patologias. Mais recentemente tornou-se possivel estudar as alterações neurofisiológicas e vasculares associadas a tarefas experimentais. Em qualquer dos casos a possibilidade de mapear no espaço e tempo as lesões ou as activações fisiológicas é de fundamental importância.

As técnicas de mapeamento funcional não invasivo actualmente disponiveis apresentam significativas limitações, sendo que o EEG e MEG são as que apresentam melhor resolução temporal (milisegundos), enquanto a RMf apresenta a melhor resolução espacial (milimetros).

Na presente tese caracterizamos o potencial do mapeamento funcional por EEG, bem como as vantagens e limitações do registo simultâneo EEG/RMf, num modelo patológico da actividade cerebral humana.

O mapeamento funcional nas epilepsias occipitais idiopáticas ilustra a necessidade da análise dinâmica detalhada da propagação da actividade paroxística, as vantagens de uma boa amostragem espacial do EEG, bem como o contributo adicional dos registos EEG/RMf.

Na epilepsia associada aos Hamartomas Hipotalâmicos ilustra-se a excelente complementaridade entre a RMf e o EEG para caracterizar a dinâmica espacio-temporal e cortico-subcortical da actividade neuronal.

Nas epilepsias submetidas a cirurgia da epilepsia validou-se metodologia de resolução do problema inverso em EEG num tipo particular de patologia cerebral (Esclerose Tuberosa), e estudou-se a concordância entre o EEG e a RMf da actividade epiléptica.

Conclui-se que a capacidade do EEG para detectar e seguir as rápidas modificações do estado funcional das redes neuronais lhe confere um papel da maior relevância entre as metodologias de mapeamento funcional. A RMf, efectuada concomitantemente, melhora a localização espacial da actividade neuronal e revela o importante contributo de áreas subcorticais.

PALAVRAS CHAVE

Mapeamento cerebral, Epilepsia, Humana, EEG, RMf

ABSTRACT

Ethical limitations to human research prevent the use of the experimental methods widely used in animal physiology to the study of brain function in man. The major advances in the area resulted from non-invasive studies of functional changes associated with structural brain lesions in various pathologies. Recent technological advances allowed detection of neurophysiological and vascular changes associated with experimental behavioral tasks. In either case, the ability to map in space and time the lesions and physiological activations is of fundamental importance.

The available non-invasive functional mapping techniques have nevertheless significant methodological limitations. Among these techniques the EEG and MEG have the best temporal resolution (milliseconds), while fMRI has the best spatial resolution (millimeters).

In the present thesis we study, in a pathological model of human brain function, the characteristics of functional brain mapping through EEG, as well as the advantages and limitations of the simultaneous EEG/fMRI recording.

The functional mapping in idiopathic occipital lobe epilepsies illustrates the necessity of a detailed dynamical analysis of propagation of paroxysmal activity, the advantages of a good EEG spatial sampling, as well as the additional contribution of EEG/fMRI recording.

In the epilepsies associated with hypothalamic hamartomas the synergy between fMRI and EEG to characterize the spatial-temporal and cortical-subcortical brain dynamics is demonstrated.

In epilepsy cases submitted to epilepsy surgery, a method to solve the inverse problem in EEG was validated in patients with Tuberous Sclerosis, and the degree of concordance between EEG and fMRI studied.

We conclude that the EEG ability to detect and follow the fast functional changes in state of brain networks gives it a role of the highest importance among functional brain mapping methods. The fMRI, recorded simultaneously, improves the spatial localization of the neuronal activity and highlights the contribution of subcortical areas.

KEYWORDS

Brain mapping, Epilepsy, Human, EEG, fMRI

RESUMO ALARGADO

As limitações de ordem ética à investigação no homem impedem a aplicação dos métodos experimentais largamente usados em outros campos da fisiologia ao estudo da dinâmica cerebral humana. Os maiores avanços nesta área resultaram do estudo, por métodos não invasivos, das alterações funcionais associadas a lesões estruturais do cérebro em diversas patologias. Mais recentemente tornou-se possivel estudar as alterações neurofisiológicas e vasculares associadas a tarefas experimentais. Em qualquer dos casos a possibilidade de representar no espaço e tempo as lesões ou as activações fisiológicas é de fundamental importância, sendo o foco de interesse do mapeamento funcional cerebral.

As técnicas de mapeamento funcional não invasivo actualmente disponiveis apresentam significativas limitações, sendo que o Electroencefalograma (EEG) e a Magnetoencefalografia (MEG) são as que apresentam melhor resolução temporal (milisegundos), enquanto a Ressonância Magnética funcional (RMf) apresenta a melhor resolução espacial (milimetros). Avanços técnicos na última década possibilitaram a realização de registos simultâneos das duas modalidades funcionais e geraram a expectativa de que estes possam contribuir para ultrapassar as limitações individuais de cada uma isoladamente. No entanto o modo mais adequado para efectuar a integração dos dois tipos de informação não foi ainda estabelecido, existindo a necessidade de um esforço de validação experimental dos resultados antes de os mesmos serem usados para uma efectiva exploração da fisiologia cerebral.

Na presente tese caracterizamos o potencial e as limitações da metodologia de mapeamento funcional por EEG, procurando dar mais robustez aos modelos obtidos. O potencial contributo da técnica de registo simultâneo EEG/RMf é também investigado.

Seleccionamos a epilepsia como um modelo experimental que, do ponto de vista do mapeamento funcional, tem requisitos de resolução espacio-temporal semelhantes ao da actividade das redes neuronais normais. Este modelo apresenta a vantagem metodológica de uma boa amplitude e especificidade da actividade EEG em relação aos ritmos fisiológicos.

O trabalho experimental consistiu no mapeamento funcional cerebral em três grupos de doentes com epilepsias focais, seleccionados de molde a documentar aspectos importantes da metodologia neurofisiológica de mapeamento funcional cerebral humano:

1. As epilepsias occipitais idiopáticas da infância constituem um conjunto de patologias com manifestações clinicas ictais diversificadas, que serviram de base à sua organização em três sindromes epilépticos bem distintos: o sindrome de Epilepsia Occipital Idiopática Precoce da Infância (Sindrome de Panayiotopoulos); o sindrome de Epilepsia Occipital Benigna Tardia da Infância (Sindrome de Gastaut); o sindrome de Epilepsia Occipital Reflexa da Infância (Sindrome de Guerrini). Todos estão associados a EEG com actividade paroxística de média a grande amplitude sobre as regiões posteriores do escalpe. Apesar de a heterogenidade das manifestações clinicas durante as crises sugerir o envolvimento de áreas distintas dos lobos occipitais, as limitações das técnicas de mapeamento funcional por EEG impediram a

determinação da localização destas áreas. Tendo em vista clarificar estas limitações metodológicas bem como estabelecer uma estratégia de mapeamento eficaz nestas situações, realizaram-se registos EEG e EEG/RMf em doentes com os diversos sindromes, procurando melhorar a resolução temporal e espacial.

O primeiro estudo efectuado combinando métodos dipolares em EEG e registos do efeito BOLD associado às pontas, revelou discrepâncias significativas na localização dos geradores, sendo que as áreas de activação BOLD foram consistentes em dois doentes com o sindrome de Gastaut e distintas do padrão de activação num doente com sindrome de Guerrini. O EEG não mostrou uma clara distinção entre os dois sindromes.

Em dois estudos subsequentes foram estudados em maior detalhe a dinâmica espacial e temporal da actividade paroxística associada ao sindrome de Panayiotopoulos. Demonstrou-se a existência de significativa propagação dos paroxísmos interictais a áreas distantes do cérebro, a partir da região occipito-temporal. Foi proposta ser esta propagação e a deficiente técnica usualmente utilizada nos registos clinicos o responsável pela convicção largamente disseminada de não existir um gerador consistente da actividade epiléptica neste sindrome, apesar de as manifestações clinicas relativamente monótonas assim o sugerirem.

Num estudo detalhado empregando EEG de alta resolução e EEG/RMf documentou-se de forma detalhada a dinâmica da actividade interictal em um doente com o sindrome de Panayiotopoulos, confirmando-se a provável origem da actividade paroxística na região occipito-temporal de um hemisfério.

2. A epilepsia associada aos Hamartomas Hipotalâmicos apresenta um gerador com localização bem conhecida numa área cerebral profunda. Os registos EEG da actividade subcortical apresentam significativas limitações, ilustradas não só na reduzida sensibilidade como na diminuta reproductibilidade da localização dos geradores fornecida pelos métodos de resolução do problema inverso. Em dois estudos analisamos em detalhe as caracteristicas dos registos ictais em doentes com epilepsia associada a hamartomas hipotalâmicos, usando EEGs analisados com métodos recentes de decomposição em componentes independentes e registos simultâneos EEG/RMf.

   A análise detalhada dos registos EEG apesar de ter permitido distinguir a existência de geradores corticais associados a geradores subcorticais, não conseguiu localizar de forma consistente a origem destes últimos.

   A técnica de registo simultâneo do EEG/RMf forneceu informação adicional importante para estabelecer a dinâmica espacio-temporal da actividade epiléptica, detalhando de forma muito precisa a origem e padrões de propagação da actividade ictal, sugerindo ser esta uma metodologia da maior importância para melhorar o mapeamento funcional de áreas cerebrais profundas.

3. As limitações das técnicas actuais de resolução do problema inverso em EEG estão criticamente dependentes da validade das restrições às caracteristicas dos geradores que é

necessário impôr para obter uma solução matematicamente única. O tipo de restrições mais adequado a cada problema concreto terá em geral que ser validado experimentalmente. Num estudo em doentes com o sindrome de epilepsia associada a Esclerose Tuberosa, em avaliação para Cirurgia da Epilepsia, foi validada metodologia de resolução do problema inverso da actividade ictal. Demonstrou-se boa concordância entre a localização sugerida pelo modelo e a área cerebral removida em 3 casos que ficaram livres de crises no pós-operatório.

Na ausência de validação prévia das restrições a aplicar aos geradores intracranianos, a utilização de métodos de filtragem espacial do tipo laplaciano, em registos EEG de alta resolução, poderá ser uma metodologia alternativa para obter informação adicional sobre os mesmos. A conjugação desta informação com a activação BOLD poderá ser uma fonte de informação adicional a incorporar no modelo final dos geradores. Num estudo em 12 doentes com epilepsias focais refractárias em avaliação para cirurgia da epilepsia, foram efectuados registos EEG de alta resolução e EEG/RMf. O co-registo dos dois tipos de informação mostrou vantagens em relação a cada método isoladamente, contribuindo a sua convergência para uma maior robustez das soluções obtidas.

Globalmente o trabalho efectuado confirmou o potencial do mapeamento funcional por EEG na análise dinâmica da actividade cerebral, sendo de particular relevância a excelente resolução temporal do método. A melhoria da amostragem espacial bem como a introdução de métodos mais sofisticados de processamento do sinal melhoram significativamente a informação fornecida. A técnica de registo simultâneo do EEG/RMf fornece informação sobre a resposta vascular associada à resposta neurofisiológica, que promete complementar de forma importante os mapas de EEG. Os métodos de análise desta modalidade estão no entanto ainda em desenvolvimento, existindo potencial para uma maior contribuição da técnica num futuro próximo.

Apesar de a técnica do EEG ter mais de 80 anos de idade, continua ainda a fornecer informação da maior relevância, que peomete ser melhorada com as melhorias na amostragem espacial, e a fácil integração com outras moddalidades de estudo funcional do cérebro, tais como a magnetoencefalografia, RMf, SPECT, PET, TMS, etc.

ACKNOWLEDGEMENTS

The work in this thesis has been made possible by the synergistic contribution of several people:

Dr. Orlando Leitão whose leadership trough example and continuous exigence during the Neurology training years greatly influenced the author, and several generations of neurologists, to become better professionals, both in the clinics and in the lab.

Dr. Luis Guerra has been responsible for the author clinical neurophysiology training and his ability to seen beyond the EEG recordings into the heart of the patients problems has been a source of inspiration and motivation.

Prof. Lopes da Silva has been a supporting and inspiring figure throughout the years, not only to the author but to several other clinicians with a desire to “do science”.

Prof. José Feijó is a long time friend whose continuous pressure throughout the years has been a powerfull motivational force for the author to go beyond clinical work and “get published”.

Dr Karin Dias is a reference figure in Portuguese Pediatric Neurology and her invitation to joint the Pediatric Neurology Department of Hospital Dona Estefânia has been a driving force to work in childhood clinical neurophysiology.

The colleagues of the Pediatric Neurology Department of Hospital Dona Estefânia with whom I have worked in the last 10 years, Dr. Eulália Calado (Head of Department), Dr. José Pedro Vieira, Dr. Ana Moreira, Dr. Ana I Dias and Dr. Rita Silva, have been a continuous source of puzzling clinical problems that provided a most stimulating working environment.

The Caselas Magnetic Ressonance staff, Dr. Constança Jordão, Prof. Mário Secca and Mrs Cristina Menezes, has been a small but very supportative group for the clinical and research studies.

My wife Alexandra and my sons Eduardo and Pedro have provided the background family support to the present work.

Abbreviations used in the text

AMPA	3-hydroxy-5-methyl-4-isoxalone proprionic acid
BOLD	blood oxygen level dependent
EEG	electroencephalography
EPI	echo-planar imaging
ERP	event-related potentials
fMRI	functional magnetic resonance imaging
GABA	gamma-aminobutyric acid
HR-EEG	high resolution electroencephalography
ICA	independent component analysis
MEG	magnetoencephalography
MRI	magnetic resonance imaging
NIRS	near infrared spectroscopy
NMDA	N-methyl-O-aspartic acid
OLE	occipital lobe epilepsy
PCA	principal component analysis
PET	positron emission tomography
SPECT	single photon emission computer tomography
TR	time of repetition

INDEX

1. INTRODUCTION 2
1.1. Functional mapping of human brain dynamics 2
1.2. General overview of the physiology of brain networks 3
1.3. Historical overview of functional brain mapping methods 7
1.4. Brain mapping with EEG 12
1.5. Brain mapping with functional magnetic resonance 16
1.6. Brain mapping with simultaneous EEG/fMRI 19
1.7. The human epilepsies as models of the behavior of brain networks 22

2. IDIOPATHIC OCCIPITAL LOBE EPILEPSY 24
2.1. Overview of idiopathic occipital lobe epilepsy 24
2.2. The BOLD effect of interictal spike activity in childhood occipital lobe epilepsy. 26
2.3. Analysis of the generators of epileptic activity in early-onset childhood begnin occipital lobe epilepsy 36
2.4. Origin of frontal lobe spikes in the early onset benign occipital lobe epilepsy (Panayiotopoulos syndrome) 48
2.5. Brain Mapping of epileptic activity in a case of Idiopathic Occipital Lobe Epilepsy (Panayiotopoulos syndrome) 58

3. EPILEPSY OF HYPOTHALAMIC HAMARTOMAS 66
3.1. Overview of the epilepsies associated with hypothalamic hamartomas 66
3.2. Analysis of the EEG dynamics of epileptic activity in gelastic seizures using decomposition in independent components 68
3.3. Functional brain mapping of ictal activity in Gelastic Epilepsy associated with Hypothalamic Hamartoma: a case report 78

4. FOCAL EPILEPSIES EVALUATED FOR SURGERY 88
4.1. Overview of focal symptomatic epilepsies 88
4.2. Analysis of the dynamics and origin of epileptic activity in patients with Tuberous Sclerosis evaluated for surgery of epilepsy 90
4.3. Comparison of high-resolution EEG and the spike-triggered BOLD activation in focal epilepsy 102

5. GENERAL DISCUSSION 116
5.1. Spatial resolution 116
5.2. The inverse problem in EEG 117
5.3. Reduced sensitivity to subcortical generators 119
5.4. Variable sensitivity to sources in sulcus or gyrus 120
5.5. Volume conductor mixing at scalp electrodes 120
5.6. Dependence on synchronization of a large cortical area 121
5.7. Fast spread between distant brain areas 122
5.8. Future perspectives 122

6. REFERENCES 124

1. INTRODUCTION

1.1. Functional mapping of human brain dynamics

The organization of human behavior is dependent on the capability of the central nervous system to receive and process sensory information from the environment and generate adaptative responses. The brain is capable of carrying out dynamical changes in a time scale ranging from a few milliseconds to several seconds and involving spatial synchronization of areas separated by a few microns to several centimeters (Freeman, 1978; Freeman and Baird, 1987; Gray and Singer, 1989; Gevins et al, 1994b). The analysis of such organization is difficult not only due to the complexity of the problem but also by the ethical restrictions to experiments in humans, which do not allow the use of the methodological paradigms widely used in the study of animal physiology and in other areas of biology in general.

Some of the major conceptual advances in our understanding of the functional organization of the human brain function resulted from the study of individual patients suffering from lesions, such as stroke or trauma, or in cases were invasive studies were justified by necessary medical procedures, as for example in surgery for epilepsy. Such was the case of patient HM in whom removal of both hippocampi to alleviate his epilepsy resulted in an enduring inability to form new memories from daily experience (Scoville and Milner, 1957), highlighting the fundamental role of the hippocampus in memory consolidation; or of patient Phileas Cage, which suffered a traumatic lesion of both prefrontal lobes, highlighting the importance of these structures in the organization of normal human behavior (Harlow, 1868). In such methology the careful characterization of particular functional brain deficits goes hand in hand with the careful detection of the brain lesions originating them. The technological advances of the last decades resulted not only in a significant increase in our capability to detect the brain lesions of individual patients but also in the ability to detect the physiological brain correlates of particular behavioral tasks, resulting in the ever expanding field of functional brain mapping.

Historicaly the neurophysiological techniques have played a major role in exploring the behavior of brain networks because they allow a direct measure of the neuronal activity underlying information transfer in the higher vertebrate brains. At the macroscopic scale, the EEG and MEG allowed the analysis with high temporal resolution of the activity of diverse networks interacting in complex patterns and establishing transitory functional connections between areas widely apart in a given hemisphere (Gray and Singer, 1989; Singer, 1993; Gevins et al, 1994). These techniques suffer from major problems from the point of view of functional mapping:

1. Reduced spatial resolution on the scalp surface.
2. Inability to localize intracranial generators from scalp surface recordings alone, due to the ill posed character of the inverse problem in EEG/MEG.
3. Reduced sensitivity for subcortical generators.

4. Significant volume conductor mixing of potentials from different brain areas on the scalp electrodes.
5. Variable sensitivity to cortical sources localized in the gyrus or sulcus.
6. Dependence on synchronization of a large, and difficult to characterize, cortical area to obtain signal on the scalp.
7. Fast spread of activity between distant brain areas can lead to erroneous localization results.

Nevertheless, in view of the non-invasive character of these methods and the limitations imposed to experiments in humans, the EEG/MEG techniques will continue to play a major role in the study of human brain physiology and behavior. It is therefore an important goal in neuroscience to improve the previous methodological problems, in order to make the EEG/MEG a more robust functional brain mapping procedure.

In recent years the combination of different brain mapping methods has been used as a productive strategy to overcome some of their individual intrinsic weaknesses (reviewed in Shibasaki, 2008). One such combination that is particularly promising is between EEG and fMRI, which associates the good temporal resolution of EEG to the good spatial resolution of fMRI in a completely non-invasive methodology. Despite significant work in the field, several problems in the integration of the two types of recordings still remain (Makeig et al, 2002; Nunez and Silberstien, 2000) and a robust experimental determination of the power of such integration in human subjects is yet to be achieved.

In this thesis we use functional brain mapping methods based on EEG and simultaneous EEG-fMRI recordings in a pathological model of human brain activity, to address some of the previously mentioned methodological problems of the macroscopic neurophysiological mapping of brain activity and also contribute to its experimental test.

1.2. General overview of the physiology of brain networks

1.2.1. The neuronal structure of the brain

The neuron constitutes the basic cellular element of the nervous system and the one responsible for its information processing capabilities. Neurons have the unique capability among the central nervous system cells of generating action potentials (Adrian, 1936) which propagate through the axon to excite or inhibit other neurons in a highly selective way. The effect on other neurons is obtained through synaptic junctions. The electrical presynaptic potential leads to the release of a chemical neurotransmitter that diffuses in the synaptic cleft and act on post-synaptic receptors. These induce membrane conductivity changes that result in changes in the post-synaptic membrane potential. In most neurons the afferent synapses are localized in the dendritic branches while efferent ones are localized in axonal branches (Cajal, 1911). A significant integration of information takes place in the dendritic tree of each neuron,

which results in electrotonic potentials that sum up (Rall, 1962) and can lead to the generation of an action potential when the membrane depolarization at the hilo of the axon reaches a given threshold (reviewed in Speckmann and Elger, 2005).

The action potentials are similar in different neurons, but the temporal organization of neuronal discharges can have distinct characteristics in diverse brain areas and physiological states. This is dependent on a large number of factors ranging from afferent synaptic distribution in the dendritic tree, synaptic neurotransmitter effects, electrotonic effects in the dendritic tree and membrane ionic channels.

In each brain area neurons are distributed in space in a structured way, and receive afferents from specific parts of the brain, projecting to a limited number of structures sometimes in distant parts of the same or the other hemisphere (Felleman and Van Essen, 1991). Some interneurons project only locally, often inducing inhibition or excitation of neuronal firing. The most numerous types of neurons project to distant regions and are associated mostly with postsynaptic excitation. Complex feedforward and feedback circuits are established which make the detailed mapping of the connections very difficult, but basic canonical circuits have been proposed for the vertebrate cortex (reviewed in Douglas and Martin, 2007).

A number of levels of complexity arise in this type of structure: the molecular level, mainly defining the membrane excitation properties; the synaptic and dendritic levels, with fundamental roles in inter-neuronal information transmission and integration; the neuronal level, mainly defining the spiking code and selective post-synaptic propagation; the local circuit level, defining the neighborhood interconnections of different neuronal elements; the network level defining the regional functional relationships between local circuits; and the macroscopic brain integrating the previous elements in a functional system capable of a complex and adaptative behavior to the particular ecological environment of the individual (reviewed in Shepherd, 2004). At each level one has to deal with complexity in different ways, using specific experimental tools and extracting information on brain physiology that sheds some light on its overall function (Scott, 1995). In the long run this will lead to a true systemic view of the central nervous system functioning. It is nevertheless very difficult to extrapolate the operation of the brain at a given level by studying only the lower levels, as new emergent properties result from the complex interactions established at each new step of the scale.

1.2.2. Functional organization of the cortex

The brain displays differences in histological organization of the grey matter that can be used to partition the cortex in different cytoarchitectonic areas (Cajal, 1911). The observations with the optical microscope revealed an organization in layers with different staining properties and where neurons with diverse morphology are localized in different levels. In these layers there is a complex spatial segregation of synaptic fields in the dendritic tree of the diverse neuronal elements, and a highly organized wiring takes place between different neuronal elements both in the plane and perpendicular to the cortex surface (reviewed in Douglas et al, 2004).

The main brain neuronal elements with long distance projections are the pyramidal cells (Sloper et al, 1979), which are organized in layers parallel to the cortex surface, with the dendritic tree near the surface and the axons projecting to deeper layers. The pyramidal neurons of the superficial layers project mainly to layer 4 of the target cortex, whereas deeper pyramidal neurons project to deep or superficial cortical areas (reviewed in Felleman and Van Essen, 1991). These types of projections have been correlated with feedforward and feedback circuits in the simple canonical representations of cortical circuits (Shepherd, 2004).

This spatial organization and the fact that these cells show an electrical polarity when the dendritic field is stimulated (reviewed in Speckmann and Elger, 2005), leads to an electric open field configuration (Lorent de No, 1947) which can be detected at the surface of the scalp and forms the physiological basis of the EEG.

The first theory of the functional organization of the cortex was only established in the 1950s in the seminal works of Mountcastle (1957) in the somatosensory cortex and Hubel and Wiesel (1962) in the visual cortex. Those investigators demonstrated that the cortex is structured in columns, with surface diameter of 0.5 mm, in which the neurons code in a similar way sensory stimulus characteristics. This spatial scale sets a natural target in spatial resolution for the functional brain mapping techniques attempting to reveal the functional organization of the cortex in higher mammals.

1.2.3. Long distance cortical-cortical and cortical-subcortical connections

The axons of pyramidal cells can reach extraordinary distances (meters for the motor pyramidal neurons) compared with the cell diameter, and a large number of these connecting fibers cross the brain white matter in different directions, establishing a complex web of functional interacting pathways between cortical columns. It is well established that the major synaptic input to any cortical area comes from other cortical areas, with the subcortical projections representing less than 1% (Braitenberg and Schultz, 1991). Because in general the projection pathways function in both directions, extensive feedback is present between the interacting cortical areas, adding to the complexity of the crosstalk.

A further element of complexity results from the important interactions between cortical and subcortical structures, which play a fundamental role in the regulation of cortical neuronal activity (reviewed in Steriade, 2005).

This web of interactions requires that in order to understand the workings of a given cortical area, one has to preserve the long distance connectivity that ultimately is bound to have a significant effect on the local physiology (reviewed in Douglas and Martin, 2007). It also highlights the fact that one has to be very careful on extrapolating to the living subject results derived from in vitro experiments, where the long-distance connectivity is reduced.

1.2.4. The temporal scale of synaptic events

Several different types of synaptic connections exist in the brain, corresponding to diverse ionic conductances, kinetics of activation and neurotransmitter specificity (reviewed in McCormick,

2004). The most common are the ones dependent on glutamate which is the main excitatory neurotransmitter released by pyramidal cells. GABA is also a widespread neurotransmitter, but associated with inhibition, released predominantly by interneurons.

The changes in postsynaptic membrane conductance that underlie the information transfer have diverse kinetics depending on the specific type of receptor that is activated. In the case of Glutamate two types of responses can be obtained: the AMPA type receptors induce rapid changes in conductance to Na^+, reaching a peak in less than 2 ms and decaying exponentially with a time constant around 7.2 ms (McCormick, 2004); the NMDA type is about 10 times slower, in fact inducing its effect when the previous AMPA conductance mediated by the same neurotransmitter has almost subsided. Inhibitory synapses, mainly mediated through GABA, also demonstrate fast ($GABA_A$ receptor mediated) and slow ($GABA_B$ receptor mediated) postsynaptic potentials.

Thus techniques for the evaluation of the physiology of brain networks should have a temporal resolution in the millisecond range in order to capture both the slow and fast synaptic effects that play a major role in information processing.

1.2.5. Organization in neuronal networks

In general our present knowledge of brain physiology does not allow the use of anatomical mapping of the cortical structures to predict their functional role (reviewed in Douglas and Martin, 2007). We also do not have good methods to determine the origin of synaptic connections in a given neuron, which makes it an overwhelming task to determine the detailed circuitry of neocortical areas.

The extensive connectivity of neurons in the brain leads to widespread crosstalk among adjacent and distant groups of neurons each time a cortical region is activated. Quantitative estimates of the synaptic connectivity between layers in the visual cortex of the cat (Binzegger et al, 2004) revealed that a given neuron receives most of its inputs from neurons in the same cortical area, while synaptic afferents from the thalamus and other unknown sources represent less than 10% each.

A given neuron can be part of more than one network and in general the study of the activity of single cells offers a limited knowledge on the physiology of the ensemble (Gurney, 1997). These networks have emergent properties that require experimental tools and analysis procedures quite different from the ones used in the study of single neurons (Lopes da Silva, 2005a).

The macroscopic methods used for the experimental study of these functional networks should have the spatial resolution to discriminate the brain basic functional unity, the cortical column (0.5 mm surface diameter), as well as enough temporal resolution (in the millisecond range) to detect the synaptic events thought to underlie the mutual interactions.

1.2.6. Functional brain mapping in the study of brain dynamics

Ultimately the understanding of the emergent properties of the brain networks involved in information processing related to behavioral organization will require its study in the intact brain. Only in this way can the long distance neuronal interactions be preserved, not only among cortical areas but also among cortical-subcortical structures. If the focus of interest is the human brain, then non-invasive methods become the only ones readily available for such a task.

Because the brain seems to be organized in networks with distinct spatial distribution in the cortex, sometimes in distant areas, the methods used for mapping should have both a good spatial resolution and coverage of a large area of the cortex (preferably the entire brain).

A further requirement for the detailed study of the dynamics of brain networks is that the evaluation should be done with the brain in a physiological state as close to the one of daily life as possible. This increases the chances of pining down the physiological mechanisms associated with the brain activity in naturalistic non-experimental conditions.

1.3. Historical overview of functional brain mapping methods

1.3.1. EEG

The EEG has been recorded from the scalp for the first time by Berger in 1929, and it is the oldest of the functional brain tests. The existence of several rhythmic activities which overlap and change throughout time became evident from the early recordings. These rhythms have a consistent relationship with the behavioral state of the patient in wakefulness, and they allowed an unprecedented insight into the sleep stage where several clearly differentiated functional states were demonstrated.

During the first decades of development of the technique the hardware devices were limited in number of channels, with the consequent bad spatial sampling. Instead, an emphasis was put on the monitoring capabilities and on the extremely good temporal resolution of the method, which allowed detection of fast transients and distinction of the detailed temporal dynamics of different brain areas, both in normal and pathological states.

The introduction of computers in the EEG field operated in the 70-80s, led to an increased interest in functional brain mapping, and resulted in the creation of EEG topography methods. These techniques produced digital color representations of the scalp potential at a given instant, with the capability to produce movies of the EEG dynamics over the head. Despite its exciting promises, the EEG topography met little success because the spatial representation produced was based on a very limited spatial sampling of the scalp EEG (typically from 19 electrodes), which reduced drastically the obtainable resolution and introduced several artifacts due to undersampling.

A more detailed representation of the spatial properties of the EEG had to wait the development of more advanced multichannel devices and better methods of processing the signal to correct for a few blurring effects induced by the skull in the brain potentials (detailed in section 1.4.2).

Several studies led to the acceptance of the concept that most of the EEG signal recorded in the scalp is due to the activity generated in the convexity of the cortical gyri, and that the sensitivity to deeper sources decreases significantly. A further requirement for detection on the scalp was that the potentials had an extended area of synchronization on the cortex, which has been proposed by Cooper (1965) to be in the order of 6 cm^2.

More detailed neurophysiological recordings of local field potentials and macroscopic EEG brought evidence that the latter signal correlates best with the slow synaptic potential activity instead of the fast action potentials due to neuronal firing (reviewed in Steriade, 2005). This data and the one obtained from cortical current density estimates using depth electrodes (Lopes da Silva and Storm van Leeuwen, 1978) led to the current concept that most of the scalp EEG originates in synaptic potentials in the pyramidal cortical cells.

A parallel field of development has been the source analysis, which attempts to recover the intracranial generators leading to the scalp potentials (reviewed in Baillet et al, 2001 and Plummer et al, 2008). Although this line of work has reached a high level of mathematical development, with multiple proposed models, it did not have a major impact on EEG brain mapping because major uncertainties affect all models. The inverse problem in EEG is an ill posed one (Helmholtz, 1853) and therefore unique solution are possible only on purely mathematical grounds. The required incorporation of constrains on the characteristics of the generators to reach a unique solution, introduces a degree of ambiguity in all models (detailed in section 1.3.d).

The recent introduction of EEG amplifiers with a large number of channels (up to 256), promises to increase even further the EEG spatial sampling. This, together with better knowledge of the conductivity of the head compartments (Gonçalves et al, 2003) and more detailed anatomical MRI, will increase the mapping capabilities of the EEG.

1.3.2. SPECT and PET

The first observations that neuronal activity is associated with a transitory increase in local blood supply goes back to the XIXth century (Roy and Sherrington, 1890; Horsley, 1892). Later reports confirmed the existence of a consistent vascular response associated with epileptic neuronal discharges (Penfield et al, 1939; Hougaard et al, 1976; Dymond and Crandall, 1976).

The ability to measure non-invasively functional changes in blood flow began with the availability of techniques based on the tomographic reconstruction of radionuclide tracers distribution in the brain: SPECT first (Kuhl et al, 1973) and a few years later PET (Phelps et al, 1975).

SPECT is based on the detection and localization of Gamma radiation emitted by a radiopharmaceutical that has been administered to the experimental subject. The products more commonly used are ^{133}Xe and the derivatives of ^{123}I or ^{99}Tc. ^{133}Xe was the first agent and it is the only one allowing quantitative evaluation of blood flow. Several problems are associated with its use: fast kinetics, requiring fast Gamma cameras, low spatial resolution (12 to 16 mm) and lack of specificity to the brain compartment. These problems led to the use of ^{123}I and ^{99}Tc

derivatives, which are radiopharmaceuticals with a rapid first-pass brain extraction (peak extraction reached 30-60 seconds after intravenous injection). The latter agents do not allow absolute quantification, and their use can only provide a snapshot of the brain regional blood flow. Although significant advances in SPECT spatial resolution (7 to 10 mm) and data processing have taken place for static tracers (reviewed in Devous, 2002), only qualitative and "single shot" measures can be obtained at the present time. For ^{133}Xe the temporal resolution of the method is better (studies can be repeated each 15 minutes) and quantitative evaluations are possible, but the spatial resolution is worse (in the centimeter range).

PET uses radiotracers with positron emission which are detected by the decay in two Gamma photons which travel in opposite directions. Because determination of the tracer localization uses information derived from the coincident detection of opposite photons and does not require collimators, an increased sensitivity as compared with SPECT is obtained. Reconstruction of the place of origin of the photons with good spatial discrimination results in an overall spatial resolution in the millimeter range for modern devices (reviewed in Cherry and Phelps, 2002). The first PET studies in brain mapping used ^{18}F-FDG to evaluate the cerebral metabolic rate in volunteers submitted to specific sensory stimuli (Greenberg et al, 1981; Phelps et al, 1981; Mazziotta et al, 1982). Robust activation of the primary sensory areas was achieved and the power of the method for functional brain mapping was demonstrated.

Better temporal resolution can be obtained by recording blood flow changes associated with neuronal activation, using isotopes with a short half-life (reviewed in Cherry and Phelps, 2002). The ^{15}O isotope has a half-life of 2 minutes and a fast diffusion when incorporated into the water molecule, resulting in the capability to evaluate extraction from plasma into tissue on its first pass by the brain, allowing a quantitative evaluation of regional cerebral blood flow. Studies can be repeated with 10 minute intervals. Because the signal to noise ratio is low, several scans are obtained per subject, followed by smoothing and averaging (both within and between subjects) in order to improve this ratio. Those procedures decrease the optimal spatial resolution, and require group analysis to obtain good statistics for the effects of interest.

Overall PET improves blood flow evaluation both in the spatial (millimeters range) and temporal domains (repeated evaluations at 10 minutes intervals), over SPECT. Because there are safety issues limiting the radiation exposure of experimental subjects, the number of scans that is possible to obtain is reduced, making inferences in individual subjects a difficult exercise.

1.3.3. MEG

The first magnetic field recording of brain activity was done by Cohen (1968), using an induction coil magnetometer. A major improvement in sensitivity occurred with the introduction of sensors based on the superconducting quantum interference device (SQUID) magnetometers (Cohen, 1972), which allowed continuous recording of neuronal magnetic activity.

MEG has several theoretical advantages over EEG for brain mapping applications (Hämäläinen, 1993):

- The record is reference-free, avoiding the effects of active reference electrodes that are important in EEG.
- The magnetic fields are not affected by the skull layer which is the major responsible for blurring of scalp EEG.
- The transparency of the head compartments to magnetic fields is expected to increase spatial resolution of cortical sources.
- The source analysis with MEG is more robust than for EEG, because less complicated volume conductor models are required.

Those theoretical advantages over EEG together with the rapid evolution of the hardware have made MEG an important functional brain imaging tool (reviewed in Hari, 2005).
It is widely accepted that there is a significant redundancy in EEG and MEG recordings, yet each technique is able to demonstrate unique activity not present in the other method (Fernandes et al, 2005), which explains the widely established fact that the simultaneous acquisition of both modalities results in an improved sensitivity to cortical generators (Stock, 1987).
But despite the fact that the inverse problem in MEG requires a simplified volume conductor model and a larger number of channels are available as compared to EEG, the fundamental requirement for constrains on the source properties remains.

1.3.4. fMRI

The nuclear magnetic resonance in bulk matter was discovered in the 1940s (Bloch et al, 1946, Purcell et al, 1946). The first imaging applications were done in the 1970s (Lauterbur, 1973) and in 1977 the first human MRI scanner was created by the FONAR Corporation. The first commercial human-body scanners started shipping to hospitals in the early 1980s.
The resonance effect is obtained by applying an electromagnetic pulse at the Larmour frequency of precession of the bulk magnetization spin of the brain. In the commonly used magnetic fields the Larmour frequency is in the radio part of the electromagnetic spectrum. After the brief stimulation, the bulk magnetization spin relaxes back exponentially to the resting state, emitting back electromagnetic radiation that is collected using the same coil used for stimulation. Because the relaxing kinetics of the spins is sensitive to the particular environment surrounding the hydrogen proton, a contrast is established between different compartments of the tissue. By applying a combination of variable magnetic gradients and changing the frequency, timing of the applied pulses (time of repetition, TR) and received echo, selective scanning of the brain volume is possible.
A wide variety of combinations of stimulating pulse sequences and contrast mechanisms have been developed, allowing exploration of several properties of the human body and an enhanced imaging of the brain tissues.
One type of image acquisition protocol that has particular importance to physiological studies is the Echo Planar Imaging (EPI) discovered by Mansfield in 1976. In this type of sequence a very

fast scanning is done, with a complete slice acquired for each stimulation pulse. This allows acquisition of a whole brain volume for each TR (2 to 3 seconds), which sets the temporal sampling rate much higher than it is possible for the other scanning imaging methods (PET and SPECT).

The functional study of the brain requires a contrast that can act as a marker of the functional state of brain networks. Because the changes in local blood flow were a well recognized target for monitoring functional changes (Roy and Sherrington, 1890), techniques were developed to detect changes in blood flow with brain activation. The use of paramagnetic contrast agents such as Gadolinium is a way to evaluate the changes in blood volume induced by local neuronal activation (Belliveau et al, 1991), but the need for repeated intravenous administrations severely reduces the usefulness of the method. A much more useful contrast is the hemoglobin molecule which in its desoxy state has been demonstrated to be paramagnetic (Pauling and Coryell, 1936), and produce detectable T2* contrast (Thulborn et al, 1982). These observations led to the discovery of the Blood Oxygenation Level Dependent (BOLD) effect (Ogawa et al, 1990) using hemoglobin as an endogenous contrast agent (detailed later). The later development resulted in the explosion of studies using brain fMRI.

1.3.5. NIRS

Jobsis (1977) was the first researcher to demonstrate that infrared light can penetrate the skull and be used to noninvasively monitor the oxygenation state of brain tissue. The application to monitoring of human brain activity was done years later (Chance et al, 1988; Hoshi and Tamura, 1993; Vilringer et al, 1993).

The opportunity to study the brain function derives from the fact that the main chromophores in the infrared window of 600-900 nm are the oxyhemoglobin and deoxyhemoglobin and also the cytochrome-c-oxidase, while the skull and scalp are transparent. Because these chromophores have distinct absorvance spectra, it is possible to measure concentration changes by optical measurements of the reflected infrared light from the brain at diverse wavelengths. The light sources are infrared lasers applied in the scalp at a distance of a few centimeters from the detector. From these measurements a continuous quantitative determination of the concentrations of oxyhemoglobin and deoxyhemoglobin, as well as the total hemoglobin is obtained (Jasdzewski et al, 2003).

Several advantages are attributed to NIRS as compared with other methods of brain mapping:

1. Direct information about oxygenation is available to NIRS and to no other method.
2. Absolute quantification of the concentration changes is possible with NIRS but not with fMRI.
3. The temporal resolution in the milliseconds range is better than the one of fMRI and PET (Jasdzewski et al, 2003).
4. The NIRS equipment is less restraining than the one of fMRI or PET, allowing more freedom for experimental setups.

The method has been used extensively to study the neurovascular coupling, a central issue in modern brain mapping (reviewed in Villringer and Obrig 2002).
The main limitation of the methodology is the poor spatial resolution which is in the order of centimeters. A further handicap is the inability to detect changes occurring bellow the more superficial layers of cortex.

1.4. Brain mapping with EEG

1.4.1. Temporal and spatial resolution

Temporal resolution:

At the present time the EEG and MEG are the only non-invasive brain mapping methods with enough temporal resolution to discriminate the fast sequence of stages involved in brain information processing.
From the early days of the human EEG recording (Berger, 1929) it became apparent that the electrical brain activity could be recovered in the scalp with high temporal resolution, limited only by the response time of the analogue pen recorders first, and later by the sampling rate of the digital devices. The temporal changes in the diverse brain waves can be reproduced well in each scalp electrode, even for the fastest components. Such millisecond resolution places the EEG in the temporal scale of synaptic events which are thought to underlie the generation of the macroscopic potentials recorded in the scalp (reviewed in Speckmann and Elger, 2005). The macroscopic scalp potentials of the EEG originate in the synchronous activation of a large number of microscopic synaptic potentials with a spatial arrangement leading to the generation of an open electric field (Lorent de No, 1947). Such potentials tend to have a rhythmic character and a particular topography, which allows the distinction of different functional networks (reviewed in Steriade, 2005).
In order to isolate the scalp potentials of relevance for a given experiment, a method has to be designed to decrease the interference of the background activity, while preserving the signal of interest. The most commonly used methodology consists in averaging multiple responses aligned by the time of occurrence of an event of interest. The averaging selectively preserves the potentials time-locked with the event of interest, while reducing the amplitude of non time-locked activity. A series of event-related potentials (ERPs) are obtained, with peaks distributed in time which have been correlated with different processing stages of information on the brain (Lopes da Silva, 2005b). The capability to distinguish the temporal sequence of such stages is of fundamental importance to gain insight into the dynamics of information processing associated with the events of interest.
The analysis of the phase relations between electrodes in the scalp is a complementary methodology (Sayers et al, 1974) which allows the detection of transitory functional connections between widely separated brain areas and an insight into the complex dynamics of brain networks (Freeman, 1978; Gray and Singer, 1989). The extensive crosstalk between groups of neurons both in the close neighborhood and across cortical distances of millimeters or

centimeters (Gevins el al, 1994) is widely thought to be an important part of the normal physiology of brain networks (reviewed in Singer, 1993).

Spatial resolution

The analysis of the EEG in the first years was based on the study of the temporal dynamics of the signal, due mainly to the very bad spatial sampling allowed by the reduced number of electrodes of the early electroencephalographs. Despite this, it became apparent that in general the scalp potential looked very similar in electrodes in the close neighborhood (Gevins et al, 1991). This observation led to the establishment of a method of spatial sampling using a standard map of 19 channels in the scalp, the 10-20 system (Jaspers et al, 1958). This system has been very influential not only in clinical but also in research EEG studies. For a long time the limited spatial resolution of the scalp EEG was assumed as a fact of life and little effort was made to improve on the spatial sampling of the 10-20 system, which had an average inter-electrode distance of 6 cm.

This lack of spatial resolution of the raw scalp potentials has been attributed to the blurring effect of the poorly conducting skull on the intracranial potentials (Nunez et al, 1994). An additional factor is the significant volume conductor mixing of electric potentials at the scalp electrodes, due to close by and far away sources. Significant problems for EEG functional mapping arise from the fact that each electrode samples not only its surroundings but also distant and poorly known brain areas (reviewed in Nunez and Srinivasan, 2005).

The development of devices with 32 to 64 electrodes and later with 128 in the 80s and 90s, reduced the inter-electrode distance of scalp electrodes to the 2-3 cm range. This led to the development of an improved spatial sampling of the scalp EEG and opened the way to new methods of data analysis hoping to improve the spatial resolution of the technique.

1.4.2. High-resolution EEG methods

The first high-resolution method was the Laplacian (Hjorth, 1975), which had several refinements (Perrin et al, 1987; Perrin et al, 1989; Nunez and Pilgreen, 1991; Law et al, 1993; Le et al, 1994) leading to the modern spline-Laplacian algorithms (Babiloni et al, 1996). The Laplacian method of computation provides an estimate of the current sources and sinks perpendicular to the skull, and it allows calculation of the dura electric potential (Srinivasan, 1999) and of the scalp current density (Yao, 2002), without requiring any information on the conductivity of the different head compartments. The high-resolution maps have been validated extensively in simulation experiments (Nunez et al, 1994), in the mapping of motor and sensory areas and in comparison studies with invasive subdural recordings obtained through array electrodes in epileptic patients (Gevins et al, 1994).

Almost at the same time, the incorporation of MRI anatomical data led to the development of the cortical imaging methods (Sidman, 1991; Gevins et al, 1991; Le et al, 1993; Gevins et al, 1994), which use the model of the volume conductor to project the scalp potentials in the dura surface and therefore correct for the skull effect. Because detailed information on the individual head

anatomy is incorporated in the deblurring process (Gevins et al, 1994), a higher spatial resolution can potentially be obtained than with the Laplacian method (Gevins et al, 1999). The correction for the variable skull thickness is a major advantage of the method (Cuffin, 1993), which can still improve its performance if better data on the conductivity of the head compartments becomes available (Gonçalves et al, 2003). Experimental test of these methods has been obtained by comparing the dura potential maps estimated from scalp HR-EEG and the ones obtained by intracranial subdural grid electrodes used in candidates for surgery of epilepsy (Gevins et al, 1994).

The maps obtained with the previous HR-EEG methods have major advantages over raw potential maps (reviewed in Nunez and Srinivasan [2005] and Gevins [2002]):

- Both methods are reference-free, overcoming the problems associated with reference potentials in the conventional scalp maps.
- They have a high selectivity for potentials in the neighborhood of the electrodes, therefore filtering out volume conductor potentials from distant sources.
- The selective spatial filter for potentials near the electrodes opens interesting possibilities for studying the functional connectivity between cortical areas without the interference of volume conduction correlations.

1.4.3. Blind source separation in EEG

The mapping of the activity of a given brain network in the scalp EEG suffers from a significant interference due to the superposition of potentials from other sources in the recording electrodes. Potentials from several sources are thought to add linearly in the scalp (Nunez and Srinivasan, 2005), and originate at each scalp electrode a complex mix of electric potentials originated in nearby and distant brain areas. This fact leads to a decreased signal to noise (S/N) ratio in the scalp EEG which makes the study in isolation of the activity of particular brain networks a dificult exercise. It is therefore an important goal in neurophysiology to isolate the EEG activity of interest from simultaneously occurring background rhythms, and in such a way improve the analysis of the spatial and temporal brain dynamics.

The classical method of averaging multiple responses time locked to an event of interest, is able to improve the S/N ratio and it has been the workhorse of non-invasive EEG studies since the introduction of computers in neurophysiology in the 50s (Dawson, 1954; Barlow, 1957; Brazier, 1960). Such methods suffer from several major drawbacks:

1. The assumed independence between the evoked activity and the background rhythms may not hold true in all circunstances (Vijn et al, 1991).
2. The method assumes that the brain network response to several stimuli is the same throughout the duration of the experiment. This assumption may not hold true for some settings due to the adaptability of the human nervous system to repeated stimuli.

3. Network activity which does not keep a constant phase with the trigger point is reduced in amplitude despite the fact that several studies have demonstrated that such activity is an integral part of the response to stimuli (reviewed in Pfurscheller and Lopes da Silva, 2005).

The realization that a given stimulus can originate a change in the EEG that is not necessarily phase-locked with it, motivated the development of methods to recover such "induced" activity (reviewed in Pfurtscheller and Lopes da Silva, 2005; Makeig, 1993).

Moreover, the demonstration that certain stimuli can produce changes in the phase of background rhythms without changes in amplitude (Sayers et al, 1974), led to the current understanding that the phase resetting of ongoing EEG rhythms is a further mechanism that brain networks use to process information (Makeig et al, 2002).

The linear sum of potentials from different sources in the scalp electrodes can be studied by decomposing the data matrix in a linear combination of components, hopefully providing a more selective representation of independent EEG generators. The first data decomposition method to gain popularity in this area was Principal Components Analysis (PCA), which reorganizes the EEG data matrix in a mathematically equivalent linear combination of orthogonal components (Harner, 1990; Lagerlund et al, 1997). The first component is determined by a least square fit along the direction of maximal variance of the data matrix. The sucessive components are obtained by repeating the process in the subspace projection obtained by eliminating the dimension along the previous component. Despite its success in decorrelating the overlapping EEG generators activity in the scalp, the reliability of the principal components to correctly express the dynamics of different brain sources has been questioned (Wood and McCarthy, 1984).

A similar technique that has gained popularity in recent years is the Independent Component Analysis (ICA). ICA was first applied to the analysis of EEG by Makeig et al (1996), using an algorithm originally developed by Bell and Sejnowski (1995). ICA algorithms try to maximize the degree of linear independence of a number of spatially fixed components equal to the number of channels in the data. The temporal evolution of the electric potential at each electrode seen in the raw EEG is transformed in the temporal evolution of the components, with each component representing spatially stable generators. The ICA decomposition proved extremely effective in artifact removal from the EEG data (Iriarte et al, 2003) and also in recovering the different elements of the ERP potentials (Makeig et al, 1997). The temporal activation of the components can be associated with the activation of distinct brain areas, providing a dynamical picture of the working brain (Makeig, 2004). The fact that some of the components have dipolar topography over the scalp further suggests that they originate in restricted brain areas.

Despite the power of these techniques to unmix the electric potentials recorded at the scalp, originating in different brain sources, they are nevertheless not able to solve the inverse problem in EEG and so in order to find the brain correlates of the components found, additional methods must be used.

1.4.4. Source analysis

The goal of source analysis methods is to recover the intracranial configuration of primary currents associated with brain network processing of information. The diverse methods repeatedly calculate the scalp potential generated by a particular configuration of intracranial sources and compute the difference to the recorded potential. The algorithms try to minimize this difference by iteratively changing the number, localization or amplitude of the brain generators (reviewed in Baillet et al, 2001). This is an ill posed problem when the only source of information is the EEG potentials on the scalp (Helmholtz, 1853), and the usual way of obtaining a single solution is constraining the problem with assumptions about the intracranial generators (reviewed in Baillet et al, 2001).

Several types of constrains have been used: the moving dipole (variable position and amplitude) (Schneider, 1972); regional dipoles (fixed position/orientation and variable amplitude) (Sherg and Von Cramon, 1985); anatomical constrains (most commonly including only gray matter in the solution space); spatial smoothing (Pascual-Marqui et al, 2002). In general it can be said that dipole models recover well the localization of focal sources in experimental configurations (Leahy et al, 1998), but in more realistic scenarios one cannot be sure of the spatial extent of the sources. Because the scalp potentials are more often associated with large synchronous activation of cortical layers (Cooper et al, 1965) than with point generators, dipole models do not provide a true mapping of the sources but only general information on their localization. The limited knowledge of the detailed conductivity of the different head tissues adds a further element of uncertainty.

From the above considerations one can say that the success of source analysis is critically dependent on the choice of the appropriate constrains to the problem at hand, as well as on the choice of the adequate algorithm. In general such a choice will have to be directed by the results of experimental validation studies in sources with similar characteristics to the one of present interest. The use of associated physiological parameters such as the BOLD activation, acquired by fMRI concomitantly with the EEG, are also being actively considered (Grova et al, 2008; Liu and He, 2008), but it is likely that such approaches will also require extensive experimental validation (Plummer et al, 2008).

1.5. Brain mapping with functional magnetic resonance

1.5.1. Brain mapping with fMRI

Although methods of fMRI became available in the late 80s, the major advance in its use for mapping of human brain function happened in the early 90s when Ogawa et al (1990) demonstrated the possible use of the BOLD contrast imaging for monitoring the neuronal physiology. In this seminal report, MR signal loss in the brain blood vessels of a rat occurred when hypoxic conditions were imposed, and then cleared when oxygen blood level was normalized. This phenomena was explained by the change in the magnetic susceptibility of

blood vessels induced by changes in deoxyhemoglobin concentration, which produced local variations in the T2* relaxation. The suggestion made by Ogawa that such effect could be used to image neuronal function proved prophetic and represented a major development in the field of fMRI.

The BOLD contrast became widely used after the first studies in 1992 (Blamire et al, 1992; Kwong et al, 1992; Ogawa et al, 1992) and proved a reliable (Buckner et al, 1998) and sensitive tool, both to fundamental and clinical research. Because of its non-invasive character the experimenter was free to repeatedly test the subjects, allowing a wide scope for possible experimental setups.

The kinetics of the vascular activation was documented (Boynton et al, 1996), and the relation with the local blood flow and changes in oxyhemoglobin and deoxyhemoglobin were established (reviewed in Logothetis and Wandell, 2004). The BOLD signal increase starts 2-3 seconds after the neuronal pulse and reaches a maximum at 5 seconds, slowly decreasing afterward. Menon et al (1995) demonstrated that an early BOLD decrease occurred in the first 2 seconds, which they interpreted as a focal deoxygenation phase preceding the much stronger oxygenation phase.

The coupling of neuronal function with the vascular response proved a more difficult subject, not solved to the present day (reviewed in Logothetis 2003).

The first fMRI studies used a block design for the experimental paradigm because such setup facilitated both acquisition and analysis of the data. The demonstration that brief stimulus of about 2 seconds can elicit a BOLD response (Blamire et al, 1992) led to the development of event-related designs, which allow a much more flexible experimental design (reviewed in Buckner, 1998). The demonstration that the BOLD response adds approximately linearly for successive events (Boynton et al, 1996; Dale and Buckner. 1997) has been an important development that opened the way to studies with a large number of trials, presented in a short period of time, and allowing complex experiments and improvement of the signal to noise ratio of the fMRI. More recent work demonstrates a refractory period effect for short inter-stimulus trials (Huettel and McCarthy, 2000).

A major contribution to the understanding of the neuronal basis of the BOLD response has been given by Logothetis et al (2001), which made simultaneous recordings of neuronal spike activity, field potentials and the BOLD effect in the visual cortex of monkeys. A linear relation was demonstrated between the amplitude of local field potentials and the BOLD signal (reviewed in Logothetis, 2004). The correlation of the BOLD signal with the neuronal spiking was less consistent. These and later experiments led to the widespread acceptance that the BOLD signal correlates essentially with synaptic network activity.

The achievable spatial resolution increased steadily with the technical advances in the scanner hardware and experimental design. In the human visual cortex several studies have been able to resolve the retinotopic organization to the millimeter range (Engel et al, 1997) and later to the sub-millimeter range (reviewed in de Zwart et al, 2006). In lower mammals, which can be

studied in higher magnetic fields, the spatial resolution allowed analysis of the cortical columnar organization (Duong et al, 2001).

A more detailed spatial resolution of fMRI in humans is promised by the use of the initial dip of the hemodynamic response function, associated with an early increase in deoxyhemoglobin. Up to now no consistent improvement in human studies has been obtained due to the low signal to noise of the method (reviewed in Kim and Ogawa, 2002).

The methods more commonly used for analysis of fMRI data are model-driven and require a previous specification of the stimuli time convoluted with a hemodynamic response function (HRF). A General Linear Model (GLM) is then used to reconstruct the signal as a linear combination of multiple variables of interest and non-interest. Alternative methods of analysis have been developed which do not require such previous model specification, and are based in ICA analysis (McKeown et al, 1998). Such approaches might be particularly helpful when there are problems in specifying a model due either to poor knowledge on the stimuli sequence or of the HRF (Duann et al, 2002). In the most general cases both methods produce similar results (Quigley et al, 2002; Nybakken et al, 2002).

1.5.2. Limitations of fMRI in the study of brain dynamics

The requirement for high magnetic fields to achieve good MRI results imposes major limitations on the potential of the technique for exploration of the brain physiology:

1. The subjects are placed in a noisy and claustrophobic environment, which can affect the experimental performances.
2. Because body movements are very detrimental to the quality of the imaging, a strong emphasis is placed on the subject immobility, a very uncomfortable requirement for long experimental designs.
3. Because the BOLD signal is affected by multiple factors, no absolute quantification is possible in fMRI, restricting the experimental designs to comparisons between activated states and a baseline.
4. Fundamental questions remain unanswered on the mechanisms of the neuronal activity coupling with the vascular response, leading to a degree of uncertainty on how much of the neuronal behavior is reflected in the BOLD signal.
5. Some areas of the brain are commonly affected by magnetic susceptibility artifacts that decrease the quality of the imaging. Such is the case for the lower temporal lobe and orbito-frontal cortex.
6. The major limitation of fMRI to the study of brain networks dynamics is nevertheless the reduced temporal resolution imposed by the slow vascular response to neuronal events. It is well established that significant information processing takes place in intervals of a few hundreds of milliseconds, at least an order of magnitude lower than the best temporal resolution of BOLD-fMRI. In experiments with fast reaction times, both

processing of the presented stimulus and response generation are performed even before any increase in the BOLD signal is apparent. No real-time monitoring and analysis of neuronal physiology is therefore possible, and fMRI provides a temporal integration of events that corresponded to a temporally smoothed version of the neuronal activity. Despite the theoretical capability to discriminate the spatial organization of neuronal networks, the inability to establish the temporal sequence of activation of different brain areas does not allow the establishment of a dynamical cause and effect relationship.

1.6. Brain mapping with simultaneous EEG/fMRI

1.6.1. Historical origin of EEG-fMRI

The first report of human EEG recording in the MRI scanner was the one of Ives et al (1993). In this study the feasibility of reducing the mutual interference of the EEG and MRI equipment to a level that valuable information for each modality could be obtained, was demonstrated. From then on significant efforts have been devoted to the development of EEG equipment with reduced interference in the EPI acquisition and small MRI-induced artifacts on the EEG recording. Different materials were tested for the electrode composition: gold, silver, sintered AgCl; non-ferrous special amplifiers were designed to operate inside the scanner room; special cables of optical and carbon fibers were selected and physical arrangements with serial resistances were employed to reduce induced currents (reviewed in Ritter, 2006).

Patient safety has always been a major concern of the method (reviewed in Lemieux et al, 1999) and with the adopted designs no injury resulting from the technique has ever been reported, until now.

The commercial and custom made systems currently available reduced the interference with image acquisition to an almost negligible level, while the artifacts in the EEG recording remain a significant problem. This led to the need for EEG artifact removal through software algorithms which have been the focus of intense work (Allen et al, 1998; Allen et al, 2000; Hoffman et al, 2000; Garrefa et al, 2003; Neguishi et al, 2004; Niazy et al, 2005; Mantini et al, 2007; Gonçalves et al, 2007).

Due to the early limitations in EEG artifact removal, the oldest systems used an event-triggered fMRI acquisition (Krakow et al, 1999) in which the fMRI acquisition started a few seconds after occurrence of the event of interest. The development of effective methods to record good EEG during EPI acquisition (reviewed in Gotman et al, 2004) led to the current standard method of simultaneous acquisition of both modalities (Lemieux et al, 2001; Lazeyras et al, 2001; Goldman et al, 2002; Sommer et al, 2003).

1.6.2. Effect of the EEG equipment in fMRI

Because conventional EEG recording is done with the use of metal electrodes and conducting wires, a major concern in developing an EEG system for EEG-fMRI was to eliminate all

paramagnetic materials and still obtain good EEG signal (reviewed in Gotman et al, 2004). Such materials can produce significant magnetic susceptibility effects with the consequent loss of signal in the neighboring of the electrodes (Krakow et al, 2000). A similar effect can be produced by some conductive gels used in EEG.
The presence of the EEG equipment in the scanner room can therefore lead to a decrease in the signal/noise ratio of the acquired images, with reduced overall quality.

1.6.3. Effect of fMRI acquisition on the EEG

The scanner room is a very noisy environment for EEG recording. The patient is exposed to constant (scanner main field) and variable (imaging gradients) magnetic fields, as well as to the radio frequency emitted by the imaging coil to excite the nuclear spins.
The constant magnetic field induces few changes in the raw EEG, resulting mainly in increased sensitivity to movement artifacts, with a sometimes prominent heart beat artifact (ballistocardiogram). Such effects are easily removed and in general the main magnetic field does not significantly interfere with EEG acquisition.
The fast gradient switches required for EPI acquisition produce electrical potentials in the EEG electrodes by magnetic induction. Their amplitude is very high, typically more than ten times the baseline amplitude. Removal of these artifacts is essential as they severely affect EEG reading and analysis. Several algorithms have been developed (Allen et al, 2000; Hoffman et al, 2000; Garrefa et al, 2003; Neguishi et al, 2004; Niazy et al, 2005; Mantini et al, 2007; Gonçalves et al, 2007) and found to be very effective in reducing the impact of the variable magnetic fields in the EEG.

1.6.4. Advantages of the simultaneous EEG-fMRI

From the previous considerations it became evident that temporal resolution is the main limitation to the ability of fMRI to map brain dynamics. On the other hand the EEG recording suffers from relatively bad spatial resolution which prevents a detailed brain mapping with this modality alone.
In view of the reduced interference of modern EEG recording in the quality of the fMRI acquired concomitantly, a major expectation for the integration of both techniques is that the EEG temporal resolution will provide the timing accuracy to the fMRI activation clusters (Makeig et al, 2003). The demonstration of the temporal sequence of activation of the several brain areas typically associated with cognitive processing provides important information to establish the flow of information between the different brain networks and their physiological role in the overall brain activity.
The EEG also allows insight on the properties of the background brain activity, an important point when a comparison of BOLD activations is to be made between different subjects or with the same subject at different times (Gonçalves et al, 2006). Because no absolute measures are obtained in fMRI, ensuring common brain background properties is essential for appropriate comparison of activation results.

The EEG record can demonstrate the existence of some scalp potentials apparently not associated with sensory stimulation, the so called endogenous potentials, whose time of occurrence can be determined precisely. Imaging with good spatial resolution the brain areas activating when such potentials occur is essential to establish their origin and the physiological processes to which they are associated.

1.6.5. Methods of integration of EEG and fMRI

The information provided by the EEG and fMRI addresses different aspects of the neuronal activity in brain networks. While the scalp EEG results from the synchronized synaptic potentials in cortical pyramidal cell, the BOLD signal is an indirect effect resulting from the vascular response to the neuronal activation. The connection between the two types of responses has been a focus of intense investigation (reviewed in Logothetis, 2003), but the detailed mechanisms leading from the synatipc potentials to the BOLD response have not been elucidated yet (reviewed in Logothetis and Wandel, 2004).

The first attempts to integrate the two types of information tried to use the BOLD clusters as direct indicators of the brain localization and number of the generators of the scalp EEG. Because these two types of information are among the most difficult ones to recover from the source analysis methods in EEG, if true this approach would represent a major advance in non-invasive EEG source analysis. Unfortunately the experimental studies on the degree of concordance between EEG source analysis and fMRI activations demonstrated discrepancies in localization of several centimeters (Lemieux et al, 2001; Bagshaw et al, 2005; Bénar et al, 2006), suggesting that the BOLD clusters do not provide a very accurate localization of neuronal generators. Problems also arise in establishing the number of intracranial generators from the BOLD clusters, because clusters very often are multiple, making it difficult to establish the ones with significance and the ones resulting from false positives.

Whether the previous discrepancy might be due to suboptimal BOLD activations caused by a deficient model specification of the design matrix extracted from the EEG (Liston et al, 2006), to the failure to incorporate important regressors (De Munck et al, 2008), to unapropriate assumptions about the homogeneity of the HRF throughout the brain (De Munck et al, 2007) or a more fundamental physiological property, is currently unknown. The efforts to improve the analysis of the fMRI data also benefited greatly from the development of data-driven methods, which in experimental settings where the activation model cannot be completely specified (such as in epilepsy), allow insight into the dynamics of the BOLD changes.

A method widely used is based on “seeding” regional dipoles at the BOLD clusters and then solve a “constrained” source analysis problem (reviewed in Wagner and Fuchs, 2001). Other authors use linear continuous models with fMRI constrains to focus the activation area (Babiloni et al, 2001). Methods based in Bayesian inference also use the BOLD clusters to provide a priori information to guide the search procedure (Grova et al, 2008).

Despite the fact that the EEG spatial sampling has improved in recent years with the introduction of recording devices with a large number of electrodes (64-128), no study

correlating high-resolution EEG and BOLD activation has been published to the best of our knowledge.

1.7. The human epilepsies as models of the behavior of brain networks

The human epilepsies are diseases characterized by spontaneous and unpredictable behavioral abnormalities (seizures) resulting from the synchronous activation of a network of neurons constituting the epileptogenic area. Such pathological networks express abnormal activity clearly distinct from normal brain rhythms between seizures (interictal spikes) and also distinct EEG activity in the seizure events (ictal activity).

From a dynamical point of view, the interictal activity is very fast (in the milliseconds range) and also expresses the long distance functional connection (sometimes to opposite areas of the brain) seen in some normal brain rhythms (Steriade, 2005). The EEG of epileptic activity has the experimental advantage of much higher amplitude than the normal physiological rhythms and it also has good specificity to express the activity of the epileptogenic area, as compared to the poorly known generators of the normal EEG activity (Steriade, 2005). Because the epileptogenic areas range in spatial extent from millimeters to several centimeters, the spatial-temporal requirements for an adequate mapping are similar to the ones of the normal neural networks. The study of this pathological model offers therefore an advantageous experimental setting in which to test the power of functional brain mapping.

The epileptic seizures represent another class of events in which a particular brain network demonstrates a peculiar dynamical behavior (reviewed in Niedermeyer, 2005), clearly distinct from the one of the normal brain. The analysis of such temporally extended and dynamical network activities, with its spreading to different brain areas, has been difficult to characterize using the current methods of brain mapping. The capability to provide information on the dynamical involvement of different brain areas in such extended behavior episodes would be of the most advantage to study normal human behaviors.

Some human epilepsies are refractory to pharmacological therapy, and then surgery for epilepsy is contemplated. In this procedure the epileptogenic area is surgically removed to eliminate the seizure events. The decision on the type of surgical procedure is established after extensive clinical, neurophysiological, neuropsychological, imagiological and psychiatric evaluations. The outcome of such procedures offers a unique opportunity for validation of the results of brain mapping, namely the EEG and EEG-fMRI studies.

In order to address the experimental goals set forth in the section 1.1, we selected three groups of epilepsy patients:

1. Patients with idiopathic occipital lobe epilepsy of childhood, providing an oportunity to compare the information obtained with EEG mapping with the one obtained through the simultaneous recording of EEG/fMRI.
2. Patients with epilepsy associated with Hypothalamic Hamartomas have a very well known source of epileptic activity, providing a useful oportunity to test the localizing capabilities of neurophysiological functional brain mapping.

3. Patients with focal epilepsies under study for surgery of epilepsy are valuable experimental oportunities to determine the degree of concordance of functional brain mapping with the structural lesions and/or the brain areas removed on successful surgery, providing validation of the maps obtained.

2. IDIOPATHIC OCCIPITAL LOBE EPILEPSY

2.1. Overview of idiopathic occipital lobe epilepsy

The occipital lobe epilepsies constitute a heterogeneous group which has in common the existence of EEG spikes over the posterior scalp areas. While the symptomatic forms associated with structural brain lesion are rare, the idiopathic (without structural lesion) cases occur mainly in childhood and are relatively common.

The idiopathic occipital lobe epilepsies have been grouped in syndromes with diverse seizure semiology, age of onset, EEG manifestations and clinical course (reviewed in Taylor et al, 2003). Three distinct syndromes have been well established: The early onset occipital lobe epilepsy of childhood (Panayiotopoulos syndrome [Panayiotopoulos, 1989]), the late onset benign occipital lobe epilepsy of childhood (Gastaut syndrome [Gastaut et al, 1992]) and the photosensitive occipital lobe epilepsy of childhood (Guerrini syndrome [Guerrini et al, 1995]). The behavioral manifestations in the seizure events are very distinct in each of these syndromes, suggesting that different cortical areas are involved in their origin. Because no structural brain lesions have been demonstrated in such cases and the clinical manifestations are not specific enough to point the particular brain area involved, it is currently unknown which particular cortical area is responsible for the epilepsy in each syndrome.

EEG studies, despite the fact that prominent spikes are easily recorded over the posterior scalp, have not been able to provide a robust indication of the localization of the generators of the epileptic activity. The Panayiotopoulos syndrome is particularly striking, because despite the relatively monotonous and easily recognizable clinical picture, patients present with multifocal EEG spikes with a changing pattern along time (Ohtsu et al, 2003) that has been the focus of major speculation in recent years (Koutroumanidis, 2007).

We performed four studies on the subject:

1. (Leal et al, 2006a [section 2.2])

   A comparison was made between the use of EEG (source analysis) and EEG-fMRI in two patients with the Gastaut syndrome and one with the Guerrini syndrome. Clearly distinct BOLD patterns of activation were found between the two syndromes, but a consistent pattern in the two patients with the same syndrome. The EEG-only analysis failed to provide a consistent distinction between syndromes and produced inconsistent results in patients with the same syndrome. In general the spatial concordance between spike related BOLD clusters and EEG sources was bad.

2. (Leal et al, 2007a) [section 2.3]

   An analysis of the complex interictal spike patterns present in patients with the Panayiotopoulos syndrome is done in a group of five patients. The use of independent component analysis allowed decomposition of the scalp occipital spikes in several components with distinct spatial and temporal configuration, suggesting significant spread of epileptic activity in each spike. A comparison with rolandic spikes present in

the same patients is done. We conclude that fast spread of epileptic occipital spikes can provide an explanation for the complex and apparently multifocal character of these events. We also identified an early area of activation in the lateral occipital-temporal area.

3. (Leal et al, 2008b) [section 2.4]

   In a follow up paper we tested the spread theory to explain the multifocal spikes by selecting three patients with predominant frontal lobe spikes despite classic clinical manifestations of occipital lobe epilepsy (Panayiotopoulos syndrome). Using independent component analysis and high-resolution EEG we identified an early occipital epileptic discharge preceding the frontal one, effectively ruling out an independent frontal lobe generator for these spikes. The posterior discharges are localized over the occipital-temporal area of a single hemisphere and are compatible with the results of the previous paper in a different set of patients with the same syndrome.

4. (Leal et al, 2007b) [section 2.5]

   The interictal spike activity in a patient with the Panayiotopoulos syndrome is studied with high-resolution EEG and simultaneous EEG-fMRI. The first study revealed an occipital topography for the interictal spikes, while the second one put in evidence multiple BOLD clusters, involving the occipital, temporal and frontal lobes. After integrating the two types of information, using dipole seeding at the BOLD clusters of activation followed by source analysis, a dynamical model was obtained, with onset in the occipital-temporal transition followed by temporal lobe spread.

2.2. Leal, A, Dias AI, Vieira JP, Secca MF, Jordão C. *The BOLD effect of interictal spike activity in childhood occipital lobe epilepsy*. Epilepsia 2006a; 47(9): 1536-1542.

Abstract

Purpose: Occipital lobe epilepsy (OLE) presents in childhood with different manifestations, age of onset and EEG features that form distinct syndromes. The ictal clinical symptoms are difficult to correlate with onset in particular areas in the occipital lobes, and the EEG recordings have not been able to overcome this limitation. The mapping of epileptogenic cortical regions in OLE remains therefore an important goal in our understanding of these syndromes.

Methods: In this work, three patients with two types of idiopathic childhood OLE were studied with EEG source analysis and also with mapping of the BOLD effect associated with spikes in simultaneous EEG/fMRI recordings.

Results: Two patients with late onset OLE provided EEG source localizations in the lateral parietal cortex and in the medial occipital areas. The BOLD activations were consistent and restricted to the medial parietal-occipital cortex in both cases. One patient with photosensitive idiopathic OLE presented with dipole sources in the medial parietal cortex, but the BOLD activations were widespread over inferior and bilateral occipital areas and also posterior temporal ones. There was little spatial overlap between the EEG and BOLD results, but the localizations suggested by the latter are more consistent with the clinical manifestations of each type of epileptic syndrome.

Conclusions: Overall, the BOLD effect associated with interictal spikes maps epileptogenic areas to different localizations than the ones suggested by EEG source analysis. These maps are similar in two patients with late onset idiopathic OLE, but different from a case of photosensitive idiopathic OLE.

Introduction

The occipital lobe epilepsies (OLEs) of childhood are a heterogeneous group of diseases with diverse clinical symptoms, age of onset and prognosis (Taylor et al, 2003). The EEG helps in the localization of the epileptic activity to the occipital lobes, but it is not syndrome-specific and very often the abnormalities also involve the parietal and temporal areas (Taylor et al, 2003). The topography of spikes rarely points to the particular region in the occipital lobes originating the seizures and the few attempts to do source analysis did not improve the generally poor electroclinical correlation (Van de Meil et al, 1997). In the case of idiopathic epilepsies, where brain imaging is normal, the particular regions of seizure onset remain unknown, despite the consistent clinical picture of each syndrome.

The detection of the BOLD effect associated with the occurrence of interictal spikes in simultaneous EEG/fMRI recordings offers a promising way to detect the epileptic neuronal dysfunction with high spatial resolution (Al-Asmi et al, 2003). Some studies with this method have been done in symptomatic OLE (Lazeyras et al, 2000; Bénar et al, 2002; Al-Asmi et al,

2003) demonstrating significant posterior activation. No work has been done in idiopathic OLE, a group of epilepsies where clues to the particular cortical area of onset are lacking.

The goals of this work are to use the BOLD effect associated with the occurrence of interictal spike activity in different types of childhood OLE to improve the electroclinical correlation and also to compare the degree of concordance of this technique with the conventional methods of EEG source analysis.

Methods and subjects

Methods

Three patients with the diagnosis of idiopathic OLE from the outpatient clinic of the Pediatric Neurology Department of Hospital Dona Estefânia were submitted to a 60-min EEG recording outside the scanner, including a sleep period, with a cap of 36 AgCl electrodes ($Fp_{1/2}$, $F_{3/4}$, $FC_{3/4}$, $C_{3/4}$, $CP_{3/4}$, $P_{3/4}$, $PO_{1/2}$, $O_{1/2}$, $F_{7/8}$, $FT_{7/8}$, $T_{3/4}$, $TP_{7/8}$, $T_{5/6}$, $FT_{9/10}$, $A_{1/2}$, F_z, FC_z, C_z, CP_z, P_z, O_z). The sampling rate was 256 Hz and intermittent photic stimulation was performed at the end of registration. Later in the same day a session of functional MRI was performed while simultaneously recording the EEG (19 electrodes at standard 10-20 positions). Each patient demonstrated a single, topographically stable, paroxysm type. This was the main neurophysiological criteria for selection of patients for this study. Informed consent was obtained from the parents of the patients.

Source analysis of the EEG was done using in spikes detected visually in recordings obtained outside the scanner in all patients and also inside for patient 1. The EEG was high pass filtered at 3 Hz (zero phase shift filter with 24 dB/oct) and spikes with good signal to noise ratio were aligned by the peak amplitude to produce an average spike. For patients 2 and 3, not enough spikes could be recorded inside the scanner to produce stable dipole solutions. The sources were obtained from instantaneous moving dipoles at the peak of average spikes (n= 43, 19 and 21 for patients 1, 2 and 3), with a standard three layer Boundary Element Model (BEM) volume conductor model (conductances of 0.33, 0.0042, 0.33 S/m for scalp, bone and brain), provided in the Source2 software package (Neuroscan, El Paso, Mexico). Standard electrode positions were also used. The confidence ellipsoids for the dipole positions represent the 1 SD interval and are directly proportional to the noise estimate in the average spikes (Fuchs et al, 2004), evaluated as 5 μV, 6 μV and 5 μV, for patients 1, 2 and 3.

The EEG/fMRI consisted in the acquisition of blocks of 100 brain volumes each one made of 16 EPI images (in plane resolution 3.75 mm and slice thickness of 7 mm, no spacing; echo time 50 μs; flip angle of 90º) obtained with a TR = 3 s, corresponding to periods of 5 min of continuous and simultaneous monitoring. 4 to 6 blocks were obtained per patient, providing 20 minutes of simultaneous monitoring for patient 1, 30 minutes for patient 2 and 20 minutes for patient 3. A brain T1 weighted anatomic sequence (in plane resolution 0.94 mm and slice thickness of 1.3 mm) was obtained in the same session.

Images were acquired in a 1.5T GE CVi/NVi scanner, while the EEG was recorded through a set of AgCl electrodes connected to an amplifier located outside the scanner room through

carbon fiber wires (MagLink, Neuroscan, El Paso, TX, U.S.A.). The cap did not produce detectable artifacts in the MRI sequences, so these could be processed without any special correction. The EEG was corrected for artifacts induced by the magnetic field and rapidly changing imaging gradients offline using commercial software (Scan 4.3.2, Neuroscan).

The time of occurrence of spikes was determined and used to classify the acquired image volumes, resulting in sequences of events of interest used to build an event-related paradigm. To model the hemodynamic function a Gamma function with derivatives was used (Huetel et al, 2004). Sixty, three and nine spikes were used, respectively for patients 1, 2 and 3. The EPI sequences were corrected for movement and slice acquisition time and smoothed with a Gaussian kernel of FWHM 8 mm. A local autocorrelation correction was used (Worsley et al, 1992) and z statistic images generated. The correction for the multiple comparison problem was done using a cluster threshold with a p=0.05. The preprocessing and paradigm-related analysis of the fMRI was performed using the FSL software package (Smith et al, 2004).

Representation of dipoles on individual brain anatomy was performed by adjusting the fiducial points (nasion, preauricular points inion and vertex) of the BEM model on the individual 3D T1 MRI. Representation on the inflated cortex was done with the FreeSurfer software package (Fischl et al, 1999).

Case 1

This 13-year-old boy is the son of healthy and nonconsanguineous parents. Gestation and delivery were normal and the cognitive and motor development milestones were reached at the appropriate ages. At the age of 7 years, there was an episode of sudden bilateral loss of vision of brief duration, without loss of consciousness or other clinical symptoms. The neurological examination performed hours later was normal.

The EEG revealed high-amplitude spikes over the posterior temporal and occipital areas in the right hemisphere, that blocked partially during recording with the eyes open. A brain 1.5T MRI scan was performed and considered normal.

Medication with Sodium Valproate (250 mg twice daily) was started and he remains seizure-free.

Case 2

This 12-year-old girl has a history of uneventful gestation and delivery. Development in early childhood was reportedly normal and intelligence is also normal.

At the age of 9 years, the parents noticed the occurrence of very frequent, daily episodes of motor arrest with purposeless hand movements, when she was watching TV. During these episodes she stared, remained immobile and did not respond to verbal stimuli. No eyelid movements or loss of tone were apparent. This behavior was also triggered by an abstract yellow pattern on the kitchen wall mosaics, which were green. She could stand for long periods of time in front of a particular mosaic without paying attention to the surroundings. Later on when asked what she was seeing she would say that “there was a lion’s head”.

The EEG showed frequent bursts of parietal-occipital spike-wave activity at 5-7 Hz, lasting seconds and persistent posterior photo-paroxysmal response to intermittent light stimulation in the range of 4-10 Hz.
A younger brother (6-year-old) presented reflex epilepsy in early childhood where the seizures could be evoked by lightly tapping the forehead.

Case 3

A 12-year-old boy with no family history of epilepsy was studied. He was born at the gestational age of 37 weeks by forceps with an APGAR score of 6/10. He had a normal motor and cognitive development.
With age 3 years, he developed partial complex seizures with occasional generalization and without fever. Later on, he presented frequent drop attacks with no apparent cause. He was treated with Carbamazepine and the seizures stopped. He remained controlled until he was 11, at which time he had three seizures characterized by sudden loss of vision followed by interruption of consciousness in two, and one with visual hallucinations where he saw images similar to a motion picture he had seen previously. Headaches followed the seizures.
The EEGs showed a persistently normal background and abundant spike activity over the right occipital and parietal areas. No photo-paroxysmal response was apparent.
He attends regular school without significant learning difficulties.

Results

The EEGs obtained inside the scanner allowed recognition of interictal spikes in all patients (Figs. 2.2.1c, 2.2.2c, and 2.2.3c), which were abundant in patient 1 and rare in the remaining. The number of spikes was clearly reduced in all patients as compared with the recording outside the scanner. This agrees well with what we would expect from comparing sleep recordings obtained outside with full awaken ones obtained inside the scanner, as sleep is a powerful activator of spikes in childhood idiopathic epilepsy.
For patient 1, the EEG background is normal and high-amplitude spikes are present over the left occipital-parietal region (Fig. 2.2.1a), most often occurring rhythmically at 1-3 Hz and with a clear reduction while recording with the eyes open. The spike morphology and topography are monotonous and demonstrate a clear bipolar scalp distribution of the electrical potential (Fig. 2.2.1b). The source analysis reveals dipoles located over the cortical right parietal-occipital region (Fig. 2.2.1b), suggesting a restricted focal epileptogenic area. The source obtained from EEG inside the scanner shows a similar localization but suffers from worse signal to noise ratio (larger confidence ellipsoid) and deficient spatial sampling over right temporal areas (solution shifted to the left) (Fig. 2.2.1c). The BOLD effect associated with the occurrence of spikes involves the more posterior and medial areas of both parietal lobes, with small clusters in the neighborhood of the calcarine fissure (Fig. 2.2.1d,e). No significant BOLD activation is apparent in the cortex adjacent to the source analysis dipoles. Deactivation analysis produces several

clusters, with a more consistent one over the right parietal area, in a localization similar to that of EEG source analysis.

Patient 2 presents a normal background EEG with bursts of spikes over the posterior hemispheres (Fig. 2.2.2a), and focal photo-paroxysmal response induced by intermittent light stimulation. The scalp potential distribution is of a dipolar type, and the source analysis suggests that the localization of the spike generators is in the midline parietal-occipital area, with a slight lateralization to the left (Fig. 2.2.2b). The regions of significant BOLD activation spread over the occipital lobes, involving the lower lateral cortex on both hemispheres, and also the more rostral medial occipital cortex and posterior temporal areas on the right (Fig. 2.2.2c,d). The areas where the dipoles of the source analysis are located show no significant BOLD activation. No significant spike-related deactivation was apparent.

Patient 3 presents spikes and sharp waves with maximum amplitude over occipital electrodes (Fig. 2.2.3a). The average paroxysm shows a dipolar potential field over the scalp, and the moving dipole solution locates the generators in the medial occipital lobe (Fig. 2.2.3b). The BOLD hotspots are located over the posterior and medial occipital cortex and also over the basal ganglia in the right hemisphere (Fig. 2.2.3d,e). The ones localized in the occipital lobe are more superficial than the dipole solutions, and point to different cortical areas as the source of scalp paroxysms. The BOLD deactivation occurs in the left frontal lobe.

Discussion

The different types of OLE reviewed demonstrate a clear discrepancy between the localization of epileptogenic cortical areas suggested by the EEG source analysis and the BOLD activations associated with the paroxysms. This occurs despite the fact that the spatial sampling of the EEG over posterior areas was increased (Van der Meij et al, 1997) resulting in five electrodes over occipital areas (as compared with two for the 10-20 system) and an even more significant increase over parietal and temporal areas (Figs 2.2.1b, 2.2.2b, and 2.3.3b).

The fact that the EEG used for source analysis was obtained outside the scanner room, evokes the possibility that this discrepancy might be due to different paroxysm types being analyzed in the two methods. This is unlikely because patients were selected to the study with the requirement that they had topographically stable, single paroxysm types in previous EEGs; the data collection was done in the same day; and the paroxysms in the EEG obtained inside and outside the scanner room show a similar topography (Figs 2.2.1a-c, 2.2.2a-c, and 2.2.3a-c).

Patient 1 presents a normal development and MRI, pointing to an idiopathic epilepsy. The clinical and neurophysiological features are typical of late onset childhood epilepsy with Occipital Paroxysms (Gastaut et al, 1992), with onset at school age, amaurosis as the main visual manifestation and occipital EEG spikes blocking with the eyes open. Little is known about the cortical areas involved in spike or seizure generation in this syndrome, but ictal semiology would suggest a locus near the primary visual area, while the dipole analysis of Van der Meij (Van der Meij et al, 1997) suggests superficial sources just beneath the skull layer. Our results show a similar superficial localization (Fig. 2.2.1b), but over lateral parietal areas, despite the

fact that we used more electrodes and a realistic volume conductor model. The electroclinical correlation between dipole solutions and clinical ictal symptoms remains poor as no reference in the literature could be found with respect to amaurosis as a manifestation of a focus in this area, and no electrical stimulation in the parietal lobe lead to this symptom. The BOLD activations located in the medial parietal-occipital cortex, and also in the neighborhood of the calcarine sulcus (Fig. 2.2.1e) provide a more consistent electroclinical correlation, as electrical stimulation in the posterior cingulate and inferior precuneus could induce blurred vision (Richer et al, 1991). The significance of the activation in the right basal nuclei is difficult to evaluate, and whether it represents an abnormal functional connection with the epileptic cortical focus as suggested by Federico et al. (Federico et al, 2005) for similar activations is uncertain.

Patient 3 had early developmental problems but the normal intelligence, lack of lesion in the MRI, and normal EEG background with posterior spikes, suggest the diagnosis of idiopathic epilepsy. Amaurosis as the main ictal symptom in recent years strongly suggests the inclusion in the syndrome of late onset childhood epilepsy with occipital paroxysms (Gastaut et al, 1992), which can also present interruption of consciousness, visual hallucinations and post-ictal headache. This syndrome can start as early as 3 years of age and be associated with partial seizures, generalized tonic-clonic seizures, and ictal falls without loss of consciousness (reviewed in Panayiotopoulos, 2002). The localization of the dipole solution provides a good electro-clinical correlation and agrees well with the previously mentioned literature experience on electrical stimulation of the region (Richer et al, 1991).

The BOLD activation on the more posterior parietal-occipital region, although in a different localization, also correlates well with results of local stimulation. Deactivation over the right frontal lobe has no clear EEG correlate in the scalp recording, remaining difficult to interpret.

The BOLD activation data of patients 1 and 3 correlates well and strongly suggests that the epileptogenic area in the Gastaut type of benign OLE is localized in the medial parietal areas of both hemispheres.

In patient 2, the normal neurological status, neuroimaging, and the evidence of a genetic component, point to an idiopathic epilepsy. The visually induced seizures, EEG with prominent focal photo-paroxysmal response and occipital spikes, strongly suggest the diagnosis of Idiopathic Photosensitive OLE (Guerrini et al, 1995). To the best of our knowledge no dipole analysis has been done in this syndrome, so little is known about the possible spike sources. In our case the dipoles are located in the lateral parietal lobe, near the midline (Fig. 2.2.2b), a region where Geller et al (Geller et al, 2000) could evoke complex visual hallucinations with electrical stimulation. The BOLD activations show a discrepant localization, but involvement of inferior occipital and temporal areas provides a better electroclinical correlation with the complex nature of visual symptoms and persistent interruption of consciousness (Salanova et al, 1992; Geller et al, 2000). The two data sets are nevertheless not mutually exclusive.

The BOLD deactivations are present only in the two patients with the Gastaut type of OLE, but their spatial distribution does not overlap. Whether this effect is due to a decreased synaptic activity as suggested by Agakhani et al (Agakhani et al, 2004) or to other unknown effect is a

matter that cannot be resolved with the present data. The overall concordance of BOLD deactivation with the source analysis is no better than for activation, a point already mentioned in the literature (Bagshaw et al, 2006).

We could obtain BOLD activations in 100% of our patients, which is significantly better than the results of larger series, where values in the order of 40-60% are mentioned (Al-Asmi et al, 2003; Bagshaw et al, 2004) for patients with focal epilepsy. A study in a population with generalized idiopathic epilepsy (Aghakahani et al, 2004) improves this value to 93%, and together with our results, suggests that the method may be more efficient in idiopathic epilepsies as compared with the symptomatic ones.

Overall, our data show different BOLD activations on the occipital lobes in different syndromes of idiopathic OLE. The epileptogenic regions identified by this method show important discrepancies with the ones suggested by dipole analysis, in line with data from the literature (Lemieux et al, 2001; Bagshaw et al, 2006), but as a possible representation of the epileptogenic area, they provide a more satisfactory explanation of the clinical ictal manifestations from the literature. The EEG/RMf technique is a powerful method for the study of occipital lobe epilepsies and can provide a way to build more detailed models integrating clinical, structural, electrical and vascular data.

Acknowledgements

The authors are grateful to Cristina Menezes, Elisa Vilar, Rita Pinto, Elizabete Lage and Bruno Mourão for technical support. The work was supported by a grant for Research in Epilepsy from Tecnifar SA and by project Topo3D (POSI/CPS/39758/2001) from FCT.

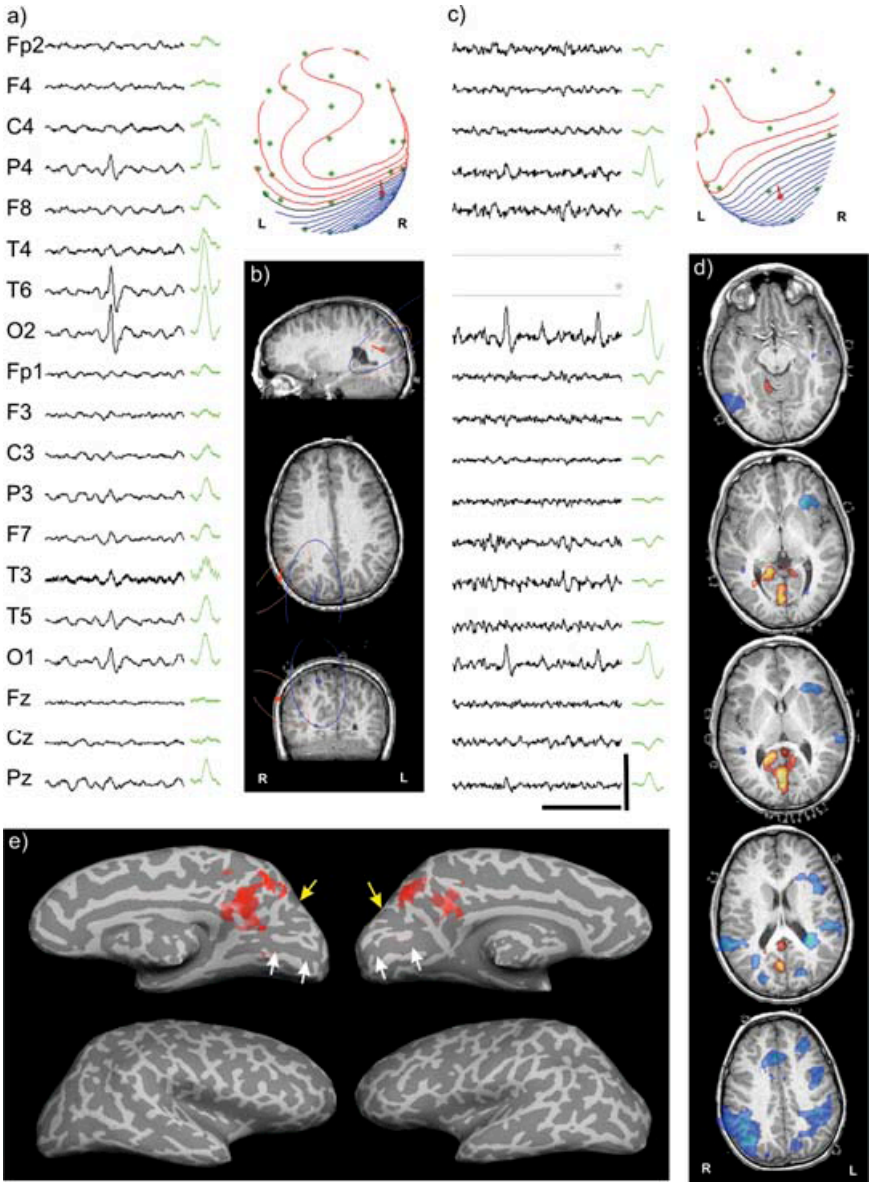

Figure 2.2.1. a) Sample of selected EEG channels demonstrating the interictal spikes in patient 1 over the posterior right hemisphere (the scale bar represents 1 s of time horizontally and 200 µvertically) and average spike at right (n=43). Above right, map of electrical potential at the peak of an averaged spike (electrodes are green, nose upward; negative potentials are blue and positive ones red). b) Moving dipole solution around the peak of an averaged spike outside (red) and inside (blue) the scanner, with a measure of dispersion represented in confidence ellipsoids (1 SD); c) Raw spikes inside the scanner after artifact correction, with average (n=15) and potential map on the scalp (* represents bad channels); d) BOLD regions of significant activation (red) and deactivation (blue) represented over the patient high resolution T1 MRI; e) Activation regions represented on the inflated white/gray matter interface. The calcarine and parietal-occipital sulci are indicated by white and yellow arrows, respectively.

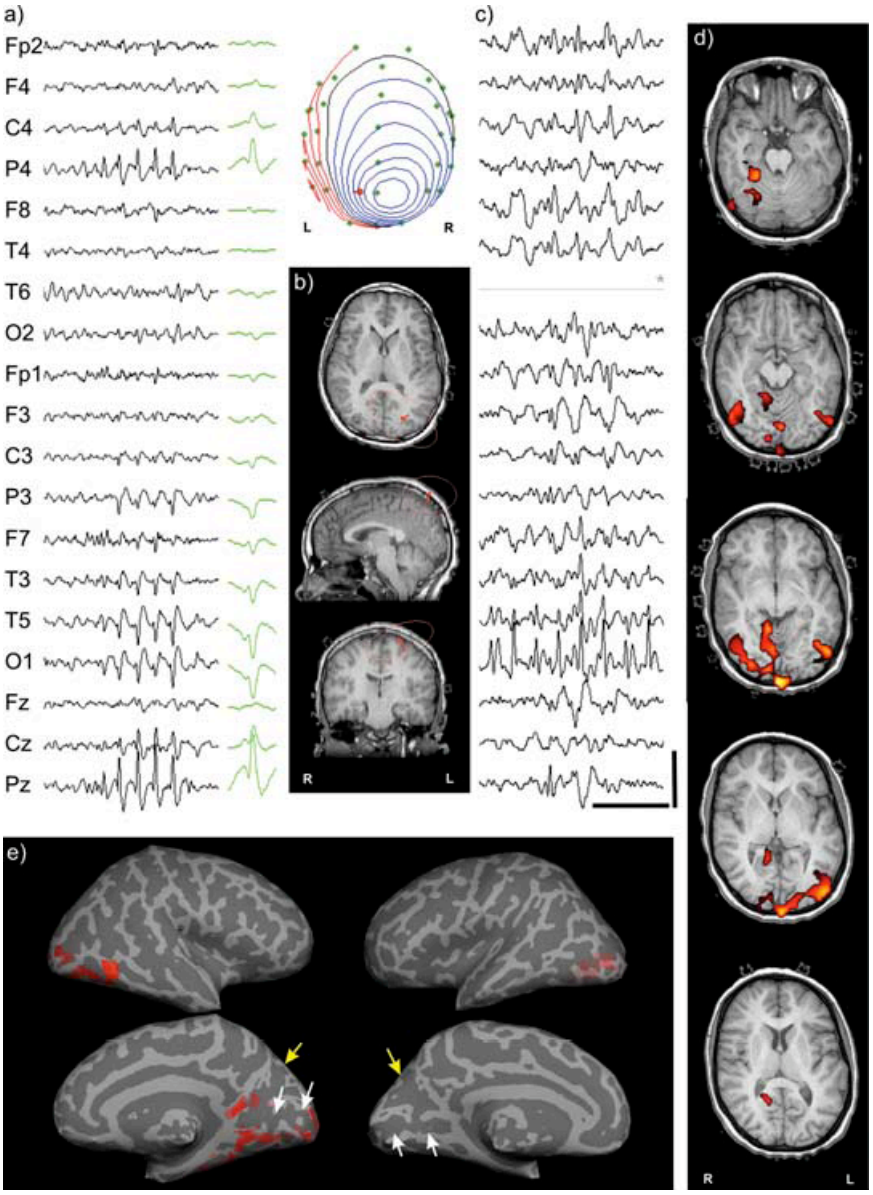

Figure 2.2.2. a) Sample of selected EEG channels with bursts of spikes over posterior scalp electrodes. Right, average spike (n=19); b) Map of scalp potential around the peak of the averaged spike (above), demonstrating the bipolar distribution. Bellow, dipole localization around the peak of the spike. c) Raw EEG inside the scanner, with small-amplitude posterior spikes. Electrode O1 shows gradient artifacts; d) BOLD activation associated with the spikes, mainly over the posterior regions of both hemispheres. No deactivation clusters were detected; e) Detailed representation of BOLD activations over inflated cortex, showing distribution over lower occipital bilaterally and posterior temporal lobes on the right (scale bars, colors, and arrows as in Fig. 2.2.1).

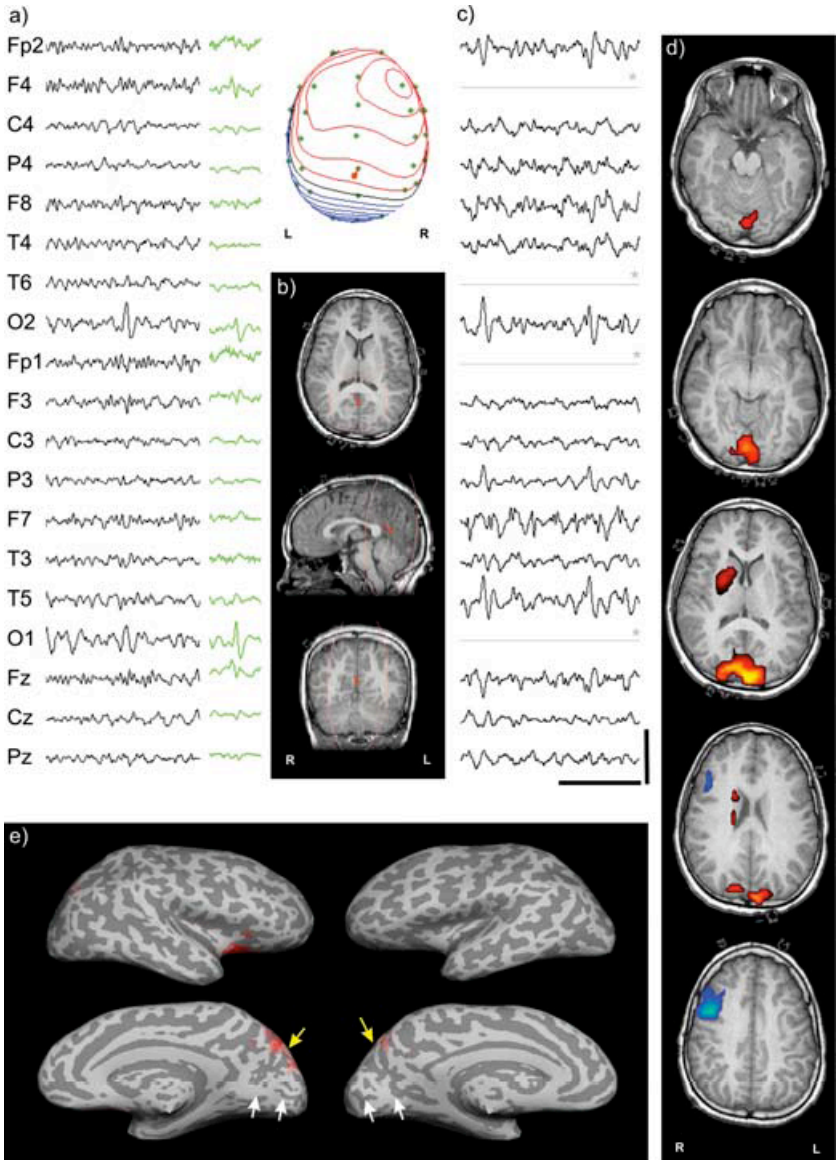

Figure 2.2.3. a) Sample of EEG with posterior paroxysms over the posterior electrodes. Right, average spike (n=21); Scalp potential map with bipolar distribution at the peak of an average spike. Bellow, dipole solution at the spike peak located near the primary visual areas, but with a large error ellipsoid associated; c) Raw EEG inside the scanner with posterior spikes; d) BOLD activation (red) associated with the spikes, in posterior areas of both hemispheres and in the basal ganglia on the right. Deactivation over the frontal lobe is shown in blue; e) Activation clusters over the parietal-occipital region. The activation in the lower right frontal lobe results from artifactual projection of the basal ganglia activation on the nearest surface (scale bars, colors, and arrows as in fig. 2.2.1).

2.3. Leal A, Nunes S, Dias A, Vieira JP, Moreira A, Calado E. *Analysis of the generators of epileptic activity in early-onset childhood begnin occipital lobe epilepsy*. Clin Neurophysiol 2007a; 118(6): 1341-1347.

Abstract

Objective: The Panayiotopoulos type of idiopathic occipital epilepsy has peculiar and easily recognizable ictal symptoms, which are associated with complex and variable spike activity over the posterior scalp areas. These characteristics of spikes have prevented localization of the particular brain regions originating clinical manifestations. We studied spike activity in this epilepsy to determine their brain generators.

Methods: The EEG of 5 patients (ages 7-9) was recorded, spikes were submitted to blind decomposition in independent components (ICs) and those to source analysis (sLORETA), revealing the spike generators. Coherence analysis evaluated the dynamics of the components.

Results: Several ICs were recovered for posterior spikes in contrast to central spikes which originated a single one. Coherence analysis supports a model with epileptic activity originating near lateral occipital area and spreading to cortical temporal or parietal areas.

Conclusions: Posterior spikes demonstrate rapid spread of epileptic activity to nearby lobes, starting in the lateral occipital area. In contrast, central spikes remain localized in the rolandic fissure.

Significance: Rapid spread of posterior epileptic activity in the Panayitopoulos type of occipital lobe epilepsy is responsible for the variable and poorly localized spike EEG. The lateral occipital cortex is the primary generator of the epileptic activity.

Introduction

The Panayiotopoulos type of Idiopathic Occipital Lobe Epilepy (IOLE) has been a focus of research in epilepsy in recent years (Panayotopoulos, 2002) but major issues still remain unsolved such as the particular brain area originating the seizure clinical symptoms and also the significance of the variability of posterior spike activity (Ohtsu et al, 2003). In this respect there is a sharp contrast with the syndrome of Idiopathic Epilepsy with Rolandic Spikes, which is associated with a consistent neurophysiological picture, pointing to the brain area of seizure onset in the rolandic fissure (Wolff et al, 2005).

The source analysis methods in EEG (Yoshinaga et al, 1999 and 2006) and MEG (Kanazawa et al, 2006), using the equivalent current dipole, suggest origin of the epileptic activity near the calcarine sulcus and parieto-occipital areas. These results do not provide a good explanation to the typical ictal clinical manifestations and also fail to explain why the visual symptoms are so rare in the syndrome.

In this work we perform a neurophysiological study of posterior EEG spikes in cases of the Payionotopoulos type of IOLE and a comparison is made with rolandic spikes also present in some of these patients. Our main goal is to determine the usefulness of the interictal EEG analysis to highlight the localization of the primary epileptic foci in this syndrome.

Methods and subjects

Five patients with the diagnosis of early onset IOLE (Panayiotopoulos type) were selected from the epilepsy outpatient clinic of Hospital Dona Estefânia. All demonstrated clinical (Table 2.3.1) and neurophysiological (Fig. 2.3.1) data compatible with the ILAE criteria for the diagnosis (Covanis et al, 2005).

Patients were studied in two moments, with a temporal interval of 3 years. In the early study a special cap with 30 electrodes (10-20 plus Fp_z, $P_{9/10}$, $PO_{3/4}$, $PO_{7/8}$, O_z, $O_{9/10}$ and PO_z) was used to perform a sleep study with one-hour duration. For the repeated study a 24-hours ambulatory EEG was performed with 30 electrodes individually glued to the scalp (10-20 plus $F_{9/10}$, $T_{9/10}$, $P_{9/10}$, $PO_{3/4}$, $O_{9/10}$ and O_z). The electrodes were photographed in several planes and their position in the scalp reproduced in a 3D rendering of a standard average brain. The sampling rate for both recordings was 256 Hz with high and low-pass filters at 1 and 70 Hz respectively.

The EEG recordings were visually reviewed by a clinical neurophysiologist (AL) and the peak of individual spikes marked. Because some of the patients had spikes with different topographies, we selected a minimum of 40 spikes (average of 91±26) for each spike type. This proved possible because all patients had abundant spikes during the sleep period.

The EEG spikes with no artifacts associated were cut in epochs (-100 to 300 ms) around the voltage peak, using the Scan 4.3.1 (Neuroscan, El Paso) software. Data was exported to the EEGLAB 4.515 package (Delorme and Makeig, 2004) for decomposition of the raw spike groups in independent components, using the Infomax algorithm (Bell and Sjenowsky, 1995) and methods detailed elsewhere (Leal et al, 2006). The spatial components with consistent activation at the time of spike peak were selected and submitted to cross-coherence analysis in order to obtain data on their temporal dynamics.

The Independent Component Analysis (ICA) components were sorted by time of activation, providing information on the spreading patterns of the spike activity, and later submitted to source analysis to improve localization of the cortical areas involved.

Source analysis was done using the sLORETA software package (Pascual-Marqui, 2002) available at http://www.unizh.ch/keyinst/NewLORETA/LORETA01.htm. The maximum of the sLORETA statistical score obtained at a given moment was taken as the source of the particular component, and because the spatial components recovered from the ICA decomposition are fixed, the source localization also remains fixed along time.

Results

Most patients (3/5) demonstrated two independent spike topographies, with maximum over posterior and central areas (Figs 2.3.1c,d,e). The latter demonstrated the typical features of rolandic spikes, with maximum amplitude in the central areas and a transverse dipolar type scalp potential, positive over the frontal areas. The posterior spikes had the features described in the literature for the Panayiotopoulos type of occipital lobe epilepsy (Ohtsu et al, 2003), (Fig. 2.3.1).

Because we were interested in evaluating the temporal stability of these interictal patterns, two studies were performed with an average separation of 3 years. When a comparison was made between the two evaluations, we found that for the three patients with central spikes in the initial study, those were also present in the second one and had a similar topography. The posterior spikes persisted in 3 out of 5 patients and disappeared in the remaining ones, despite the fact that a long recording session (24h) was done in the second evaluation. In two out of three patients the topography of these spikes remained very similar in the two studies, but there was a shift toward the parietal lobes in the remaining one.

The averaged spikes demonstrated a dipolar type of scalp potential, which produced a clear focal maximum in the sLORETA source analysis method (Fig. 2.3.1).

Because we are interested in evaluating the dynamics of the interictal activity, the independent spikes of each topographic group were submitted to decomposition in independent components instead of averaging, reconstructing the signal as a linear combination of fixed spatial and variable temporal components (Makeig et al, 2004). The spatial components provide information on the localization of brain generators, while the temporal components provide the temporal sequence of activation. Furthermore the number of ICs with consistent activation time-locked to the spike peak provides information on the minimum number of intracranial generators to include in the model (Marco-Pallarés et al, 2005).

The posterior spikes produced several ICs (Fig. 2.3.2, 2.3.3 and 2.3.4), with distinct spatial and temporal characteristics. The analysis of the relative time of activation of their generators, suggests that in these spikes different brain areas contribute to the potential in the scalp, and the consistent temporal shifts between them (Figs 2.3.2 and 2.3.3) further suggests that this is due to spread of the epileptic activity to nearby areas, from a primary source in the polar or lateral occipital lobes (Fig 2.3.4).

The central spikes produced only one or two close-by ICs for each patient, with a single maximum (Fig. 2.3.5). This suggests that no significant spread of epileptic activity takes place in these paroxysms. They also remained stable throughout time in three out of three patients.

Discussion

The analysis of the spatial and temporal dynamics of occipital and rolandic spikes in the Panayiotopoulos type of occipital lobe epilepsy reveals an important distinction: while rolandic spikes decompose in a single component with maximum over the central areas, suggesting a focal area of onset with little spread, the occipital spikes produce several ICs with distinct spatial distribution and times of activation, supporting the existence of significant spread of epileptic activity to neighbor areas from a point of origin in the superficial posterior and lateral occipital lobe.

The general characteristics of the clinical manifestations in our patients are typical of the ones described for the Panayiotopoulos type of childhood occipital lobe epilepsy (Panayiotopoulos, 1989), with autonomic ictal manifestations associated with decreased consciousness and eye deviation. The seizures lasted several minutes and were rare events (Table 2.3.1), which are

also common features of the syndrome. Patient 5 had cerebral palsy but exhibited long lasting seizures with autonomic manifestations and decreased reactivity which fulfils the criteria for the syndrome, despite the static neurological deficit.

The interictal EEGs demonstrated the typical high-amplitude posterior spikes, which in 3 out of 5 cases was accompanied by independent rolandic spikes. The coexistence of these spike types was reported by Panayiotopoulos (2002) and has in fact motivated the suggestion that a continuum might exist between this syndrome and the Benign Epilepsy with Rolandic Spikes. In two of our patients the posterior spikes disappeared in the second study, while rolandic spikes persisted. This supports an age-dependent expression of the spike activity, with posterior spikes disappearing before the central ones.

The decomposition in independent components of the EEG time series is a proven and robust procedure to decrease the mixing of different brain generators in the scalp electrodes due to volume conductor effects (Makeig et al, 2004). In our patients this analysis suggests that for rolandic and posterior spikes, despite a similar surface morphology, very different number of brain generators are involved; while in the first case a single and focal generator explains well the surface morphology (Figs 2.3.3b and 2.3.5), for the latter spike type several focal generators are required (Figs 2.3.2, 2.3.3a and 2.3.4), suggesting the existence of significant volume conductor mixing in the scalp record of these spikes. The detailed analysis of the time of onset of the ICs demonstrates consistent time lags, which are more compatible with epileptic activity spread between the different areas than with a simultaneous onset. From an area of onset in the posterior or superficial occipital lobes different patterns of spreading can be defined and this may be related with different clinical manifestations. The reduced number of our patients precludes a robust analysis of this possibility, but several trends are apparent such as: persistent existence of interruption of consciousness in patients with temporal lobe spread (patients 1, 4 and 5); vomiting in patients with parietal lobe spread (patients 2, 3, 4 and 5); eye deviation in patients with lateral occipital lobe foci (patients 1, 3 and 4).

The source analysis method used to obtain the spatial localization of the independent generators belongs to the class of linear methods (Pascual-Marqui, 1999), where a large number of fixed dipoles contribute to the overall solution. Such methods are not so sensitive to errors produced by a wrong choice of the number of intracranial generators (Pascual-Marqui, 1999) and can incorporate easily anatomical constrains, which is a major advantage as compared to equivalent current dipole models. In our study the method was used to give an anatomical context to the spatial independent components, making more understandable their intracranial dynamics.

Acknowledgements

The authors wish to express their gratitude to Elisa Vilares, Adilia Seabra and Ana Beato for technical support.

Table 2.3.1- Clinical data

	Patient 1	Patient 2	Patient 3	Patient 4	Patient 5
Age of onset (Y)	6	3	6	2	4
Development	Normal	Normal	Normal	Normal	Cerebral palsy
Ictal symptoms					
Vomiting	No	yes	Yes	Yes	Yes
Eye deviation	Yes	No	Yes	Yes	No
Decreased reactivity	Yes	No	No	Yes	Yes
Other		Nistagmus, sialorrea	Pallor		Decreased tonus
Seizure duration		>20 min	5-10 min	>15 min	>20 min
Number of seizures	1	4	2	4	3

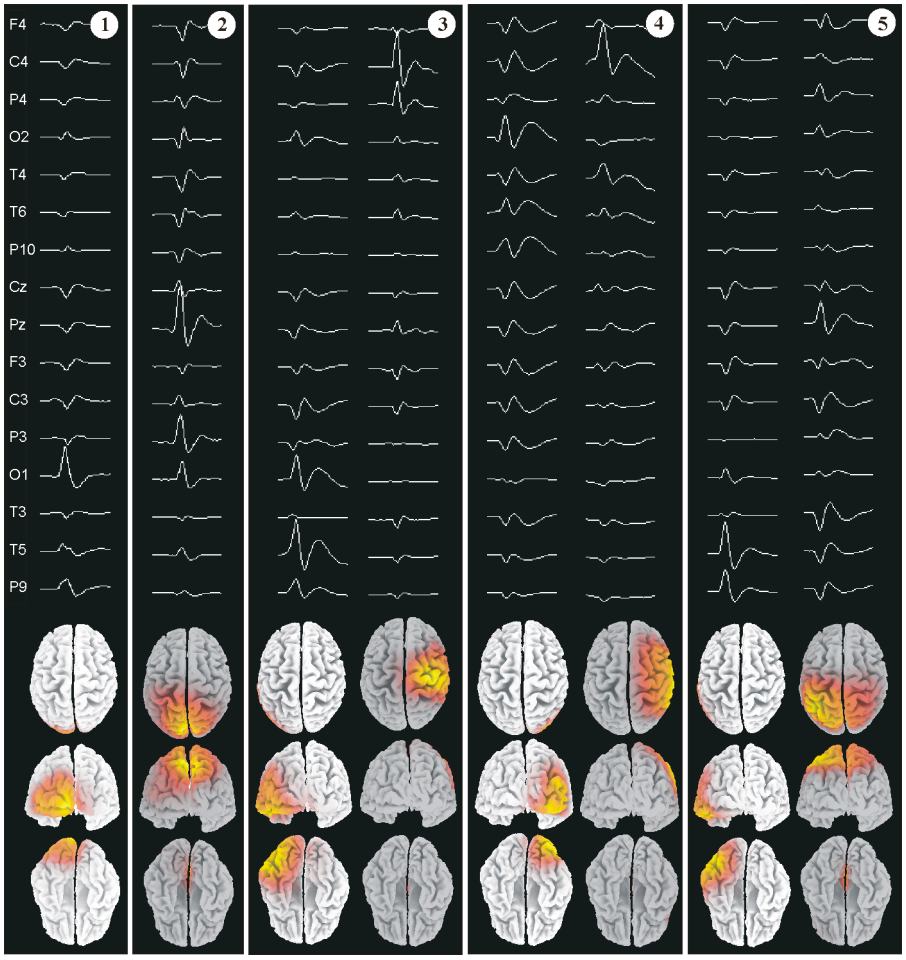

Figure 2.3.1. Topographies of interictal spikes for the five patients. Above, sub-sample of the averaged spikes, demonstrating multifocal activity for patients 3, 4 and 5, with a combination of rolandic and posterior spikes. Bellow, current source distribution at spike peak using the sLORETA algorithm constrained to the cortical volume, demonstrating single maxima of the statistical score in the more superficial cortical areas.

Table 2.3.2 - Neurophysiological data

	Patient 1	Patient 2	Patient 3	Patient 4	Patient 5
Early study					
Age	7	7	8	9	9
Background	Normal	Normal	Normal	Normal	Normal
Interictal	Left occipital spikes	Parietal spikes	Right central and Left occipital spikes	Right central and occipital spikes	Left central and occipital spikes
Early generator	Left occipital	Parietal-occipital	Left occipital	Right occipital	Left occipital
Spread areas	Left temporal		Left temporal and parietal	Right parietal	Left parietal
Second study					
Age	10	10	11	11	12
Background	Normal	Normal	Normal	Normal	Normal
Interictal	Left occipital spikes	Parietal spikes	Right central spikes	Right central and parietal spikes	Left central spikes
Early generator	Left occipital	Parietal-occipital		Right parietal	
Spread areas	Left temporal			Right central	

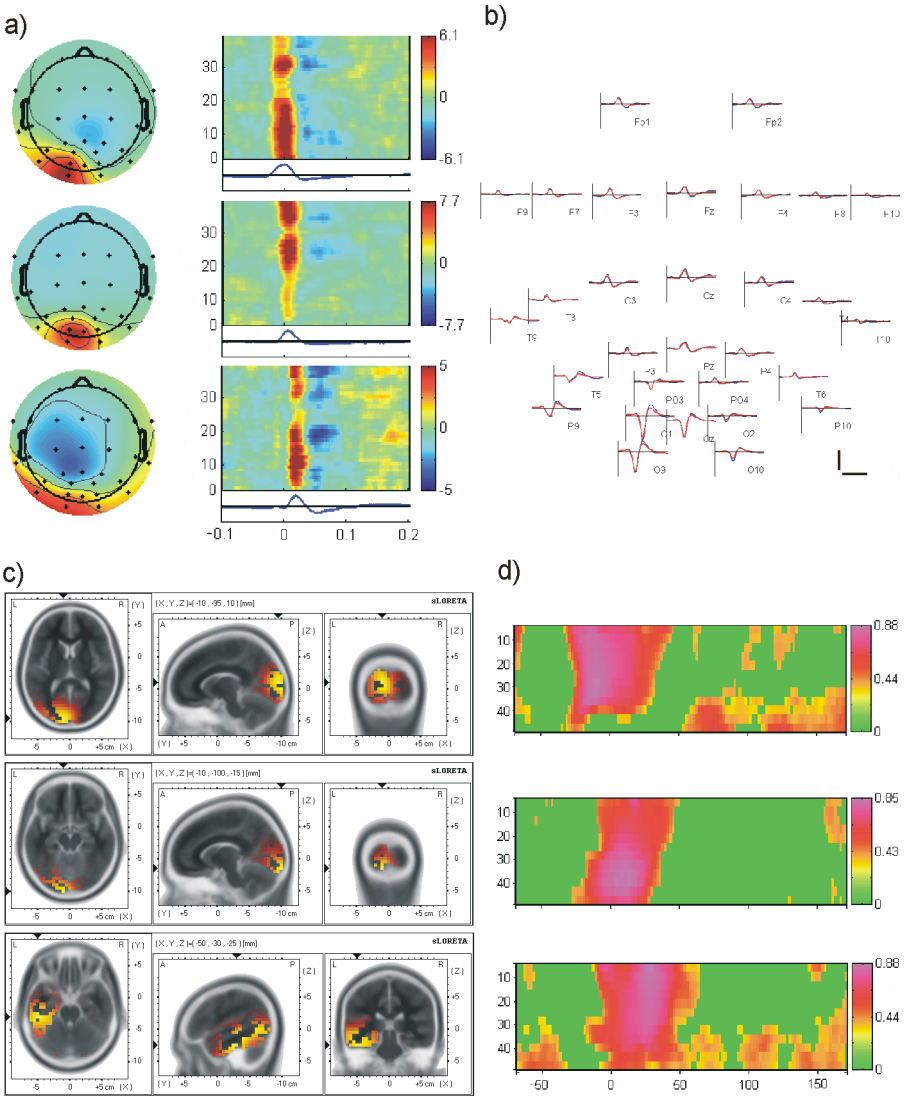

Figure 2.3.2. a) Three ICs with activation time-locked with the spike peak (t=0) for patient 1. Components were ordered from the one with earliest activation (above) to the one activating last (bellow), time in seconds. Spatial components at left. b) Simultaneous plot of original averaged spike (bleu) and the spike reconstructed from the 3 ICs in the left (red). The linear combination of the three ICs recovers most of the spike activity. c) Statistical score at the spike peak for the ICs, using the sLORETA algorithm, demonstrates maxima over the occipital and temporal lobes. d) Cross-coherence between components 1-2, 2-3 and 1-3, suggests a time lag between the components, defining a temporal spread from occipital (ICs 1 and 2) to temporal lobe (IC 3).

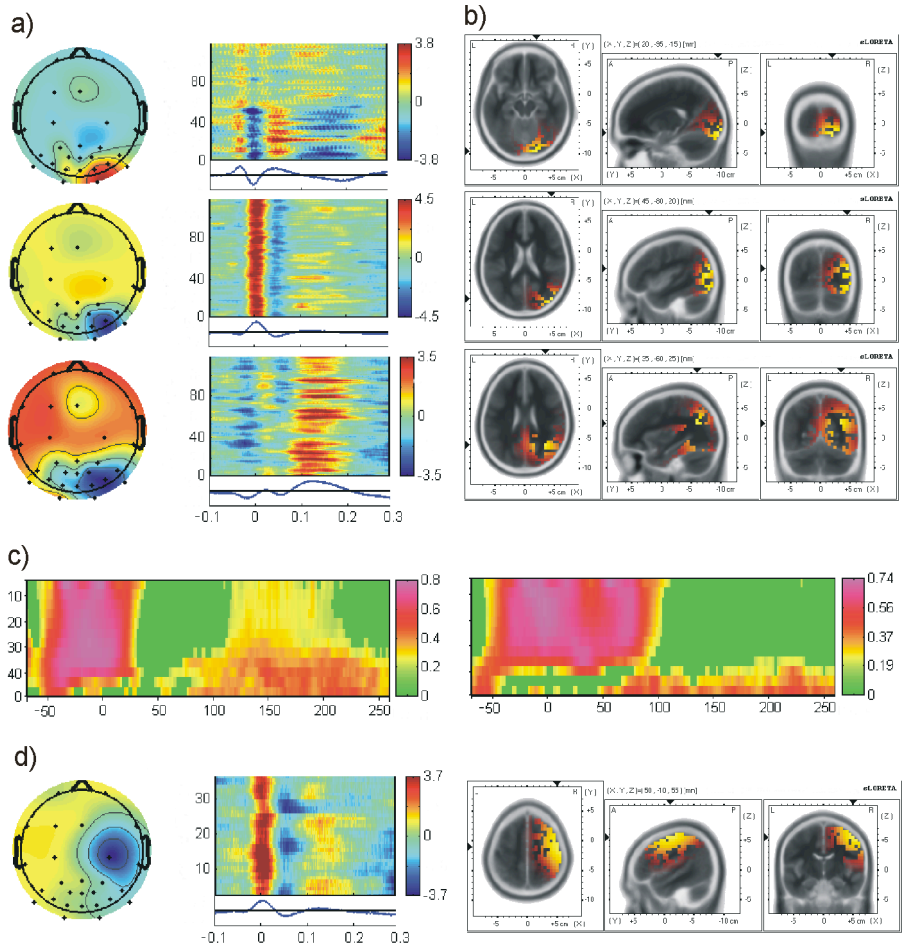

Figure 2.3.3. a) ICs time-locked with the spike peak for patient 4, ordered by sequential time of activation. b) Statistical score maxima for the different ICs using the sLORETA solution at spike peak. c) Cross-coherence between components 1-3 and 1-2. d) IC for the central spike, with sLORETA solution compatible with a rolandic focus.

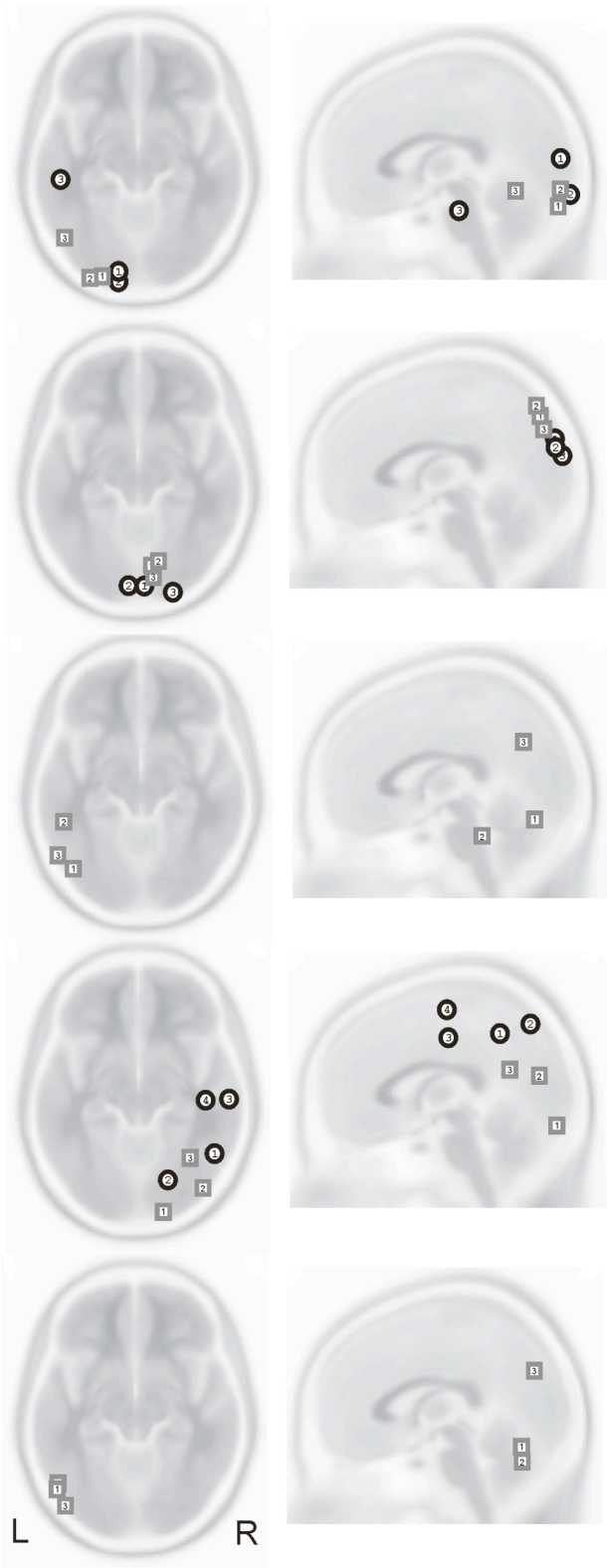

Figure 2.3.4. Propagation patterns for the posterior spikes (patients 1 to 5, from above-down), demonstrating early components (1) in posterior or lateral occipital cortex, spreading to the temporal lobe (patients 1 and 3) or to the parietal lobe (patients 3,4 and 5). Results for the first (squares) and second study (circles), demonstrate overlap of results (patients 1 and 2), discrepant results (patient 4) or disappearance of posterior spikes (patients 3 and 5).

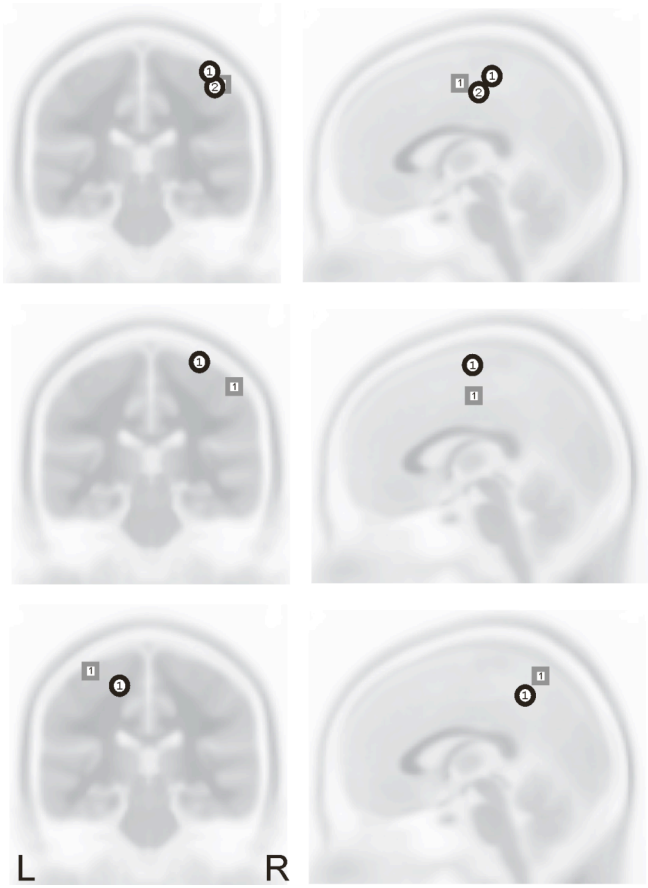

Figure 2.3.5. Propagation patterns and temporal evolution of central spike generators for patients 3 (above), 4 (middle) and 5 (bellow). No significant spread is apparent, and the localization of the generators remained stable in the three-year interval of the two records (squares, first study; circles, second study).

2.4. Leal A, Ferreira JC, Dias AI, Calado E. *Origin of frontal lobe spikes in the early onset benign occipital lobe epilepsy (Panayiotopoulos syndrome)*. Clin Neurophysiol 2008b; 119(9): 1985-1991.

Abstract

Objective: Early onset benign occipital lobe epilepsy (Panayiotopoulos syndrome [PS]) is a common and easily recognizable epilepsy. Interictal EEG spike activity is often multifocal but most frequently localized in the occipital lobes. The origin and clinical significance of the extra-occipital spikes remain poorly understood.

Methods: Three patients with the PS and interictal EEG spikes with frontal lobe topography were studied using high-resolution EEG. Independent component analysis (ICA) was used to decompose the spikes in components with distinct temporal dynamics. The components were mapped in the scalp with a spline-laplacian algorithm.

Results: The change in scalp potential topography from spike onset to peak, suggests the contribution of several intracranial generators, with different kinetics of activation and significant overlap. ICA was able to separate the major contributors to frontal spikes and consistently revealed an early activating group of components over the occipital areas in all the patients. The local origin of these early potentials was established by the spline-laplacian montage.

Conclusions: Frontal spikes in PS are consistently associated with early and unilateral occipital lobe activation, suggesting a postero-anterior spike propagation.

Significance: Frontal spikes in the PS represent a secondary activation triggered by occipital interictal discharges and do not represent an independent focus.

Introduction

The early onset benign idiopathic occipital lobe epilepsy, presently reported as Panayiotopoulos syndrome (PS), has generated a lot of interest in recent years (Lada et al, 2003; Carabalo et al, 2007; Koutroumanidis, 2007). Despite the relatively easy recognition of clinical symptoms (Ferrie et al, 2006), the highly variable characteristics of the interictal EEG activity have prevented the determination of a consistent localization for the epileptic focus (Panayiotopoulos, 2002). Such variability has even suggested to some researchers that a generalized hyper-excitability might be present (reviewed in Koutroumanidis, 2007). This theory fails to explain why there are consistent clinical manifestations of the seizures along time in the same patient and among different subjects.

An alternative view suggests that the variable EEG topographies of the spikes are due to fast spread of epileptic activity between distant cortical areas (Leal et al, 2007a,b) with the epileptic activity originating in the posterior parts of the brain. In order to test the latter hypothesis we decided to study patients with the typical clinical picture but with predominant frontal lobe spikes in the interictal EEG. The demonstration of an occipital origin for this extreme topography might be a good test of the theory postulating a common posterior onset of the epileptic discharges.

Patients and Methods

Three patients with the diagnosis of Panayiotopoulos syndrome and predominant or exclusive frontal lobe spikes in the EEG were selected from the pool of patients evaluated at our department with this syndrome. All the patients had a history of seizures with prominent autonomic manifestations (Table 2.4.1) and expressed the major features of the syndrome as set forth in a recent consensus view (Ferrie et al, 2006).

We performed a 2-h long EEG recording, including a sleep period, using a 64-channel montage in an electrode cap (EasyCap, Herrsching-Breitbrunn Germany) with the 10-10 positions (Fig. 2.4.2). The electrodes were made of sintered AgCl and were connected to an EEG amplifier (Micromed, Italy). The sampling rate was 512 Hz, and we used high- and low-pass filters at 0.5 and 70 Hz, respectively. The EEG was imported to a software environment which allowed offline high-pass filtering at 1 Hz, detection of frontal spikes, segmentation in epochs of 1 s around the spike peaks and visual inspection to remove the ones with artifacts (Scan 4.3, Neuroscan El Paso, USA).

The evaluation of potential maps of the average frontal spikes at fixed intervals before the spike peak revealed a pattern of early negativity over occipital areas which moved to the frontal lobes when approaching the spike maximum (Fig. 2.4.1). The instant in time when this change took place was determined for each patient and later used to separate early onset activity from the late onset one. The processed individual spikes were imported into the EEGLAB software (Delorme and Makeig, 2004) where decomposition in independent components was performed using the Infomax algorithm (Bell and Sejnowski, 1995). We selected the independent components (ICs) with a clear single maximum around the raw spike peak, classifying them in either early components if they had a maximum before the instant in time where the shift of topography from occipital to frontal lobes occurred, or late components with a maximum after that instant. The EEG recovered from these two groups of components consistently separated the frontal and occipital contribution to the recorded spikes (Figs 2.4.2a, 2.4.3a and 2.4.4a).

To better establish the localization of origin of the two components of the average spike we increased the spatial resolution of our recordings using a spline-laplacian montage (Babiloni et al, 1996) as implemented in the software ASA 2.2 (ANT, Enschede, The Netherlands). The scalp surface was obtained from an age-matched normal subject MRI and the standard electrode coordinates of the cap were fitted to the reconstructed scalp in order to match the configuration used in our patients.

The ICA decomposition was repeated in a sub-sample of 19 EEG channels, corresponding to the electrodes of the 10-20 system, to determine whether this analysis method is able to reproduce the same results of the full dataset.

Results

The preliminary analysis of the average frontal spikes revealed a significant change in scalp potential topography from spike onset to spike peak (Fig. 2.4.1). A consistent pattern of early negativity at posterior electrodes was followed by a progressive shift towards the frontal areas.

Such behaviour suggested to us the existence of multiple intracranial generators with different temporal dynamics.

The decomposition of the spikes using ICA, consistently separated the contribution of frontal and non-frontal ICs (Figs 2.4.2b, 2.4.3b and 2.4.4b). The temporal activation of the two groups of ICs demonstrated a pattern of early activation over the posterior areas of the scalp, and a later frontal involvement (Figs 2.4.2a, 2.4.3a and 2.4.4a) in the three patients studied.

The spline-laplacian improved the spatial resolution of the scalp EEG and demonstrated a complex pattern of current sources and sinks over one occipital lobe in three patients (Figs 2.4.2b, 2.4.3b and 2.4.4b, above) and also over the posterior temporal lobe in one (Fig. 2.4.2b, above), for the early activity. This component could be clearly identified in most single spikes for all patients (Figs 2.4.2d, 2.4.3d and 2.4.4d), which suggests that the large majority, if not all, frontal discharges originate in the posterior brain areas. The late activity produced an even more complex, bilateral and widespread, configuration of current sources and sinks over frontal and anterior temporal scalp areas (Figs 2.4.2b, 2.4.3b and 2.4.4b, below).

The repetition of the ICA analysis with the 19 electrodes of the 10-20 system produced similar early-onset components over the posterior scalp areas, with a similar scalp topography (Figs 2.4.2c, 2.4.3c and 2.4.4c left). The comparison of these components with the average spikes (Figs 2.4.2c, 2.4.3c and 2.4.4c, right) demonstrates that they explain well the early negative component seen in the average spikes of patients 2 and 3, but they are very small and hard to recognize in patient 1 (Fig. 2.4.2c, right).

A dynamic model with onset of spike activity over one occipital lobe followed by widespread and bilateral activity over frontal and anterior temporal areas explains well the temporal changes in scalp potential for the three patients and suggests a posterior origin for the interictal activity.

Discussion

The main conclusion from this study is that in 3 patients with the PS the epileptic interictal spikes over the frontal lobes are in fact propagated events from an earlier epileptic discharge at posterior localizations within the occipital lobes.

The absence of a consistent EEG topography for the high amplitude spikes seen in PS has led to speculation that this form of epilepsy might not be related to a particular onset zone, but to a general brain hyper-excitability (reviewed in Koutroumanidis, 2007). Despite this suggestion, very few detailed EEG studies have been made in these patients, and most authors used only the 10-20 map of electrodes to sample the scalp potential spikes (Ohtsu et al, 2003; Lada et al, 2003). Studies using a higher electrode density (Leal et al, 2007a) and a more careful evaluation of the temporal spike dynamics (Leal et al, 2007b) suggest that significant spatial spread of the potential over the scalp takes place from spike onset to spike peak, with the posterior brain areas consistently being the earliest to activate. These studies imply the possibility that the multifocal spike activity described in the scalp might be due to fast propagation of the epileptic activity between different brain areas, from a common area of onset. The severe spatial under-sampling of the 19 electrodes of the standard 10-20 system,

associated with simple methods of analysis, did not allow a clear distinction between the two possibilities.

The significant variation in scalp topography of the scalp potential at different moments from spike onset till spike peak in our data (Fig. 2.4.1) supports a differential temporal involvement of distinct brain areas. The concomitant activation of several generators is expected to be picked up by the surface electrodes, producing volume conductor mixing, which makes the visual analysis of the raw EEG a difficult one.

The techniques of blind source separation based on ICA are powerful tools in the temporal dynamic analysis of such type of signals, where there is a linear mix of the potentials generated by several generators (Makeig et al, 2004). In this study, the ICA algorithm was very effective in separating the dominant frontal potential from an early activating one over the occipital brain areas (Figs 2.4.2a, 2.4.3a and 2.4.4a), suggesting that these two components explain most of the scalp potential complexity of the spike. While this propagation could be suspected from the raw visual analysis of the spikes in two patients (Figs 2.4.3 and 2.4.4), in the remaining patient the small amplitude of the early component prevents such recognition.

The inference of which brain areas are involved in the generation of particular potential components in the scalp is a difficult one due to the uncertainties of the inverse problem in EEG (Plummer et al, 2007). Because our aim was to establish the dynamic relation of the occipital versus frontal activity, we decided to use a standard method to improve the resolution of the EEG using a spline-laplacian montage. This method does not recover the intracranial generators of the scalp potential, but its high selectivity to sources near the recording electrodes (Nunez and Pilgreen, 1991) suggests a contribution of the underlying cortex when focal configurations of sources and sinks are found in the scalp. The spline-laplacian maps of the ICA separated components implicate the occipital and frontal cortex in the production of the epileptic spikes in the three patients studied, with the occipital activity leading consistently the frontal one. This consistent relative timing of the discharges strongly suggests that the unknown generators of the epileptic spikes are localized over posterior brain areas, justifying the early occipital activation.

The previous effect could also be obtained with the 19-electrode sampling, suggesting that better methods of analysis of conventional EEG recordings can also support the main conclusions of our study.

Our conclusion regarding the consistent secondary contribution of frontal lobes to spike generation is in contrast with the study of Saitoh et al (2006) in which they found an independent MEG frontal lobe dipole in an atypical case of PS. The reportedly low goodness of fit (0.65-0.70) suggests that the choice of a single dipole solution was inappropriate and most likely a more complex magnetic field was present than can be explained by such a simple model. The search for additional generators that could provide a better fit to the recorded data was not done.

Overall our data demonstrate that the EEG frontal spikes in patients with PS are consistently preceded by occipital lobe activation, suggesting that they are propagated events from earlier

discharges originated in the posterior part of the brain, and supporting the dynamical model postulating an occipital onset of epileptic activity in PS.

Acknowledgements

The authors are grateful to Daniel Carvalho, Rita Pinto and Elisabete Lage for technical assistance and to Dr Jan de Munck for reviewing the manuscript and helpful suggestions.

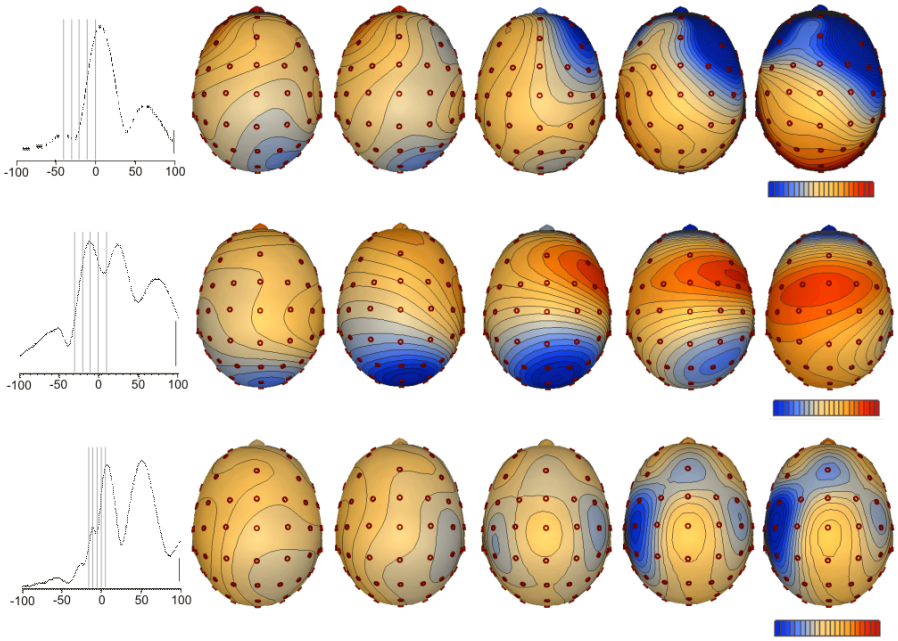

Figure 2.4.1. Maps of scalp potential at several moments in time, from spike onset till spike peak. The maps show significant changes in this temporal interval, with a pattern of the maximum negativity shifting from the posterior areas to the frontal lobes. Each row represents a patient (1 to 3 from top down). The mean global field power is in the left and the time point of each map is represented in doted lines. Temporal scale of the graph is in milliseconds; potential scale is 6.3, 10.0 and 25.2 μV/step for patients 1, 2 and 3; vertical scale is 10 μV.

Table 2.4.1 - Clinical and neurophysiological data

	Patient 1	Patient 2	Patient 3
Age	6 y	8 y	6 y
Sex	M	M	M
Cog. develop.	Normal	Normal	Normal
Seizures			
Age of onset	3 y	6 y	5 y
Nausea	Yes	No	Yes
Vomiting	Yes	No	Yes
Urinary incontinence	Yes	No	No
Eye deviation	Yes	Yes	Yes
Reduced responsiveness	Yes	Yes	Yes
Pallor	No	Yes	Yes
Loss of muscle tone	Yes	Yes	No
Duration	> 15 min	> 10 min	> 15 min
Seizure freq.	Single event	Single event	Single event
MRI	Normal	Normal	
EEG	Frontal lobe spikes only	Frontal lobe spikes	Frontal lobe spikes

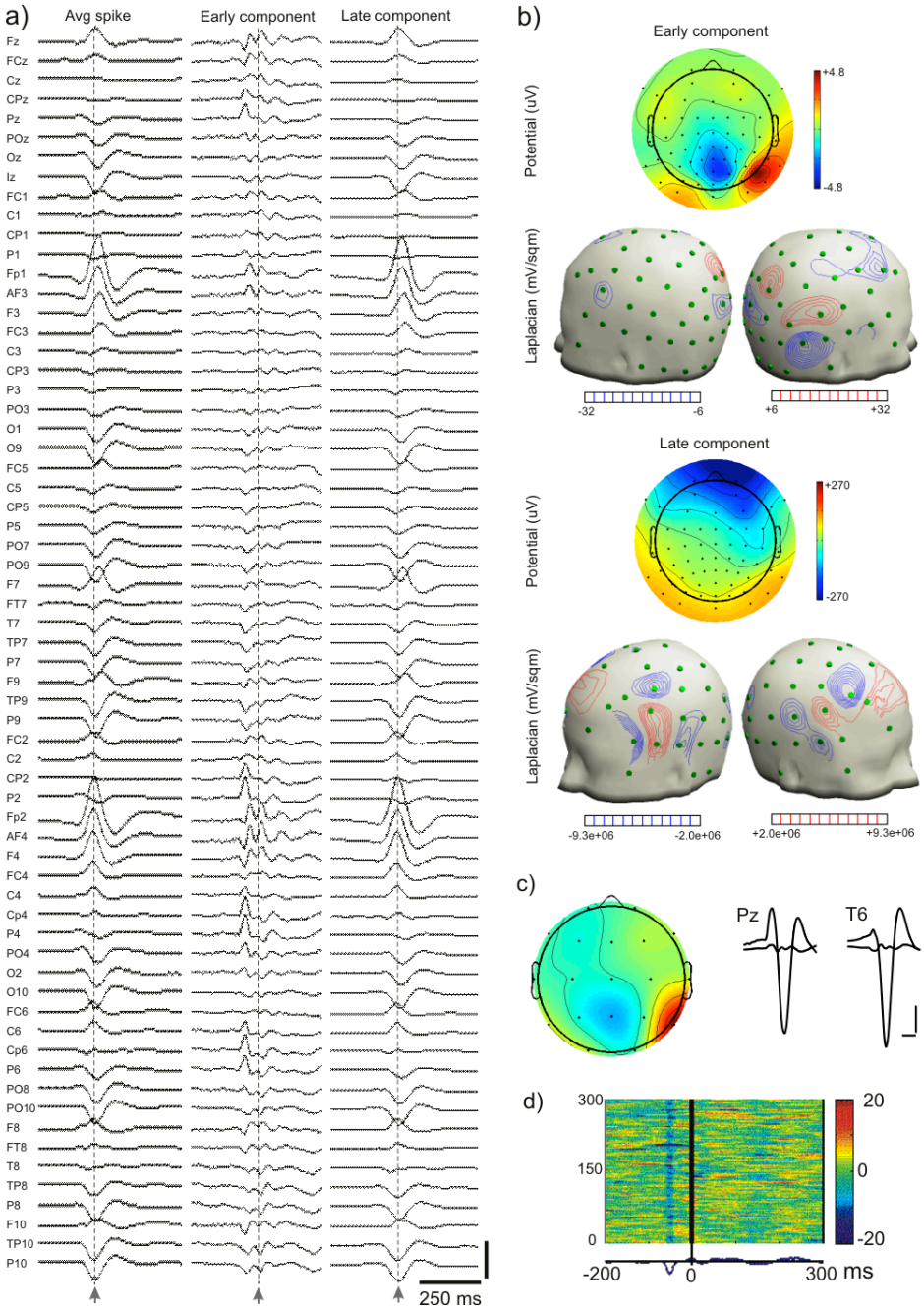

Figure 2.4.2. (a) Average spike for patient 1 (left), with a clear maximum over the frontal lobes. The two components produced by the ICA procedure demonstrate an early posterior component (middle) and a late frontal one (right). Vertical scale is 12 μV for the middle trace and 250 μV for the other traces. (b) Potential maps and laplacians of the early (above) and late (below) components. For each component the potential map on the plane and the spline-laplacian map on the scalp surface, at spike peak, are represented. A localized configuration of sources and sinks is apparent over the right posterior area in association with the early component, while a more widespread and bilateral configuration is associated with the late component. (c) Early component recovered with the ICA procedure from a sub-sample of 19-channels of the original record. The configuration is similar to the one recovered from the original 64-channel record (b, above). Superposition of the original potential and the one associated with the early component (right). The early component contributes very little to the overall potential seen at the posterior scalp electrodes. Vertical scale 30 μV, horizontal scale 20 ms. (d) Color representation of the potential of the early component for every spike included in the average. A consistent brief negativity is apparent -30 ms before spike peak in almost every spike (blue vertical strip). Left scale is the number of the spike, right scale is μV.

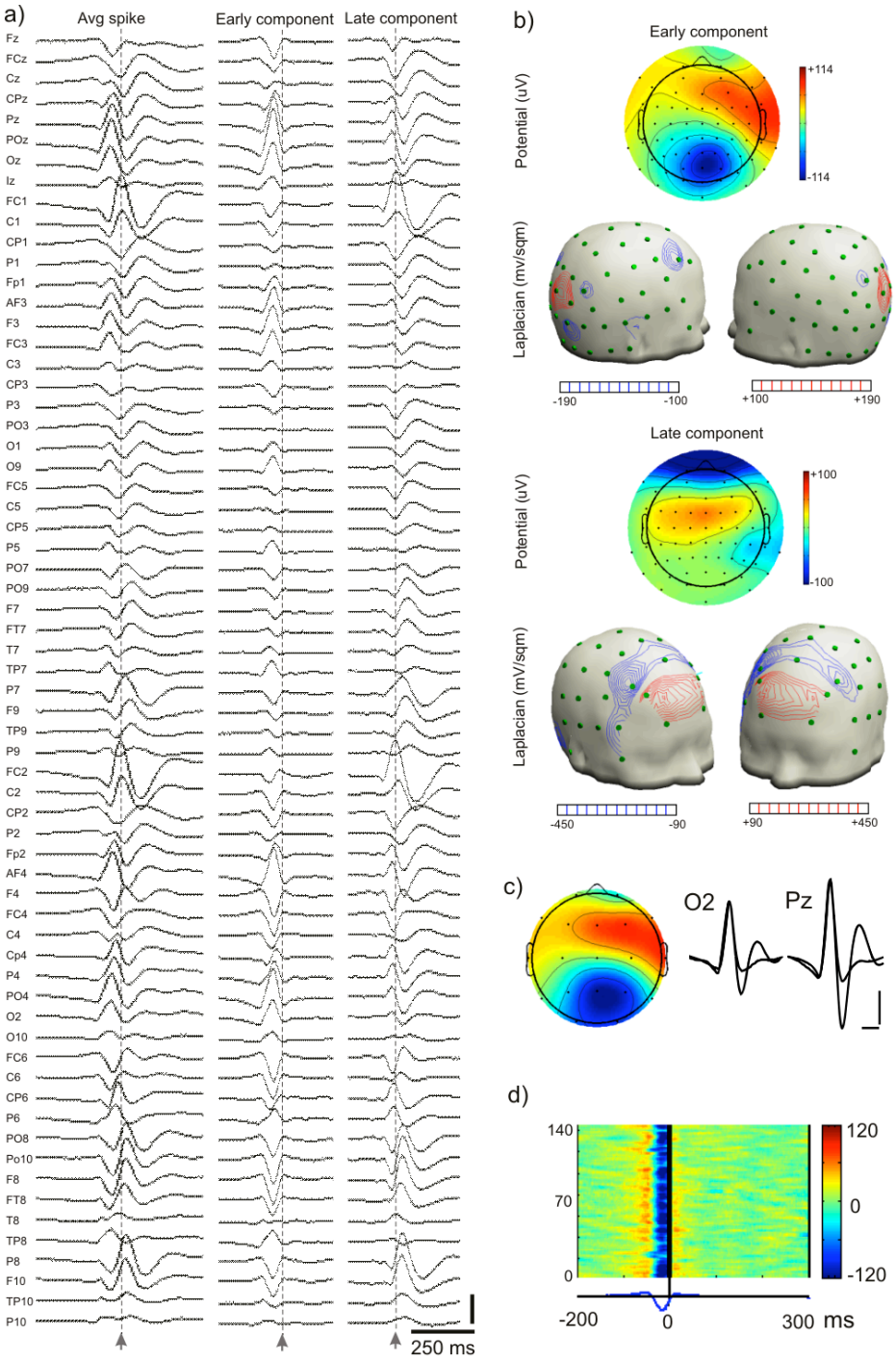

Figure 2.4.3. (a) The average spike for patient 2 (left) reveals a negative spike over the posterior scalp areas just before the frontal spikes, with a partial overlap. The ICA decomposition separates the two components (middle and right). Vertical scale 100 μV. (b) Potential and spline-laplacian maps of the early (above) and late (below) components, demonstrating a focal posterior activation preceding the more widespread frontal one. (c) The ICA procedure in a sample of 19-channels recovers the early component (left). The recovered early component explains most of the early component of the raw potential. Vertical scale 30 μV, horizontal scale 20 ms. (d) The negative potential of the early component is present in most spikes. Scales as for Fig. 2.4.2.

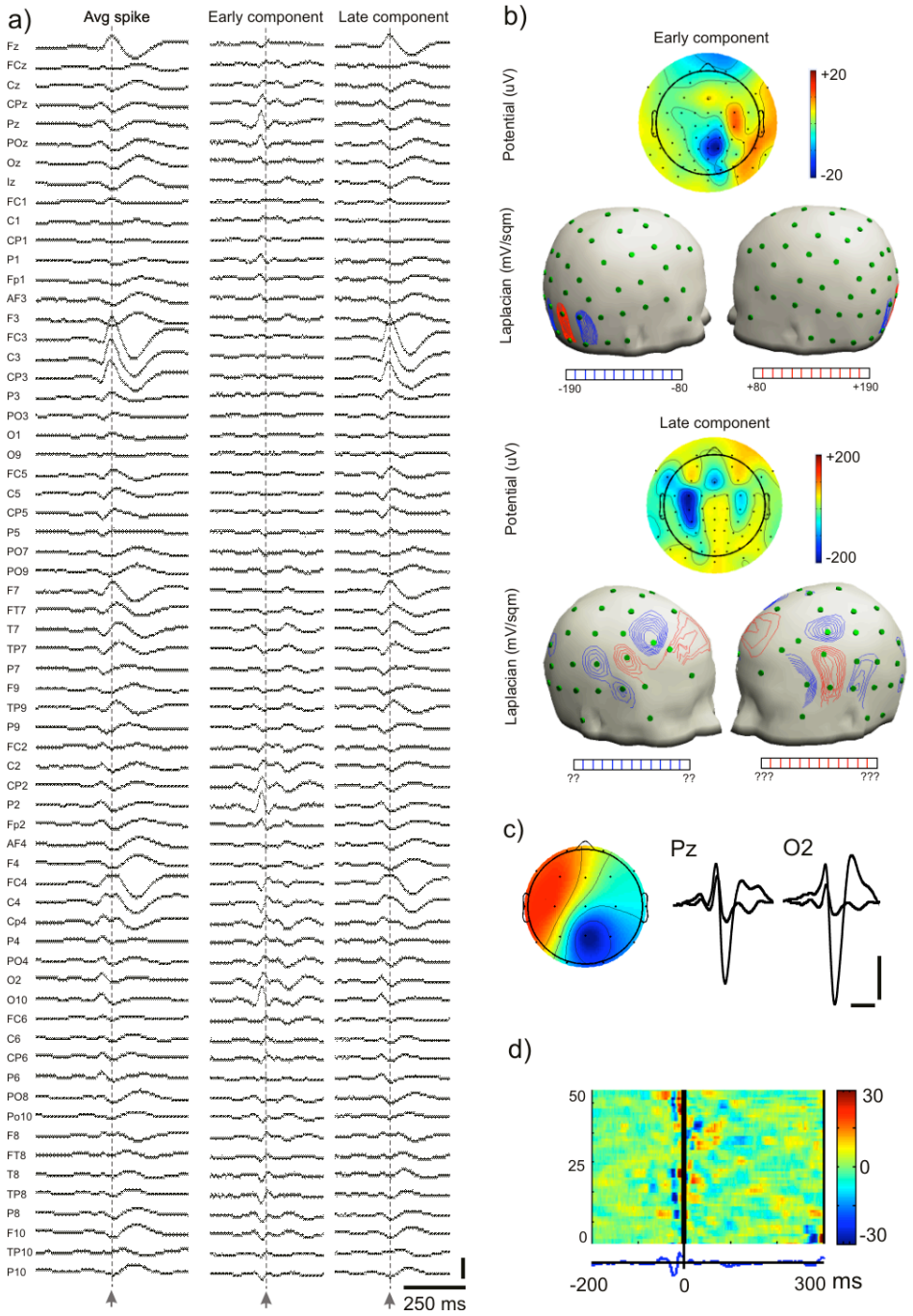

Figure 2.4.4. (a) Average spike for patient 3 (left), with the ICA decomposed early component (middle) and the late component (right). Vertical scale is 250 μV for the left and middle traces, while for the middle trace it is 20 μV. (b) Potential and spline-laplacian maps at the spike peak for the early (above) and late components (below). An early and posterior area of onset is associated with a late widespread frontal activation. (c) Early component recovered from the 19-channel EEG sample. The early component explains most of the negativity seen in the scalp posterior electrodes. Vertical scale 30 μV, horizontal scale 20 ms. (d) A brief early component negativity can be seen in most spikes preceding the spike peak. Scales as in Fig. 2.4.2.

2.5. Leal A, Nunes S, Martins A, Forjaz Secca M, Jordão C. *Brain Mapping of epileptic activity in a case of Idiopathic Occipital Lobe Epilepsy (Panayiotopoulos syndrome)*. Epilepsia 2007b; 48(6): 1179-1183.

Abstract

The Panayotopoulos type of occipital lobe epilepsy has generated great interest, but the particular brain areas involved in the peculiar seizure manifestations have not been established.
We studied a patient with the syndrome, using high-resolution EEG and simultaneous EEG and functional magnetic resonance imaging (fMRI). Resolution of the scalp EEG was improved using a realistic spline Laplacian algorithm, and produced a complex distribution of current sinks and sources over the occipital lobe. The spike–related blood oxygen level dependent (BOLD) effect was multifocal, with clusters in lateral and inferior occipital lobe and lateral and anterior temporal lobe.
We also performed regional dipole seeding in BOLD clusters to determine their relative contribution to generation of scalp spikes.
The integrated model of the neurophysiologic and vascular data strongly suggests that the epileptic activity originates in the lateral occipital area, spreading to the occipital pole and lateral temporal lobe.

Introduction

The most common syndrome of idiopathic occipital lobe epilepsy (IOLE) has been a source of puzzling questions since its description by Panayiotopoulos (Panayiotopoulos, 1989). The cardinal ictal manifestations of vomiting, eye deviation and long periods of interruption of consciousness, with rare visual symptoms, constitutes an unusual constellation of symptoms and up to now very little is known about the particular cortical structures involved in their generation.
The consistent clinical picture in affected children suggests that a common epileptic network is at work and persists with little change throughout the evolution of the syndrome. The variability of the EEG (Panayiotopoulos, 2002) has resulted in a failure to provide consistent generators in this type of epilepsy. Attempts to improve its localizing capabilities, and also of MEG, using source analysis (Yoshinaga et al, 2005; Kanazawa et al, 2005; Yoshinaga et al, 2006) have resulted in localizations which do not explain the peculiar clinical symptoms and the lack of visual manifestations.
In this study we perform detailed brain mapping of a single case and demonstrate how this data provides a better integration of clinical and EEG data.

Case report

A healthy 11-year old boy, with no previous history of seizures, was found with the eyes turned to one side, not responding to verbal stimulation and a pale face, while resting in the beach. He

recovered normal behavior after a few minutes. Hours later, while resting in a sofa, he repeated the symptoms, which also lasted for a few minutes. Medical evaluation at an emergency department half an hour later failed to find any abnormality and he was discharged with an EEG booked for the next day.

The EEG revealed almost continuous spike activity over the left posterior areas, and he was admitted to the Intensive Care Unit for vigilance, despite the fact that he remained alert and with a normal neurological status. No evidence supporting persisting clinical seizures was found.

An ambulatory device using the full 10-20 system was used to monitor continuously the EEG (24h). The prominent left posterior spike activity with the eyes closed was confirmed, as well as its striking decrease while recording with the eyes open, which led to he diagnosis of IOLE. The patient was medicated with Sodium Valproate and remains seizure free after 6 months.

Methods

To improve the spatial mapping of the epileptic activity on the scalp a high-resolution (64 electrodes), 2 hour-long recording, was done using a special AgCl electrode cap (Fig. 2.5.1b), a 256 Hz sampling rate and filters between 0.5-70Hz. The electrode positions in the scalp were determined using an electromagnetic digitizer (Polhemus, Colchester). A realistic spline Laplacian montage as implemented in the ASA 2.2 software package (ANT, Enschede) was applied.

The patient was later submitted to a 1-hour session of simultaneous EEG/fMRI recording, using a special EEG cap (Fig. 2.5.1d) designed for passive recording inside the scanner (Maglink system from Neuroscan, El Paso). A 37 channels EEG DC recording with a sampling rate of 1000 Hz and low pass filter at 70Hz was used. The echo planar imaging (EPI) artifacts were removed with the Scan 4.3.3 software package (Neuroscan, El Paso), allowing clear detection of spike onset (Fig. 2.5.1d). Four blocks of 100 brain volumes, each one made of 16 EPI images (in plane resolution 3.75 mm and slice thickness of 7 mm, no spacing; echo time 50 ms; flip angle of 90º), were obtained with a TR = 3 s, corresponding to periods of 5 minutes of simultaneous EEG/fMRI. A head 3D T1 spoiled gradient recalled gradient (SPGR) sequence was also acquired (in plane resolution of 0.94 mm and slice thickness of 1.3 mm for a field of view of 24x24 cm). Images were obtained in a 1.5T GE CVi/NVi scanner.

EPI sequences were corrected for slice acquisition time and movement, and smoothed with a gaussian kernel of full-width at half-maximum of 5 mm, using the FEAT 5.63 software package (Smith et al, 2005). The initial two sequences were obtained while the patient remained with the eyes closed, but in the last two the patient alternated periods of 30 seconds with eyes open and closed (Fig. 2.5.2a). EPI volumes were then submitted to independent component analysis (ICA) using the infomax algorithm (Bell and Sejnowski, 1995) as implemented in the GIFT 1.3b package (available at http://icatb.sourceforge.net/). The independent components (IC) were then submitted to temporal sorting by the multiple regression coefficients obtained by adjusting their time courses to a regressor constructed by the time of occurrence of the spikes convolved with a standard gamma hemodynamic response function (Fig. 2.5.2a) obtained from visual

evoked potentials (Huettel et al, 2004). The components with the highest covariance with the previous regressor were selected for further analysis (Fig. 2.5.2b), and images were thresholded with a Z score of 2.3. The blood oxygen level dependent (BOLD) images were registered to the 3D T1 sequence using FLIRT 5.0 (Jenkinson et al, 2002).

Determination of the relative contribution of the BOLD activation areas was done by seeding regional dipoles in the center of the BOLD clusters and determining the temporal contribution of each source to the average spike in the scalp, using a three shell spherical volume conductor model.

Results

The long-term EEG demonstrated a single and stable topography of the spike activity over the left occipital lobe, a feature confirmed with the high-density recording (Figs 2.5.1a,b). This topography at spike peak was dipolar (Fig. 2.5.1b) but the use of a realistic spline Laplacian reference improved the spatial resolution and demonstrated a more complex configuration of sources and sinks of current over the left occipital lobe, suggesting that multiple cortical generators are involved in spike production. Also, because of the well known selectivity of the laplacian to superficial sources (Nunez et al, 1994), this result supports involvement of the more superficial occipital cortex in epileptic activity.

The spikes recorded inside the scanner demonstrated strong modulation with opening and closing of the eyes (Fig. 2.5.1d), allowing creation of a baseline (eyes open) condition and an activated state (eyes closed). The absence of baseline in the two sequences acquired with the eyes continuously closed prevented detection of significant BOLD effect.

The ICA procedure used did not require any information on the time of occurrence of the spikes or the opening and closing of the eyes, but recovered three components (out of more than 50) whose activation exhibited strong temporal correlation with those two regressors of interest (Figs 2.5.2a,b). The component more clearly time-locked to the opening and closing of the eyes corresponded to activation of the primary visual areas (Fig. 2.5.2c) and reflects the normal activation of the visual pathway. The other two components showed consistent activation with the eyes closed and are time-locked to the occurrence of spikes, expressing the BOLD activation due to these pathological events (Fig. 2.5.2c). The remaining components either expressed known artifacts or did not show a compatible modulation of the temporal activation.

One of the selected components expressed a maximum at the left occipital pole and two secondary ones at both temporal poles (Fig. 2.5.2c, middle). The other produced BOLD activation of the left temporal-occipital junction, the lateral left temporal lobe and also in the right frontal lobe (Fig. 2.5.2c, bellow). Overall a widespread, spike induced, BOLD activation of the left occipital and temporal lobes is suggested, supporting either a diffuse epileptogenic area or significant spread of the interictal activity.

There is spatial overlap of BOLD cortical activation with the Laplacian mapping for the posterior occipital regions (Figs 2.5.3a,b), but at frontal and more anterior temporal areas no scalp electrical activity can be demonstrated in the Laplacian montage (Figs 2.5.1c and 2.5.3a). The

average reference montage does not show significant electric activity at these areas either (Fig. 2.5.1b).

The analysis of the seeded dipole activation curves suggests that the lateral and inferior occipital area originate the epileptic activity, which later spreads to the occipital pole and temporal lobe (Fig. 2.5.3c).

Discussion

The normal neurological status as well as the lack of any abnormality in the brain MRI supports the diagnosis of idiopathic epilepsy, which is also supported by the EEG demonstration of abundant and high amplitude posterior spike activity.

The ictal manifestations of tonic deviation of the eyes, decreased consciousness and pallor are common features in the Panayotopoulos type of IOLE, which associates autonomic manifestations with eye movement and consciousness disturbances (Ferrie et al, 2006). The absence of prominent autonomic manifestations, such as vomiting, is atypical but does not exclude the syndromic diagnosis (Ferrie et al, 2006). The alternative diagnosis of Gastaut type of IOLE seems unlikely because the usual ictal visual manifestations and preservation of consciousness in this syndrome are absent in our patient.

Most studies using source analysis to localize spike generators in this syndrome, either using EEG (Yoshinaga et al, 2006) or MEG (Kanazawa et al, 2005), have used such a dipolar distribution of the scalp potential to postulate a single dipole generator which they located near the calcarine sulcus and the parietal-occipital sulcus. These results suggesting an epileptogenic area near the visual cortex are not compatible with the rarity of visual symptoms and are also not compatible with our results, which show a complex distribution of sources and sinks of current over the left occipital lobe. The spatial filtering properties of the laplacian, which strongly favor superficial cortical sources (Nunez et al, 1994), further suggest that in our patient the epileptogenic area is extended and not focal, involving the pole and superficial lateral occipital cortex.

The lack of data on the characteristics of the BOLD response (Duann et al, 2002) in normal and epileptic tissue, which makes it difficult to choose the right parameters for a conventional model-based processing of the fMRI data, motivated us to use a data-driven approach which in previous studies produced results similar to the ones of the model-driven method (Nybakken et al, 2002; Quigley et al, 2002), but does not require apriori knowledge of model parameters. This approach seems particularly useful in the detection of the BOLD effect of interictal spikes, as those events are sometimes difficult to detect, resulting in decreased sensitivity of model-driven methods (Liston et al, 2006).

The occipital BOLD clusters show good agreement with the laplacian map, which suggests at least two cortical generators, one in the left pole and another one in the more lateral and inferior area (Figs 2.5.3a,b). The BOLD activations over the temporal and frontal areas are not associated with detectable scalp electrical activity.

The activation curves obtained by the dipole seeding at the BOLD activation clusters suggest that the scalp spikes originate in the lateral occipital lobe and spread to the pole and lateral temporal cortex of the same hemisphere. No contribution from other sources was apparent.

The previous results provide a tentative explanation of the peculiar ictal clinical manifestations of our patient. The interruption of consciousness can be attributed to epileptic propagation to the temporal lobe, while the eye deviation is likely to be due to the localization of epileptic activity to the occipital-temporal junction, a cortical area well known to be activated in smooth pursuit and saccadic eye movements (Petit and Haxby, 1999). The limited autonomic manifestations in our patient (pallor) offer little opportunity to determine the possible generators of more typical manifestations such as vomiting. Comparison of brain mapping in patients with diverse clinical manifestations within the same syndrome might offer an opportunity to determine the brain areas associated with particular symptoms.

Acknowledgements

The authors are grateful to Cristina Menezes, Daniel Carvalho, Rita Pinto and Elisabete Lage for technical support and to Prof Alexandre Andrade and Rosalina Fonseca for revision of the paper.

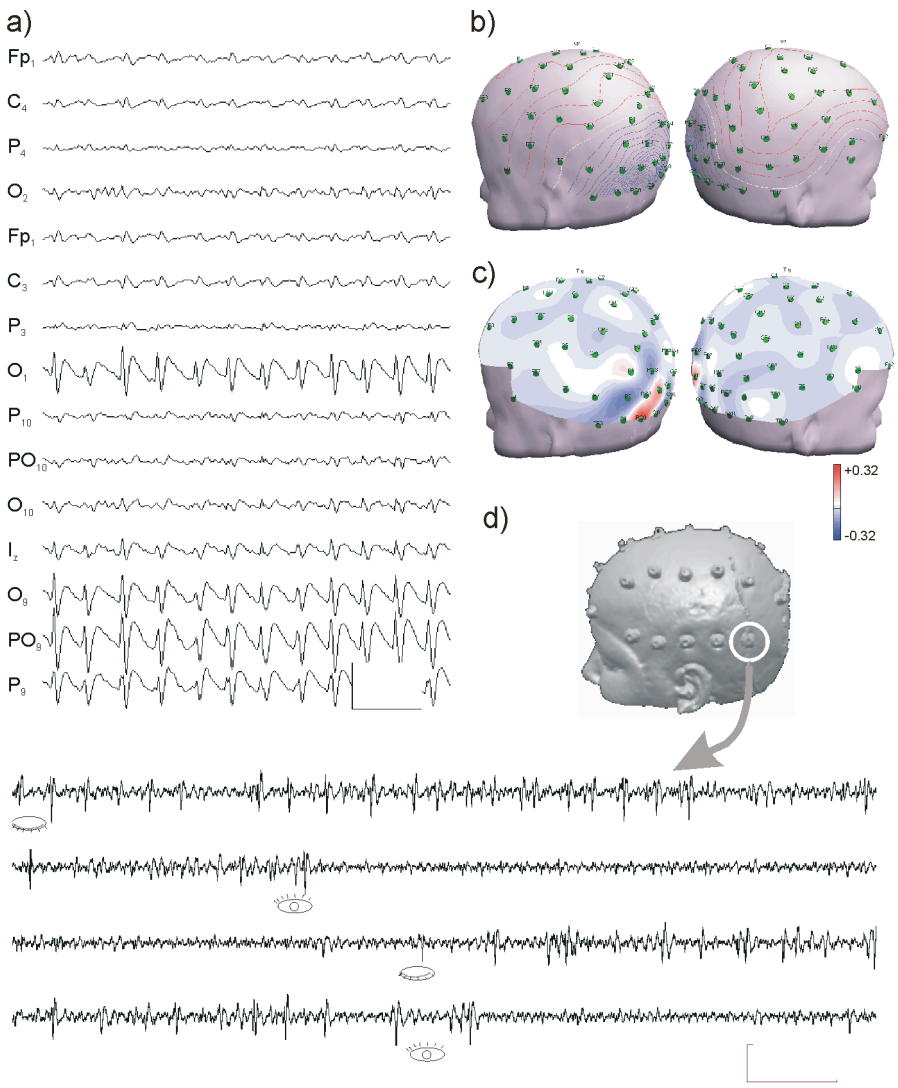

Figure 2.5.1. a) Sub sample of the 64-channel EEG recording, demonstrating almost continuous spike activity over the posterior derivations on the left hemisphere with the eyes closed. Vertical bar is 200 μV, horizontal bar 1 second. b) Dipolar distribution of the scalp potential obtained with 64 channels over a realistic head surface and with average reference. c) Map of the spline Laplacian, showing current sources and sinks with a complex spatial distribution over the posterior left hemisphere. Color scale bar in μV/sqm. d) EEG obtained inside the scanner, demonstrating strong modulation of the spike activity with opening and closing of the eyes (electrode T5). Vertical bar 256 μV, horizontal bar 3.1 seconds.

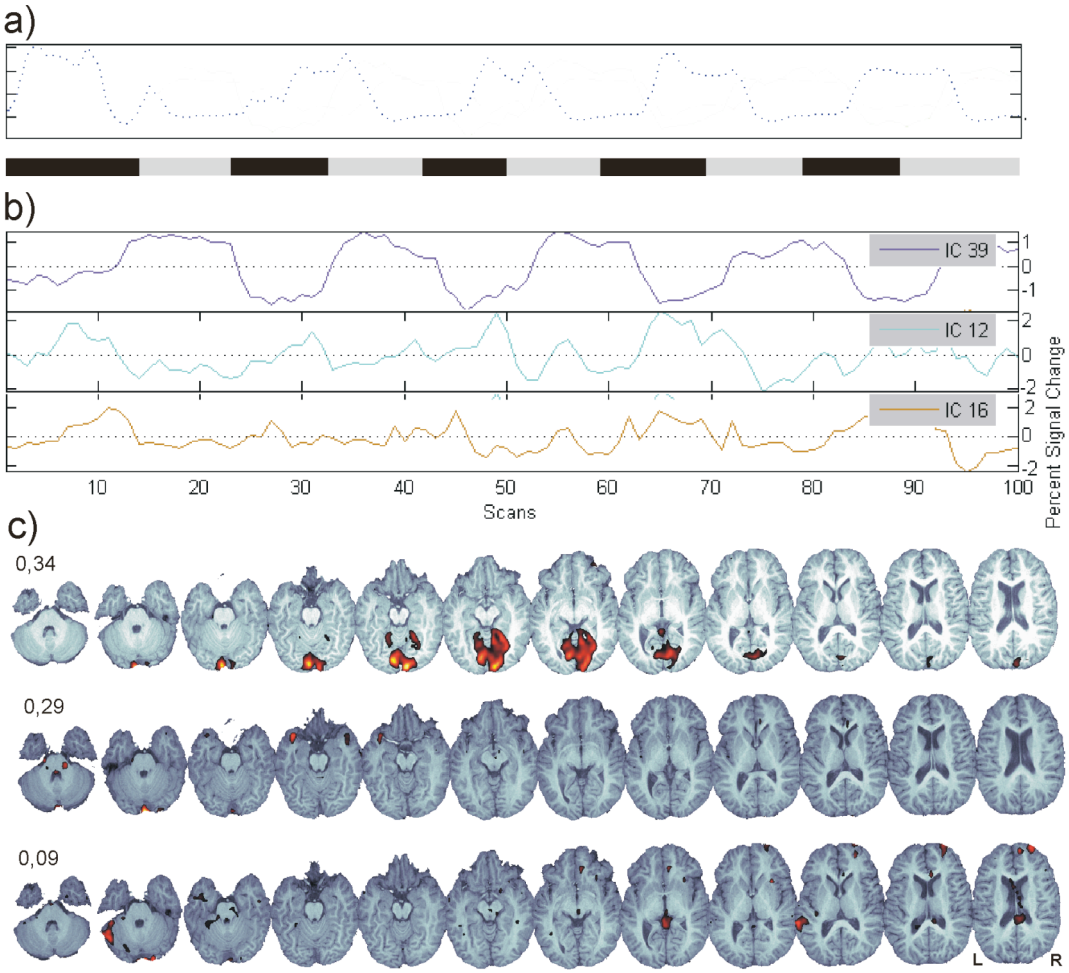

Figure 2.5.2. a) Temporal evolution of the opening and closing of the eyes (bellow: black-closed, grey-open)) and the associated amount of spike activity (convoluted with a standard gamma function), above. b) Time course of the 3 independent components more clearly correlated with the opening/closing of the eyes and with the occurrence of spikes. Component 39 is produced by visual cortex activation, while components 12 and 16 are spike-related. c) Spatial ICs, sorted by the coefficients of the multiple regression (number on the left) fitting the components to the number of spikes regressor in a), above. The images were thresholded with a Z=2.3.

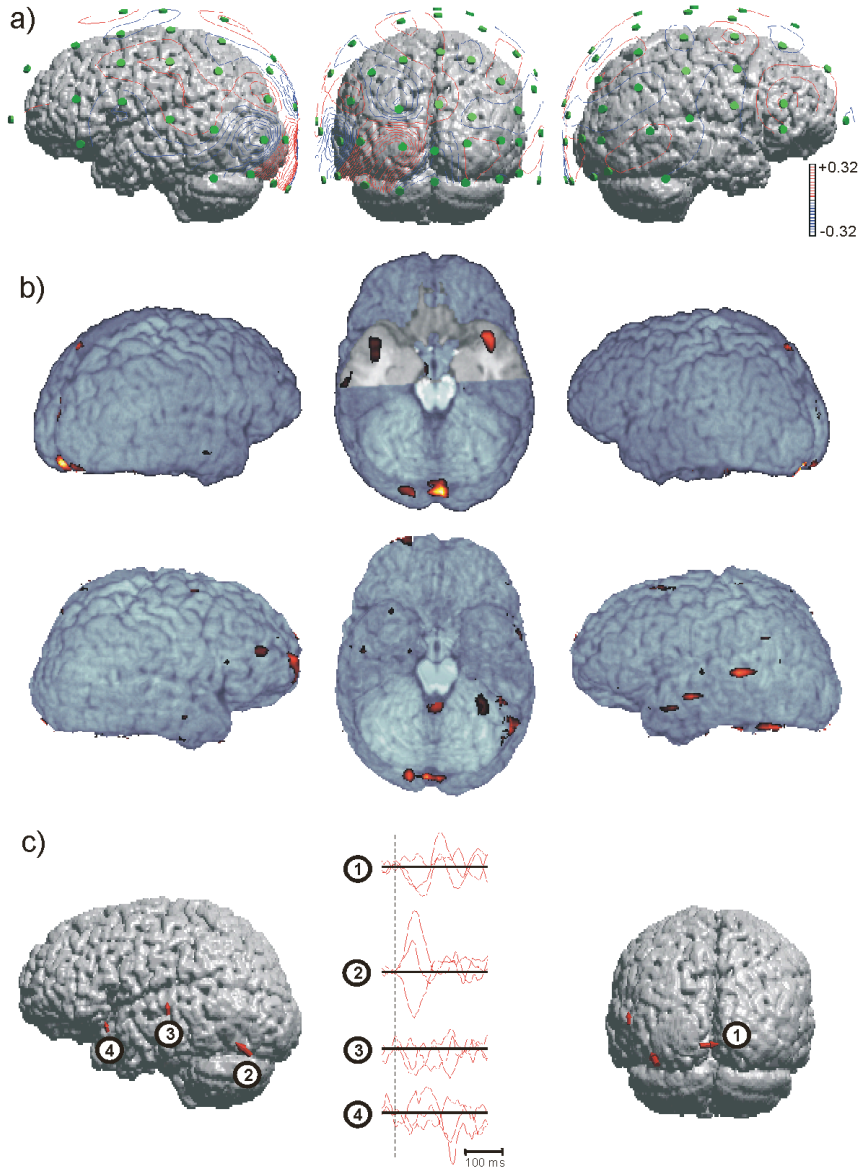

Figure 2.5.3. a) Spline Laplacian map at the peak of an average spike, represented over a 3D rendering of the patient brain. The complex distribution suggests a multifocal and extended epileptogenic area over the left occipital lobe. Red represents current sources, while blue represents current sinks (color scale bar in μV/sqm). b) 3D representation of the BOLD activation clusters co-registered with the patient brain for the two ICs spike related. The more posterior cluster of IC12 (above) and the occipital-temporal junction cluster of IC16 (bellow) are compatible with sources suggested by the Laplacian map in a), but no electrical activity is apparent near the remaining BOLD cortical clusters. c) Regional dipole seeding at the BOLD clusters allows an estimate of the temporal contribution of each activation area to the scalp average spike. The recovered activation curves (middle) suggest an origin of epileptic activity in the occipital-temporal junction (2) source and rapid spread to the nearby occipital pole (1) and temporal lobe (3 and 4).

3. EPILEPSY OF HYPOTHALAMIC HAMARTOMAS

3.1. Overview of the epilepsies associated with hypothalamic hamartomas

Hamartomas are dysplastic lesions in which the neuronal and glial cells have differentiated normally, but which have an anarchic network organization and are in general very epileptogenic (Munari et al, 1995). When connected to the hypothalamus these lesions produce a peculiar type of epilepsy associated with laughing spells (gelastic epilepsy), highly refractory to medical therapy and with an unfavorable clinical course (Berkovic et al, 1998).

This epilepsy has been the focus of interest in recent years and it has been well demonstrated that despite the often dramatic course, with multiple seizure types, multifocal spikes in the EEG, cognitive impairment and repeated status epilepticus, in the largest majority of cases there are no associated structural brain lesions besides the hamartoma. The striking resolution of all symptoms in cases where complete surgical removal of the lesion was achieved (Palmini et al, 2002) confirmed that the origin of the epileptic activity is in the hamartoma, with secondary spread to several brain areas through poorly defined propagation pathways.

Ictal SPECT studies have been able to detect a hamartoma hyperperfusion (Arroyo et al, 1997; Kuzniecky et al, 1997), while a more difuse hypometabolism was detected with PET (Cascino et al, 1993). The latter technique demonstrated predominantly areas of cortical hipometabolism likely to be associated with secondary cortical involvement of epileptic activity and of significance in relation to the progressive cognitive impairment these patients exhibit (Ryvlin et al, 2003).

Because the seizure events are brief (typically less than one minute) and few consistent ictal activity is detected in the EEG, this technique despite the good temporal resolution is too insensitive to provide a dynamical picture of epileptic origin and propagation. On the other hand the SPECT and PET techniques have the sensitivity but not the temporal resolution to contribute to clarification of the ictal dynamics.

In the following papers we present:

1. (Leal et al, 2006b) [section 3.2]

   A study of ictal events was performed, using modern techniques of blind source separation, to both extract interfering artifacts and detect the contribution of different brain areas to the seizure EEG. The proposed method of analysis improved significantly the signal to noise ratio of ictal rhythms, over the conventional visual analysis, allowing a more clear characterization of its topographic properties. Source analysis was used to recover early activating generators localized in deep brain areas, supporting a subcortical onset of seizure activity. Little spatial consistency of the localization of deep sources was present among patients.

2. (Leal et al, 2008c) [section 3.3]

   A study of ictal events using EEG and combined EEG-fMRI was performed. The fMRI clearly detected the seizure onset in the hamartoma-hypothalamus area, followed by secondary involvement of diverse deep and superficial neocortical structures. This technique was unable to distinguish the sequence of activation of the neocortical structures due to limited temporal resolution. Incorporation of the temporal information of the ictal EEG led to a dynamical model of the origin and propagation of the epileptic seizures with good spatial and temporal resolution.

3.2. Leal A, Dias AI, Vieira JP. *Analysis of the EEG dynamics of epileptic activity in gelastic seizures using decomposition in independent components*. Clin Neurophysiol 2006b; 117(7): 1595-1601.

Abstract

Objective: Gelastic seizures are a frequent and well established manifestation of the epilepsy associated with hypothalamic hamartomas. The scalp EEG recordings very seldom demonstrate clear spike activity and the information about the ictal epilepsy dynamics is limited. In this work we try to isolate epileptic rhythms in gelastic seizures and study their generators.
Methods: We extracted rhythmic activity from EEG scalp recordings of gelastic seizures using decomposition in independent components (ICA) in three patients, two with hypothalamic hamartomas and one with no hypothalamic lesion. Time analysis of these rhythms and inverse source analysis was done to recover their foci of origin and temporal dynamics.
Results: In the two patients with hypothalamic hamartomas consistent ictal delta (2-3 Hz) rhythms were present, with subcortical generators in both and a superficial one in a single patient. The latter pattern was observed in the patient with no hypothalamic hamartoma visible in MRI. The deep generators activated earlier than the superficial ones, suggesting a consistent sub-cortical origin of the rhythmical activity.
Conclusion: Our data is compatible with early and brief epileptic generators in deep sub-cortical regions and more superficial ones activating later.
Significance: Gelastic seizures express rhythms on scalp EEG compatible with epileptic activity originating in sub-cortical generators and secondarily involving cortical ones.

Introduction

Gelastic seizures are a rare type of epileptic manifestation where laughter spells occur without a concomitant sense of joy. They are usually brief (less than one minute) and can occur several times daily. Historically these seizures have been associated with hypothalamic hamartomas (List et al., 1958), and more recent invasive EEG recordings demonstrated the existence of paroxysmal activity limited to the hamartoma during such events (Munari et al., 1995). Nevertheless cases have been reported where no hypothalamic lesions could be found (Arroyo et al., 1993) and this suggested the existence of extra-hypothalamic generators.
In previous studies we used source analysis techniques of the interictal spike activity of patients with hypothalamic hamartomas to demonstrate the existence of deep generators in the neighborhood of the lesion (Leal et al., 2002) and also that the EEG scalp topography can show frontal or temporal dominance depending on the particular anatomy of the connection of the hamartoma to the hypothalamus (Leal et al., 2003).
The scalp EEG recordings during the seizures have not been very informative (reviewed in Munari et al., 2000) because no clear paroxysmal activity is usually found and the poor signal to noise ratio of such recordings has prevented more detailed analysis. Nevertheless visual inspection of ictal EEG reveals the existence of rhythmical activity in the theta-delta range which

could provide useful information on the dynamics of this type of epilepsy. In this study we perform analysis of ictal EEG recordings in patients with gelastic seizures, trying to separate true epileptic activity from artifacts and gain a deeper understanding of the dynamics and possible localizations of the epileptic generators.

Methods and subjects

Seizures of three patients with gelastic epilepsy were recorded during long-term video-EEG monitoring (12h) using setups with 32, 30 and 21 scalp gold electrodes. Clinical data is presented in table I, and has been detailed previously for patients 2 (Leal et al., 2003) and 3 (Leal et al., 2002).

The sampling rate of EEG acquisition was 256 Hz and it was filtered with a high pass filter at 0.5 Hz and a low pass at 70 Hz. All seizures were signaled by the patient or by an accompanying family member. The seizure onset time was determined by careful analysis of behavioral manifestations in the video recording. The appearance of high frequency scalp EMG activity on the EEG (Figs 3.2.1a and 3.2.2a) resulting from a characteristic sudden agitation preceding the first laughter, or EEG desynchronization with increase of fast rhythms (Fig. 3.2.3a) were additional features used to determine seizure onset.

Seizures were segmented between -30 and 30 seconds in relation to seizure onset. All lasted less than a minute and most less than 30 seconds. A total of eleven seizures were collected for patient 1 and three for each one of the two remaining patients. The segmented seizures were imported into the EEGLAB software (Delorme and Makeig, 2004) running in MatLab 6.1 (MathWorks), merged in a single dataset for each patient and submitted to Independent Component Analysis (ICA) for decomposition in independent components (Makeig et al., 2004)(appendix A). Afterward we selected the components with rhythmical activity after seizure onset (Figs 3.2.1b, 3.2.2b and 3.2.3b) which represented all rhythmic activity in the teta-delta range in the raw EEG (Figs 3.2.1a, 3.2.2a and 3.2.3a). These components were submitted to a FFT analysis and the statistically significant changes at the different frequencies were color coded to produce a graphical representation of the spectral changes induced by the seizure, a so called Event Related Spectral Perturbation (ERSP) (Makeig, 1993). Significance of the changes was quantified using a Bootstrap method (appendix A).

Source analysis was performed on the spatial component of each rhythmical activity after seizure onset, using a spherical volume conduction model to determine the localization of the generator of each scalp rhythm (Apppendix A).

Results

Seizures in the different patients showed a remarkable similarity, with early desynchronization of the EEG, which reduced in amplitude due to the disappearance of the alpha, theta and delta activities, followed seconds later by onset of slow rhythmic activity in the theta-delta frequency range. Such rhythms can be diffuse such as in patient 3 (Fig. 3.2.3a) or focalized such as in

patient 1 (Fig. 3.2.1a). A typical increase in diffuse EMG activity and also movement artifacts is seen at seizure onset (Figs 3.2.1a and 3.2.2a).

The ICA components with rhythmical activity are significantly reduced in number as compared with the number of EEG channels expressing such rhythms (Figs 3.2.1b, 3.2.2b and 3.2.3b) representing a significant convergence of information. This components express a dipolar type of distribution of the potential over the scalp (Figs 3.2.1c, 3.2.2c and 3.2.3c), suggesting that a focal source might be a good representation of the intracranial generators of such rhythms. Furthermore no significant activity of these components is observable in the 30 sec period preceding the seizure, suggesting that they represent a true ictal phenomenon (Figs 3.2.1c, 3.2.2c and 3.2.3c).

The topography of ictal rhythmical components falls in one of two categories: type 1 has polarities on opposite sides of the head, compatible with a deep source; type 2 has polarities closer together, typically in the same hemisphere, which is more compatible with superficial sources. All patients have one or more components of type 1, but only patients 1 and 3 have components of type 2.

The ERSP graphs demonstrate a clearly demarcated activity in the frequency range of 2-3 Hz, and the early onset of such activity in type 1 components supports an earlier activation as compared to the ones of type 2.

Source analysis of the different types of components leads to deep generators for type 1 and superficial ones for type 2 (Figs 3.2.1d, 3.2.2d and 3.2.3d). Adjusted dipoles for type 1 components lie in the deep frontal and Thalamus-Hypothalamus regions showing residual variances (RV) of 3%, 9% and 9-11% for patients 1, 2 and 3, respectively. Localization of type 2 dipoles is superficial in the frontal, parietal or temporal lobes and the RVs are of 5-7% for patient 1 and 20% for patient 3.

Discussion

The main result of this study is that gelastic seizures produce rhythmical activity on the scalp EEG, of probable epileptic nature and with generators in the deep subcortical regions (Thalamus/Hypothalamus) and also in cortical areas.

Gelastic seizures typically do not exhibit clear spike activity (Munari et al., 2000) and the frequent coexistence of movement and muscular artifacts makes the identification of epileptic rhythms difficult. It has historically been assumed that no relevant information can be obtained about the seizure generators from scalp ictal recordings and this fact was attributed to the focal and deep localization of such generators (Munari et al., 1995). Despite this historical background, our analysis of the raw EEG of several seizure recordings persistently revealed the existence of small amplitude rhythmical activity not attributable to artifacts (Figs 3.2.1a, 3.2.2a and 3.2.3a). Because this seems to be a seizure related rhythm we decided to explore the possibility that it contains information on the dynamics of epileptic activity in these very peculiar seizures.

The strong association with hypothalamic hamartomas (Munari et al., 2000) and the seizure disappearance after successful removal of the lesion (Cascino et al., 1993), clearly established the hypothalamus as the brain structure more strongly associated with gelastic seizures, despite the fact that they occasionally occur in patients without lesions demonstrated in Magnetic Ressonance Imaging (MRI) (Striano et al., 1999). The ability to extract information about the localization of the epileptic sources in gelastic seizures from scalp recordings, would be of value in the latter patients, as sometimes cortical generators are postulated, based on extrapolation from interictal spike activity (Munari et al., 1995).

Two of our patients have clearly defined hypothalamic hamartomas in MRI (Table I), but patient 1 has only an assimetry of the position of mammillary bodies, suggesting the existence of a small expansion of the right hypothalamus. The existence of small hamartomas has been demonstrated (Striano et al., 2002), and agrees well with the work of Sherwin et al. (1962), proving that this is an anatomical area with frequent microscopic malformations.

Our ictal EEG recordings showed the usual desynchronization, movement and EMG artifacts as well as slow wave rhythmical activity (Figs 3.2.1a, 3.2.2a and 3.2.3a). The decomposition in independent components is a technique well suited to separate the contribution of artifacts from EEG activity (Makeig et al., 2004) and the much improved signal to noise ratio, resulting from their selective removal, makes the analysis of small amplitude rhythmical activity possible. In our patients it reveals convergence of such rhythmical activity in a small number of components with distinct dipolar scalp topographies (Figs 3.2.1c, 3.2.2c and 3.2.3c). Due to the well known ill-posed character of the inverse problem in EEG, no general solution can be found to the intracranial generators of such scalp potential maps without introducing a priori properties for these generators. The dipolar distribution of the scalp potential for the components of interest in our data, suggests that a punctual source model such as the Equivalent Current Dipole (ECD) might be apropriate and provide further insight on the dynamics of ictal epileptic activity.

Inverse source analysis of rhythmic ICA components strongly suggests the presence of deep sub-cortical sources in all patients, and cortical ones in 2 out of 3 patients. ECD models have a limited power to identify the anatomical brain structures generating scalp potential patterns and these are even more pronounced when a small number of electrodes, spherical volume conduction models and single dipole models are used. Our goal in using a simple model with all the previous handicaps was to give only a rough anatomical localization, highlighting instead the dynamics of the generators of scalp slow activity. It is one of the major goals of this work to suggest that these rhythms, up to now not studied, are an epileptic activity deserving a more detailed study with optimized source analysis methods.

The occurrence of ictal delta rhythms at consistent times after seizure onset and in different events, seems to be a replicable feature across patients and in the same patient, as is shown in Figs 3.2.1c, 3.2.2c and 3.2.3c. This is also compatible with deep sources strongly attenuated and low pass filtered before their detection in scalp electrodes and agrees well with a similar trend demonstrated for interictal spikes in a previous study in patients with hypothalamic hamartoma (Leal et al., 2002). The more consistent superficial ictal generators are located in

the lobes with more consistent interictal spike activity (Table 3.2.1), which suggests a selective propagation of deep epileptic activity to particular cortical areas, frontal in patient 1 and temporal in patient 3.

The recent improvement in structural MRI allowed the demonstration of small HH in cases of gelastic seizures and other brain lesions (Palmini et al., 2005) or no lesions at all (Arroyo et al., 1997). These reports shed doubt in previous cases attributing gelastic seizures to extra-hypothalamic sources (Arroyo et al. 1993) on the basis of negative findings in MRI and the demonstration of ictal sub-cortical generators in such cases can be a further reason to carefully look for small HH.

Overall, analysis of two patients with hypothalamic hamartoma and one with a suspected hypothalamic lesion reveals the existence of ictal rhythmical activity in the scalp EEG generated in deep subcortical regions and with secondary involvement of frontal and temporal cortical areas.

Appendix A: Decomposition in independent components was performed with the INFOMAX algorithm (Bell and Sejnowski, 1995) implemented in EEGLAB (version 4.515), using 36000 frames to determine a number of ICA components equal to the number of electrodes (21, 32 and 30 for patients 1, 2 and 3 respectively).The initial learning rate was 0.001 and the process stopped when weight change was smaller than 1E-7.

The ICA components with ictal rhythmic activity on visual inspection were submitted to ERSP analysis using an FFT algorithm with a sliding window of 256 points, filtered with a Hanning window and 50% overlap. To evaluate the significance of the spectral changes we used a Bootstrap method with surrogate data generated by FFT of similar spectral windows (N=200) with onset randomized in the pre-ictal period. From the surrogate baseline distribution obtained we derived the ERSP significance level of 1% used to construct figures 3.2.1c, 3.2.2c and 3.2.3c.

Dipole fitting was done with the software Source2 (Neuroscan, El Passo), using a moving dipole in a volume conductor model of 3 spheres with conductivities of 0.33, 0.0042 and 0.33 S/m. Electrode positions were taken from their 10-20 standard position and the final representation done in a registered average brain. Confidence ellipsoids for dipole position were calculated using the method of Fuchs et al. (2004), for an average noise level of 10 μV.

Acknowledgements

The authors are grateful to Dr Jan de Munck, Elisa Vilar, Rita Pinto, Elisabete Lage and Bruno Mourão for technical support.

Table 3.2.1 - Clinical and neurophysiological data

	Patient 1	Patient 2	Patient 3
Age	6 y	8 y	6 y
Sex	M	M	M
Cog. develop.	Normal	Normal	Normal
Seizures			
Age of onset	3 y	6 y	5 y
Nausea	yes	no	yes
Vomiting	yes	no	yes
Urinary incontinence	yes	no	no
Eye deviation	yes	yes	yes
Reduced responsiveness	yes	yes	yes
Pallor	no	yes	yes
Loss of muscle tone	yes	yes	no
Duration	> 15 minutes	> 10 minutes	> 15 minutes
Seizure freq.	single event	single event	single event
MRI	Normal	Normal	
EEG	Frontal lobe spikes only	Frontal lobe spikes	Frontal lobe spikes

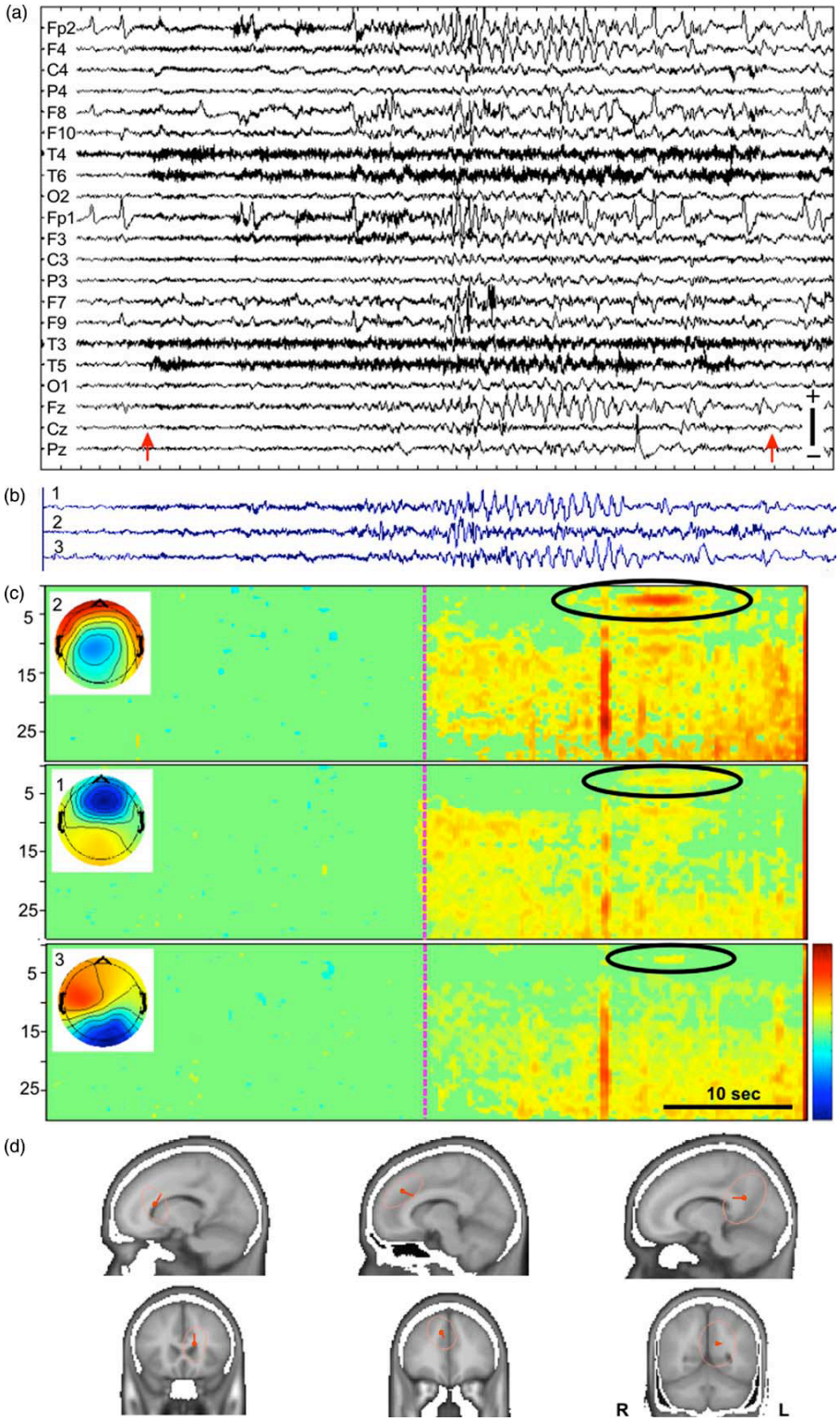

Figure 3.2.1. (a) Representative EEG of a gelastic seizure for patient 1 (arrows signal seizure onset and offset). There are no spikes, but a rhythmical delta activity is seen over the frontal electrodes (time scale in seconds, amplitude scale is 500μV). (b) Time course of ICA components with rhythmical activity during the gelastic event. (c) Event Related Spectral Perturbation (ERSP) for the three ICA components between -30 and +30 seconds centered on seizure onset, for 11 merged seizures. There is an increase at 2-3 Hz, with an early onset in component 2 (left scale in Hz, color scale -25 dB blue an +25 dB red; green is non-significant at the Bootstrap level of 1%). (d) Best fit dipole solution for components 2 (left), 1 (middle) and 3 (right), with 1 SD confidence ellipsoids (Fuchs et al., 2004). A deep localization is seen for component 2 while the others have more superficial solutions.

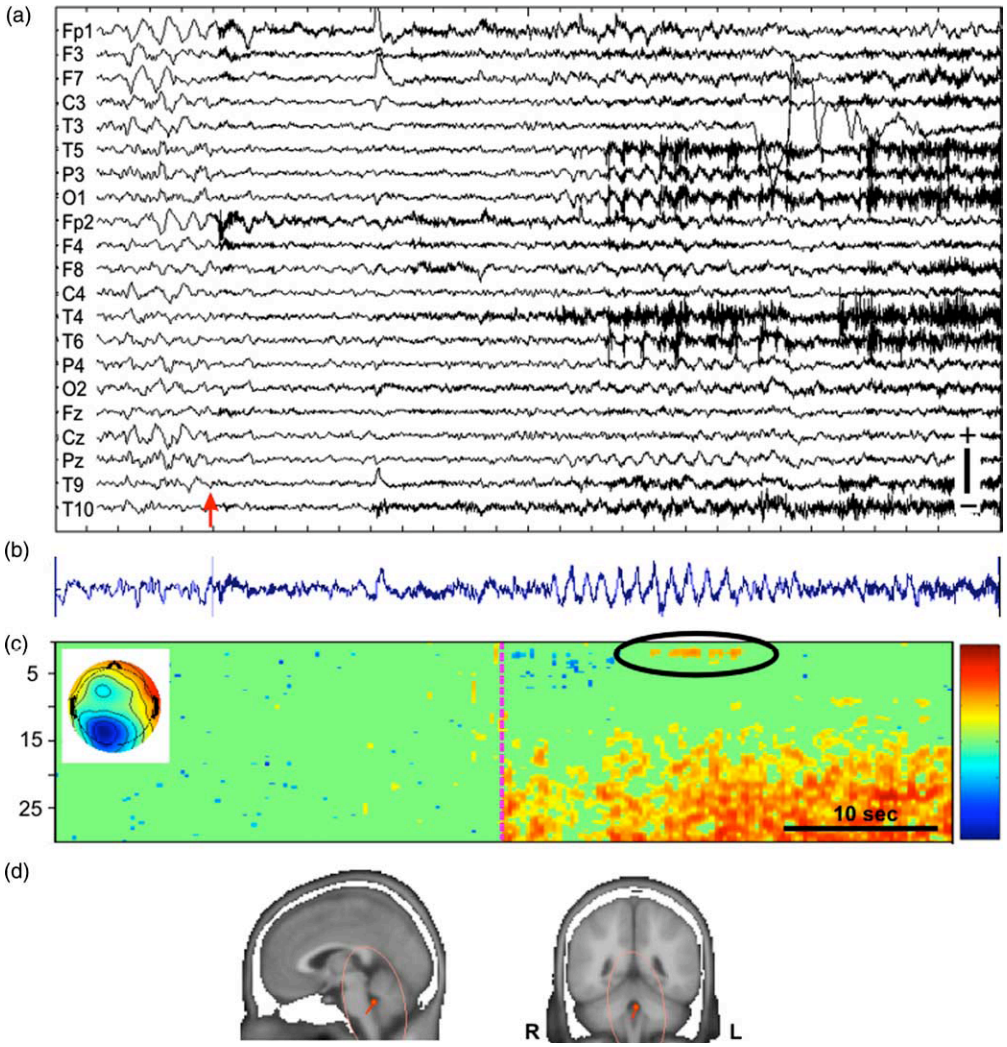

Figure 3.2.2. (a) Representative EEG of a gelastic seizure for patient 2 (arrow signals seizure onset). There are no spikes, but a diffuse rhythmical delta activity is seen. (b) Time course of the only rhythmical ICA component obtained from the merged gelastic events. (c) ERSP for the ICA component, for three merged seizures. There is an increase in the 2-3 Hz frequency a few seconds after seizure onset (scales as in Fig. 1). (d) Best fit dipole solution for the ICA component, with the 1 SD confidence ellipsoids. A deep posterior localization is obtained.

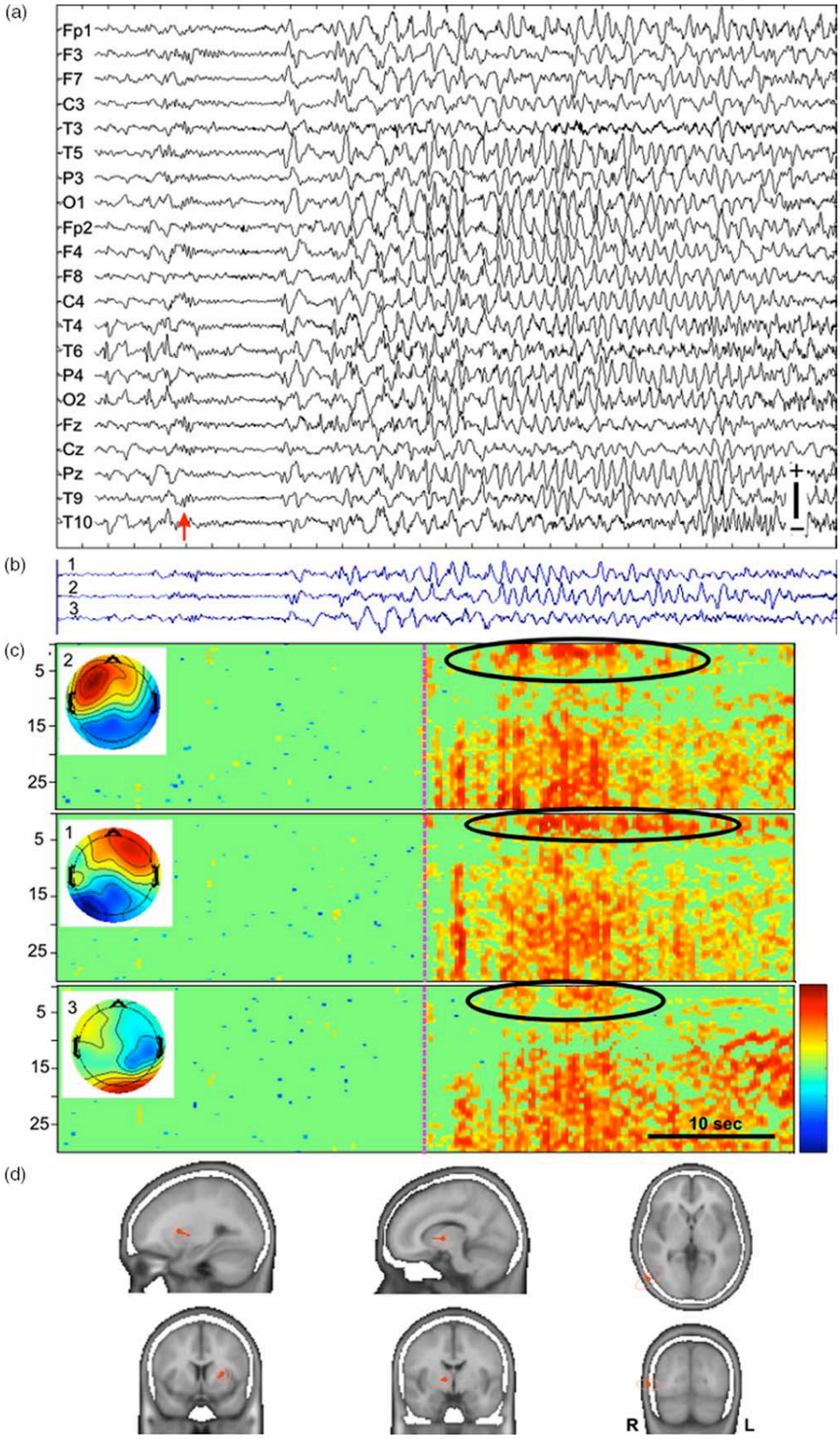

Figure 3.2.3. (a) Representative EEG of a gelastic seizure for patient 3 (arrow signals seizure onset). There are no spikes, but a diffuse rhythmical delta activity is seen. (b) Time course of the three rhythmical ICA components obtained from the merged gelastic events. (c) ERSP for the ICA components, for three merged seizures. There is an increase in the 1-2 Hz frequency a few seconds after seizure onset, firstly in component 2 (scales as in Fig. 1). (d) Best fit dipole solution for the ICA components. A deep localization is obtained for components 2 and 1, and a superficial one for component 3.

3.3. Alberto Leal, José P Monteiro, Mario Forjaz Secca, Constança Jordão. *Functional brain mapping of ictal activity in Gelastic Epilepsy associated with Hypothalamic Hamartoma: a case report*. Epilepsia 2008c, in press.

Abstract

Hypothalamic hamartomas (HH) have been demonstrated as the cause of gelastic epilepsy, both by intracranial electrodes and functional imaging. The neocortex becomes secondarily involved, through poorly characterized propagation pathways. The detailed dynamics of seizure spread have not yet been demonstrated due to the limited spatial-temporal resolution of available functional mapping.

We studied a patient with epilepsy associated with HH and gelastic epilepsy. Simultaneous EEG and fMRI of several seizure events were obtained, with BOLD activation of the hamartoma and left hemisphere hypothalamus, hippocampus, parietal-occipital area, cingulate gyrus and dorsal-lateral frontal area. Integration of regional BOLD kinetics and EEG power dynamics strongly suggest propagation of the epileptic activity from the HH through the left Fornix to the temporal lobe and later through the cingulate fasciculus to the left frontal lobe.

The EEG/fMRI method has the spatial-temporal resolution to study the dynamics of seizure activity, with detailed demonstration of origin and propagation pathways.

Keywords: hypothalamic hamartoma; epilepsy; BOLD; EEG-fMRI; seizure; functional mapping

Introduction

Epilepsy associated with Hypothalamic Hamartomas (HH) has generated a lot of interest since the work of Berkovic et al (1988), which described the peculiar features of the syndrome. More recent studies have demonstrated the intrinsic epileptic character of the Hamartoma (Munari et al, 1995; Kuzniecky et al, 1997), as well as the excellent outcome of cases where surgical removal was possible (Nishio et al, 1994; Fohlen et al, 2003; Rosenfeld et al, 2007). Overall these data suggest that the epileptic activity in these patients originates in the Hamartoma, propagates to the hypothalamus, and afterwards to the neocortex.

Several studies in children with the syndrome have reported a restricted participation of neocortical areas in epileptic activity (Mullati et al, 2003; Ryvlin et al, 2003), with epileptic spikes involving predominantly the frontal or temporal areas, most often in a single hemisphere (Leal et al, 2003). This and the monotonous character of clinical seizure manifestations in the first years of the syndrome suggest the existence of selective and stable propagation pathways from the Hamartoma to the neocortex, which nevertheless remain poorly characterized. The PET and SPECT brain mapping techniques can show the participation of the Hamartoma in the seizure events (Arroyo et al, 1997; Kuzniecky et al, 1997), as well as the neocortical dysfunction (Ryvlin et al, 2003), but their lack of temporal resolution does not allow insight into the dynamics of the propagation. The scalp EEG has the required time resolution but it is insensitive to the activity in

the Hamartoma and deep neocortical structures in general, and therefore has not allowed a complete characterization of the ictal events (Leal et al, 2006). A full understanding of the dynamics of the epileptic activity throughout the seizure will require brain mapping methods with both good spatial and temporal resolution and enough sensitivity to detect activity onset in the Hamartoma.

The technique of simultaneous recording of the EEG and fMRI (EEG/fMRI) promises to combine the good temporal resolution of the EEG with the good spatial resolution of the fMRI (Ritter and Villringer, 2006) and it can be used to record both interictal and ictal activity. In this study we apply this method to a case of epilepsy associated with HH and very frequent seizure events.

Methods and subjects

Clinical data

A first-born 2-year old boy was referred for neurophysiological evaluation of refractory epilepsy at the program of Surgery for Epilepsy of the Hospital Center of West Lisbon. The parents were not consanguineous, no history of epilepsy was uncovered and the only pathology present was Rheumatoid Arthritis in the father, a condition he had had since the first decade of life.

The seizures were detected at the age of 9 months, and consisted of brief episodes in which he suddenly stopped playing, remained “frozen” for a few seconds, and presented a few eyelid rhythmic movements more apparent in the right eye and also a fearful facial expression. During the event he had a variable lack of responsiveness to stimulation. The events lasted less than 20 seconds and could occur hourly, but with time they became more prolonged (up to 30 seconds) and more frequent (more than 5 per hour) and sometimes the patient exhibited an inappropriate laughter.

An EEG was performed at the age of 21 months, which revealed normal background activity and abundant left frontal lobe spikes. One month later he had a Magnetic Resonance brain scan, which showed a large (grade IV in the Delalande and Fohlen (2003) classification) HH, with no other structural abnormalities (Fig. 3.3.3c).

Motor and cognitive developments were normal at age 24 months and the neurological examination did not demonstrate pathological features.

Several anti-epileptic drugs were tested without any significant seizure reduction.

Methods

An indication for surgery of epilepsy was established and the following complementary studies were obtained with this goal in mind, after informed consent was obtained from the parents.

The patient was submitted to a 24-h video-EEG recording using 27 electrodes in the scalp (10-20 plus Fpz, Oz, F9/10, M1/2 and P9/10). The high- and low-pass filters were set at 0.5 and 70 Hz, and the sampling rate was 256 Hz.

Two types of interictal spikes with distinct scalp topographies were identified visually, one with maximum over the left occipital lobe and another with left frontal maximum (Fig. 3.3.1a). Each type was averaged after detection using a template match algorithm implemented in the software BESA 5.1 (MEGIS, Graefelfing, Germany). More than 60 seizure events were recorded in the 24-h period, with ictal activity localized in the left hemisphere (Fig. 3.3.1b). The EEG of seizures without significant artifacts (N=55) was cut in epochs from minus 10 to plus 20 seconds after onset and submitted to Event Related Synchronization / Desynchronization (ERS/ERD) of the full bandwidth, using the Scan 4.3.3 software (Neuroscan, El Paso, USA). The percentage reduction in mean global field power (MGFP) as compared to the 10-second period preceding seizure onset was determined, using bipolar derivations to evaluate the relative dynamics of the major left hemisphere lobes (Fig. 3.3.3a). A FFT analysis using an Event Related Spectral Perturbation (ERSP) (Makeig, 1993) plot in the band 1-70 Hz was obtained for each lobe, using as statistical measure of significance a Bootstrap test where the baseline for comparison of spectral responses was the distribution obtained by calculating the spectra of epochs with 200 points, randomly chosen in the pre-seizure period. 1000 resamples were used for the distribution, and a significance level of 1% was used. This analysis was done using the EEGLAB software package (Delorme and Makeig, 2004).

The patient was also submitted to a brain MRI (1.5T, Cvi/NVi GE scanner), with acquisitions of: 1. A volumetric T1 Spoiled Gradient Recovery (SPGR) 3D sequence, with an in-plane resolution of 0.94x0.94 mm and a slice thickness of 0.6 mm; 2. Six sequences of simultaneous EEG and fMRI, with a continuous acquisition of 150 EPI brain volumes per session, composed of 24 slices per volume (in-plane resolution 3.75x3.75 mm, slice thickness 5 mm) obtained with a Repetition Time (TR) of 2.275 s. The EEG was recorded with a 37-channel DC amplifier through a MR-compatible MagLink system (Neuroscan, El Paso, USA). The EEG artifacts induced during EPI acquisition were removed with the Scan 4.3.3 software and the cleaned signal visually inspected to detect the rhythmical spike activity typical of seizure events (Fig. 3.3.1b). A design matrix was obtained after convolution of the previous activations with a standard Gamma Hemodynamic Response Function (HRF), which was used to obtain the ictal BOLD activation using the GLM theory as implemented in the FSL 4.0 software package (Smith et al, 2004).

Results

The interictal EEG demonstrated a persistent slow wave abnormality over the left temporal-occipital area, associated with abundant spike activity with occasional contra lateral propagation. Abundant spike activity also occurred over the left hemisphere frontal lobe. A more detailed analysis of the scalp potential topography at successive moments in time from spike onset to spike peak revealed spatial stability of the posterior spikes while the frontal ones changed significantly in configuration (Fig. 3.3.1a), from an occipital bipolar potential at spike onset to a bipolar frontal potential at spike peak. This suggests that the frontal lobe spikes are mixed events resulting from the overlap of the scalp potentials induced by early activating occipital generators and late activating frontal ones.

The effect of Sevoflurane anesthesia on the spike activity recorded inside the scanner was minimal, as judged by visual inspection, and both interictal spikes and ictal rhythms could be easily recognized (Fig. 3.3.1b).

The BOLD response associated with the occurrence of left occipital spikes consisted only of scattered deactivation clusters (Fig 3.3.2a, above), involving the left temporal and parietal lobes, as well as the frontal lobes on both hemispheres. No significant response was obtained near the hypothalamus.

More than 60 seizures were recorded in the 24-h video-EEG monitoring, with durations of 20 to 30 seconds and almost exclusive involvement of the left hemisphere. The ictal EEG pattern was very monotonous and consisted of early diffuse desynchronization, followed by the build up of spike activity over the left occipital and temporal areas and in the later stages of the seizure over the frontal area (Fig. 3.3.1c). Occasionally secondary propagation of spike activity to the right temporal areas occurred. The clinical manifestations of the seizures consisted of slowing of motor activity, variable interruption of consciousness, eyelid rhythmic movements with bilateral nistagmus to the right and occasionally gelastic laughter.

The EEG ictal recordings were so consistent that we could merge the MGFP of a large number of artifact free events (N=55) to establish the recovery of each brain area after the initial desynchronization (Fig. 3.3.3a). Because this recovery was due to the build up of spike activity (Fig. 3.3.1c), a dynamical sequence of the epileptic activity of different cortical areas in the seizure event was obtained, with data supporting an early participation of the temporal and occipital lobes and a late frontal lobe involvement. The parietal lobe remained desynchronized throughout the seizures.

Multiple clusters of BOLD seizure activation were obtained with fMRI, from a single session in which 5 seizure events occurred, involving not only the Hamartoma but also the hippocampus, occipital lobe, cingulate gyrus and dorsal-lateral frontal lobe in the left hemisphere (Fig. 3.3.2a, bellow). An analysis of the seizure-induced deactivation revealed only cerebellum and right temporal clusters. The overall fit of the BOLD signal from the significant voxels and the seizure events convoluted with the standard HRF is shown in Fig. 3.3.2b. The BOLD temporal evolution showed a trend to an earlier and more pronounced activation (seizures 1, 3 and 4 of Fig. 3.3.2c) of the hamartoma-hypothalamic area, as compared with the cortical clusters. No temporal lead of a particular cortical brain area could be demonstrated (Fig. 3.3.2c).

The integration of the temporal evolution of ictal spike activity over the left hemisphere major lobes (Fig. 3.3.3a) with the spatial areas of BOLD activation in each lobe (Fig. 3.3.2a, bellow), suggests a dynamical model of seizure propagation (Fig. 3.3.3b). After onset in the hamartoma (stage 1), the epileptic activity propagates to the left hippocampus and occipital lobe (stages 2) and later to the left cingulate gyrus and dorsal-lateral frontal lobe (stage 3).

Discussion

The brief seizures associated with variable interruption of consciousness and inappropriate laughter seen in our patient are compatible with the characteristics of ictal events reported in the

literature for patients with HH (reviewed in Nguyen et al, 2003). The interictal EEG demonstrates multifocal spikes commonly seen in HH cases, but a clear predominance over the frontal and occipital-temporal areas in the left hemisphere is seen, demonstrating a selective and restricted neocortical involvement. A similar tendency of spike activity to concentrate in the frontal and temporal lobes has been noted in a series of HH patients (Mullati et al, 2003; Ryvlin et al, 2003) and correlated with the anatomical characteristics of the connection of the lesion to the Hypothalamus (Leal et al, 2003). The more detailed analysis of the average spikes in our study (Fig. 3.3.1a) suggests a stable synchronous configuration of posterior brain generators for the occipital-temporal spikes from spike onset to peak (right), while the frontal ones demonstrate asynchronous generators with distinct spatial distribution, with early posterior brain activation (-40 and -30 ms before spike peak, left). This data, together with the prominent slow wave activity over the left occipital-temporal area, suggests the existence of a posterior left hemisphere focal neocortical dysfunction with strong epileptic activity, which leads secondarily to frontal lobe involvement.

The EEG ictal recordings exhibit a very consistent pattern of early diffuse desynchronization, followed by the appearance of rhythmic sharp waves and spikes over the left temporal and occipital lobes and only later a build up of rhythmical spike activity over the left frontal lobe (Fig. 3.3.1c). The large number of ictal events allowed a quantitative determination of this trend by evaluating the signal power in representative bipolar channels (Fig. 3.3.3a). If it is assumed that the seizures originate in the Hamartoma, as suggested by the early BOLD activation of the hamartoma-hypothamalus area, then the EEG data support an early cortical activation of the left occipital-temporal area, which later spreads to the frontal lobe on the same hemisphere. This hypothetical temporal sequence agrees with the previously analyzed dynamics of interictal spikes and supports the existence of very selective propagation pathways for the epileptic activity in our patient.

Our EEG-fMRI recordings were obtained under light Sevoflurane anesthesia, using the conventional clinical protocol for small children at the MRI center. At these concentrations Sevoflurane is not expected to reduce significantly the epileptic activity (Komatsu et al, 1994), as was observed in our case where both interictal and ictal spikes were comparable, both in morphology and topography, to the data obtained without anesthesia. The later observation suggests that the recorded activity is the usual epileptic activity of the patient and not some pharmacologically induced abnormal rhythm.

The BOLD response associated with the occurrence of posterior spikes did not present any significant brain activation, but widespread deactivation clusters were apparent in the left temporal and parietal areas, as well as over the frontal lobes (Fig. 3.3.2a, above). No significant BOLD response was apparent from the hypothalamus, most likely because the spike activity recorded in the scalp does not faithfully reproduce the dynamics of activation of the Hamartoma, preventing the generation of an appropriate design matrix.

In contrast with the interictal events, the seizures produced several clusters of activation but restricted deactivations (Fig. 3.3.2a, bellow). A significant (95% confidence level, corrected for

multiple comparisons) increase in the BOLD signal was apparent in the left Hypothalamus, Hippocampus, Occipital lobe, anterior Cingulate Gyrus and dorsal-lateral frontal lobe at seizure onset (Fig. 3.3.2b). The analysis of the BOLD dynamics of the voxels belonging to regions of interest (ROI) in the previous structures (Fig. 3.3.2c) shows a trend to an early and more pronounced activation of the left Hypothalamus-Hamartoma cluster, but no clear separation of the time response of each of the several cortical areas was possible, most likely due to the limited temporal resolution of our activation paradigm. This prevents the determination of the cortical temporal dynamics of ictal activity from fMRI data alone.

The combination of the brain areas with BOLD activation with the sequential temporal evolution of ictal spike activity, leads to a model of seizure propagation from the Hamartoma to the left Hypothalamus, followed by the posterior temporal-occipital area and later the frontal lobe. Such a model suggests that propagation of epileptic activity through major white matter projection pathways is taking place, the left Fornix (Hypothalamus to posterior temporal area) and the left cingulate fasciculus (from posterior temporal to frontal lobe). These pathways overlap the circuit of Papez (Papez, 1937), which is a main crossroad to important physiological rhythms such as the limbic Theta activity (Kocsis et Vertes, 1994).

The Mammillary bodies are able to support epileptic activity (Raftopoulos et al, 2005) and in the few cases of epilepsy of these structures, the epileptic discharges were associated with temporal lobe activity in the scalp EEG (Rijckevorsel et al, 2005). This suggests the existence of a selective pathway for seizure propagation between the two brain areas, most likely through antidromic conduction in the Fornix formation. The anatomical projection of this pathway to the posterior hippocampus can also explain the focal slowing and abundant interictal spike activity over the left occipital and posterior temporal lobes.

An alternative projection pathway for seizure spread has been suggested by Kahane et al (2003) in their patients studied with depth electrodes. They documented an early propagation from the HH to the cingulate gyrus in 3 patients, which they propose to be mediated through a mamillo-thalamo-cingulate pathway. In contrast to those cases, in our patient the involvement of the frontal lobe was always limited to the late phases of the seizure EEG event, and was always preceded by left side occipito-temporal spike activity. This suggests that the alternative pathway of the Papez circuit through a mamillo-hippocampus-cingulate provides a better explanation of our data.

The present study highlights with good spatial resolution the brain areas involved in seizure expression in a patient with epilepsy associated with HH. The integration of the early BOLD activation of the hamartoma-hypothalamus with the temporal information of cortical activity provided by the EEG, leads to a dynamical model of seizure spread through well defined anatomical pathways, which can help the planning of surgical therapy.

Acknowledgements

The authors are grateful to Daniel Carvalho and Rita Pinto for technical support in the neurophysiological recordings and to Cristina Menezes for help in the imaging. We confirm that

we have read the Journal's position on issues involved in ethical publication and affirm that this report is consistent with those guidelines.

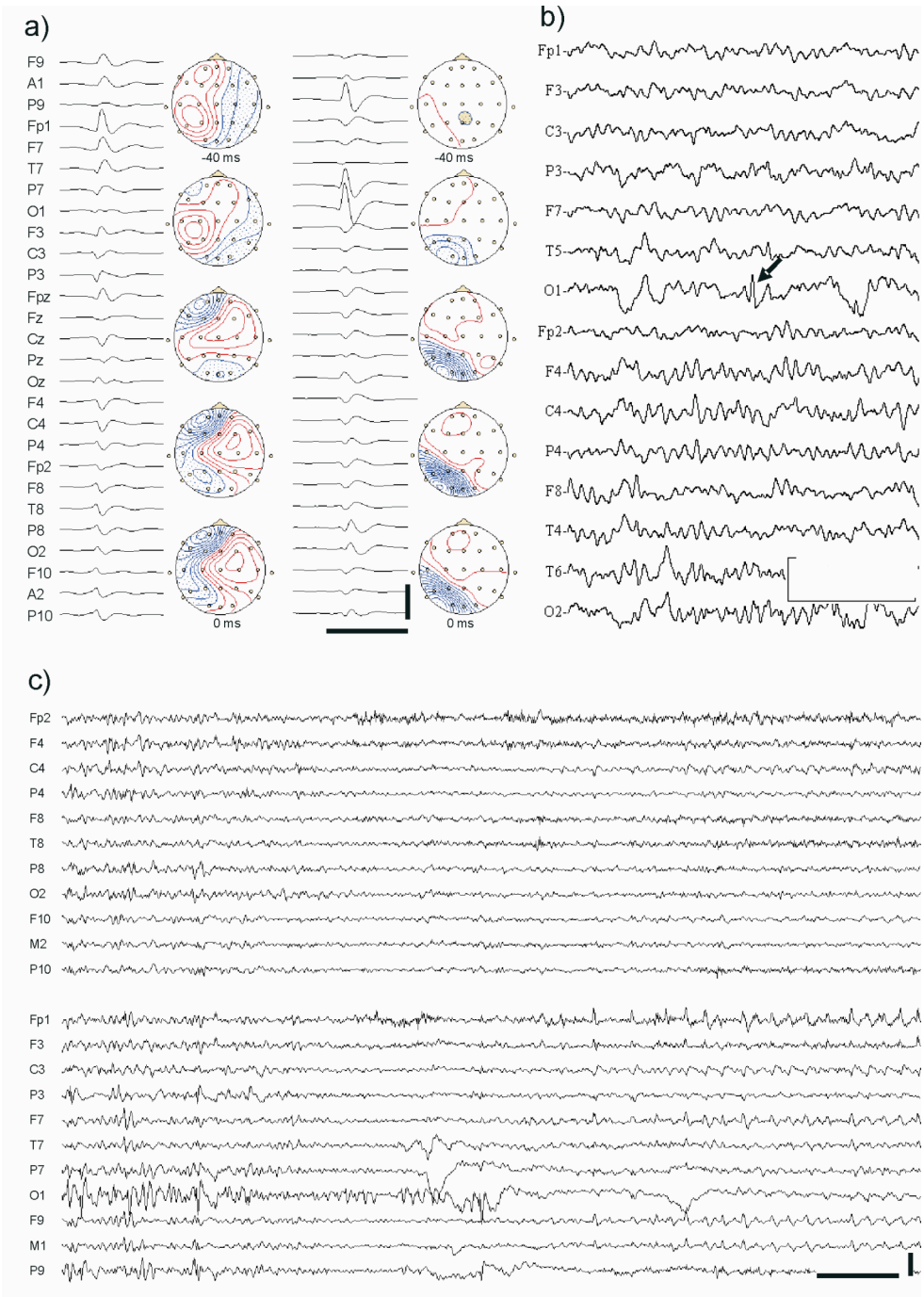

Fig. 3.3.1 a) Average interictal spikes for the frontal (left, N=81) and occipital (right, N=503) classes. The scalp instantaneous potential maps at 10 ms intervals from spike onset (top) to spike peak (bottom) demonstrates a stable topography for occipital spikes, but a prominent change through time for the frontal spikes. (Vertical scale is 300 μV and the horizontal 0.5 s). b) Sample of EEG under Sevoflurane anesthesia, allowing easy recognition of normal background rhythms and spikes (arrow). Vertical scale 500 μV, horizontal scale 1 s. c) Sample of ictal EEG, with diffuse desynchronization at seizure onset (arrow), followed by spike build up at the left occipital electrode (O1) and later in the temporal electrodes (F9 and M1) and frontal ones (Fp1). Vertical scale 500 μV and horizontal scale 2 s.

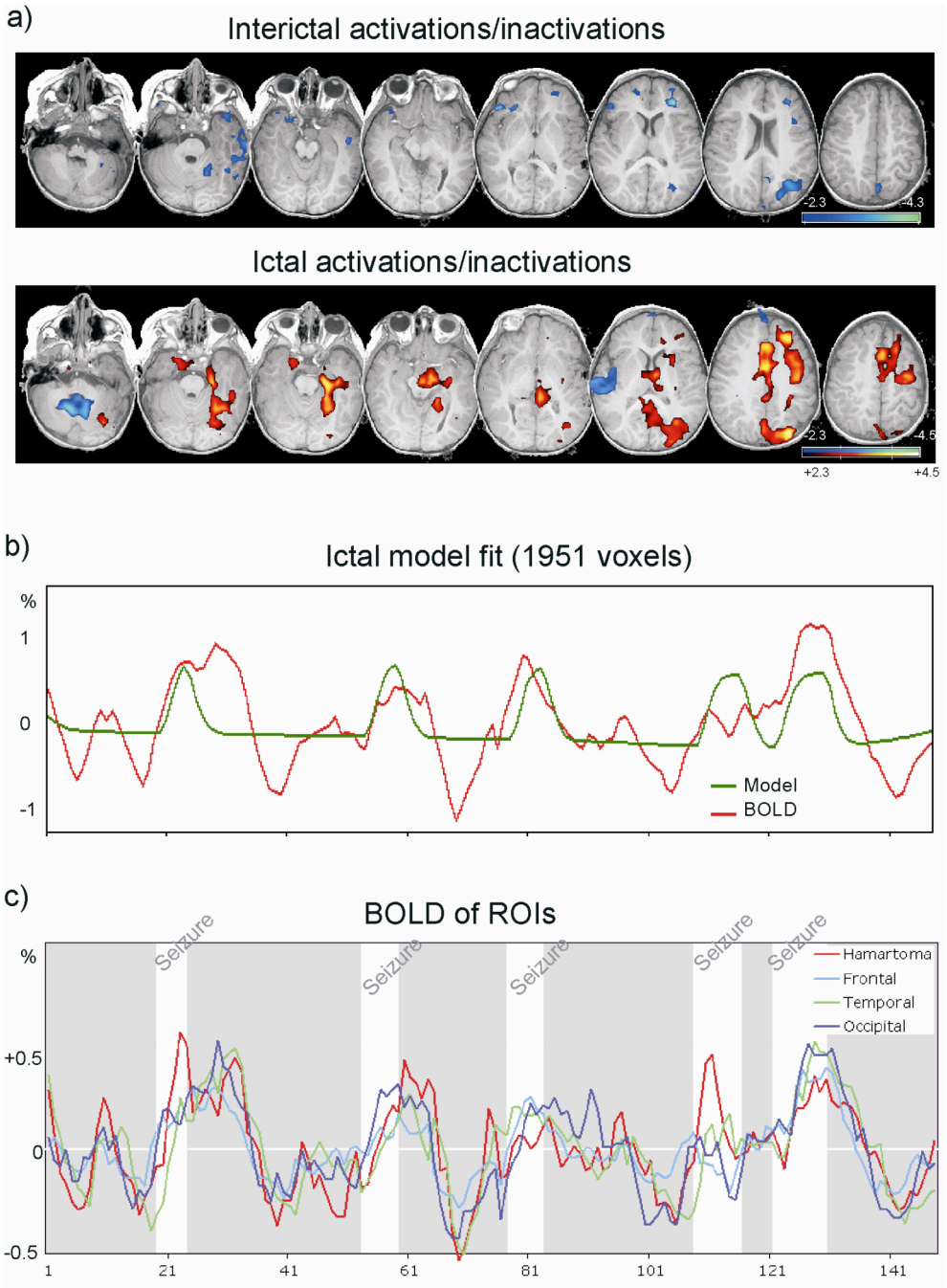

Fig. 3.3.2 a) BOLD activation (red) and deactivation (blue) for the interictal spikes (above) and ictal events (bellow). Only deactivations are apparent for interictal spikes. The seizures induce a significant activation of the Hamartoma as well as several cortical areas in the left hemisphere. (Color scales in Z scores). b) Temporal evolution of the BOLD signal for the 1951 voxels found to be significantly activated (red). In green is represented the model obtained by convoluting the seizure events with a standard Gamma HRF. c) Variation of the BOLD signal in a EEG/fMRI sequence with 5 seizures (white). In 3 of the events a strong and early activation of the Hamartoma cluster is seen (brown), while no dynamical difference can be found between the other clusters. Horizontal numbers are the volumes in the sequence.

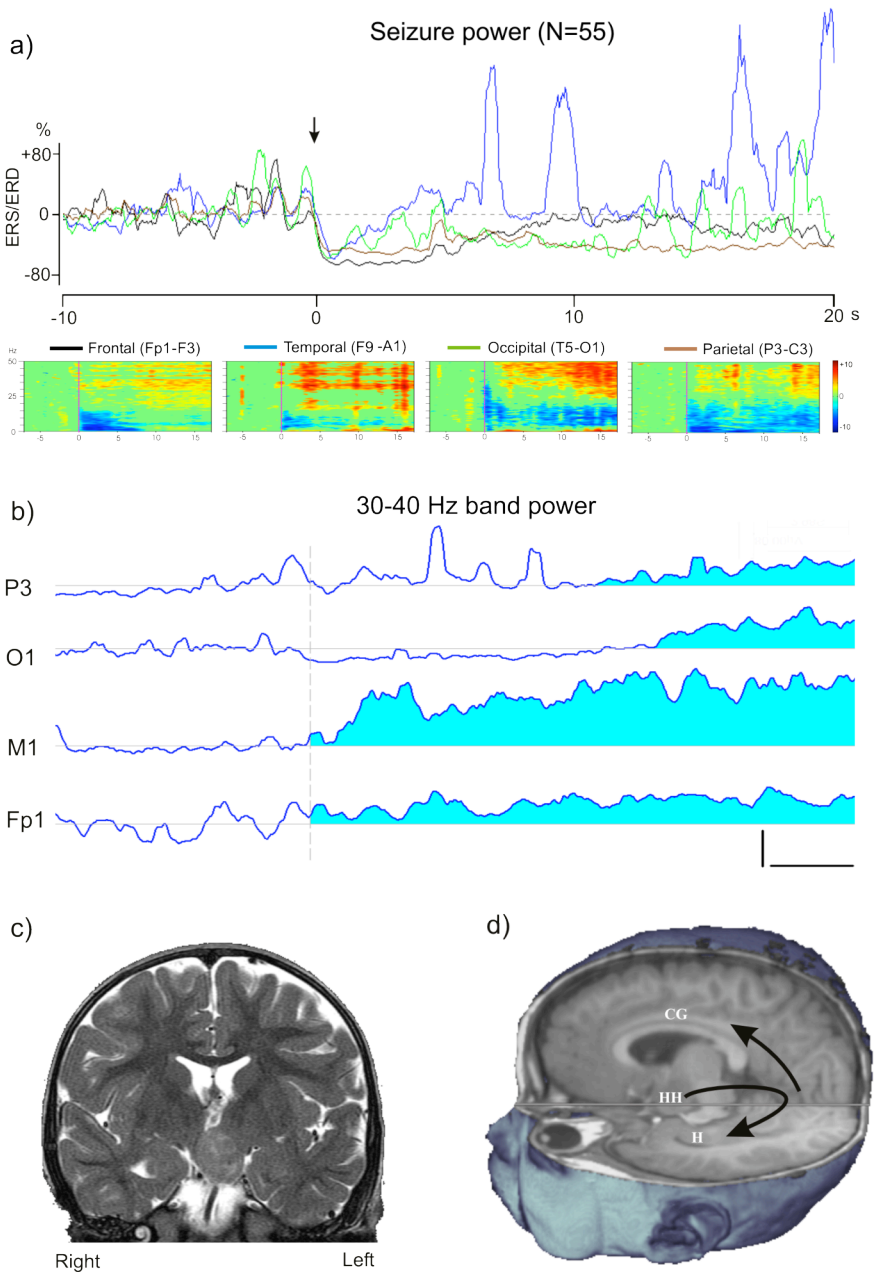

Fig. 3.3.3 a) Mean Global Field Power (MGFP) variation from 10 seconds before to 20 seconds after seizure onset (t=0), for bipolar derivations representing activity in the major lobes of the left hemisphere. Diffuse desynchronization at seizure onset, at frequencies below 20 Hz, is followed by an early recovery in the left temporal lobe and a late one in the frontal lobe. The ERSP plots (below) demonstrate no significant (Bootstrap test with a 1% significance level) recovery of desyncronization in the occipital or parietal lobes. A significant and persistent increase in power in a 30-40 Hz band after seizure onset occurred in the temporal and frontal lobes. b) The dynamics of the power in the 30-40 Hz band at representative monopolar electrodes (average reference), demonstrates an earlier activation of the left temporal area, as compared with the left frontal one. Vertical scale is 80% and horizontal scale 3 s. c) Coronal fast spin echo T2 sequence, demonstrating the selective connection to the left hemisphere and the large dimensions of the hamartoma. d) Diagram illustrating the main propagation stages postulated for the dynamics of seizure events. Seizure activity propagates from the hamartoma to the left hypothalamus, followed by spread to the posterior hyppocampus through the Fornix, and later to the cingulate gyrus through the cingulate fasciculus.

4. FOCAL EPILEPSIES EVALUATED FOR SURGERY

4.1. Overview of focal symptomatic epilepsies

Focal epilepsies are commonly refractory to pharmacological therapy and seizure events persist with significant impact on the quality of life of the patients. Some of these cases are considered for surgery of epilepsy after extensive clinical, neurophysiological, imagiological, psychological and psychiatric studies. The very detailed information obtained and the importance of being able to understand the origin and dynamics of epileptic activity is one of the more demanding task put on both, clinical neurophysiology and brain imaging. Because these patients are operated, a careful comparison of the results after surgery with the models obtained before surgery is a unique opportunity to test the validity of the functional brain mapping methods.

A great importance is given to the EEG and to the clinical manifestations of the seizure events in localizing the origin and secondary propagation of the epileptic activity (reviewed in Foldvary, 2001). The poor spatial resolution of both methods makes this a very difficult exercise and often invasive intracranial EEG recordings have to be made (reviewed in Hamer and Morris, 2001). The availability of new brain mapping methods with good spatial and temporal resolution offers hope that they can make a significant contribution to the selection for surgery of epilepsy.

Two papers were written on the subject:

1. (Leal et al, 2008a) [section 4.2]
   A group of 4 patients with refractory focal epilepsy and brain lesions secondary to Tuberous Sclerosis, undergoing evaluation for surgery of epilepsy were studied with independent component analysis (ICA) of both the interictal and ictal EEGs. The ICA was very successful in removing artifacts and in isolating the ictal rhythmic activity that later was submitted to source analysis. A clustering of solutions for the different ictal events around a single lesion among the several present in each patient was apparent. In the three successfully operated patients, removal of that lesion resulted in a seizure-free outcome. The interictal analysis did not provide a consistent picture in this respect. We conclude that modern EEG analysis allows the extraction of significant information from ictal EEG recordings, which traditionally have been difficult to analyze due to the bad signal to noise ratio.

2. (Leal et al, 2008d) [section 4.3]
   A group of 12 patients with focal epilepsy undergoing evaluation for surgery of epilepsy was submitted to both a high-resolution (64 channel) EEG and simultaneous EEG-fMRI recordings. A comparison of the localization of BOLD clusters projected in the superficial cortex and of the superficial EEG maps of interictal spikes was done. A further correlation with the structural lesions present in some patients was performed. BOLD activation was obtained in 75% of the cases, and in general multiple clusters were present. The EEG results revealed the advantage of using both the average and laplacian methods to improve localization. In the cases with no structural lesion the

convergence of the BOLD and EEG localization provides an important source of information.

4.2. Leal A, Dias AI, Vieira JP, Moreira A, Távora L, Calado E. *Analysis of the dynamics and origin of epileptic activity in patients with Tuberous Sclerosis evaluated for surgery of epilepsy*. Clin Neurophysiol 2008a; 119(4): 853-861.

Abstract

Objective: The epilepsies associated with the Tuberous Sclerosis Complex (TSC) are very often refractory to medical therapy. Surgery for epilepsy is an effective alternative when the critical link between the localization of seizure onset in the scalp and a particular cortical tuber can be established. In this study we perform analysis of ictal and interictal EEG to improve such link.
Methods: The ictal and interictal recordings of four patients with TSC undergoing surgery for epilepsy were submitted to independent component analysis (ICA), followed by source analysis, using the sLORETA algorithm. The localizations obtained for the ictal EEG and for the average interictal spikes were compared.
Results: The ICA analysis of ictal EEG produced consistent results in different events, and there was good agreement with the tubers that were successfully removed in 3 of the 4 patients (one patient refused surgery). In some patients there was a large discrepancy between the localization of ictal and interictal sources. The interictal activity produced more widespread source localizations.
Conclusions: The use of ICA analysis of ictal EEG followed by the use of source analysis methods in 4 cases of epilepsy and TSC was able to localize the epileptic generators very near the lesions successfully removed in surgery for epilepsy.
Significance: The ICA analysis of ictal EEG events may be a useful add-on to the tools used to establish the connection between epileptic scalp activity and the cortical tubers originating it, in patients with TSC considered for surgery of epilepsy.

Introduction

Tuberous Sclerosis (TS) is one of the most common neuro-cutaneous syndromes and the patients very often have pharmacoresistant focal epilepsy (Holmes et al, 2007). These epilepsies are usually associated with complex and multi-focal spike activity in the scalp EEG that leads to the false impression that several brain areas are producing seizure activity and so these patients were formerly not considered for surgery (Jansen et al, 2007). It became apparent in recent years that interictal spikes are a poor predictor of the localization of seizure onset, and many patients have consistent seizure onset foci and can benefit from a surgical procedure, despite having the previous complex interictal pattern (Perot and Weir, 1966; Bebin et al, 1993).
The selection process remains nevertheless difficult because of the complex and variable temporal characteristics of the EEG and ictal behavioral manifestations. In this setting it becomes important a better understanding of the relationship between ictal and interictal activity, in order to select wisely the good surgical candidates.

We propose a strategy of study favoring ictal EEG analysis, combining Independent Component Analysis (ICA) and source analysis, to establish the critical connection between EEG scalp recordings and the underlying brain lesions.

Methods

Four consecutive patients from the Pediatric Neurology Department of Hospital Dona Estefânia with the diagnosis of Tuberous Sclerosis (TS) and epilepsy refractory to medical treatment were included in the present study. The patients were being considered for surgery of epilepsy and the neurophysiological and brain imaging data were obtained with this goal in mind.

All patients underwent long-term video-EEG recordings, using 19 (patients 2 and 4) or 27 (10-20 plus $F_{9/10}$, $T_{9/10}$, $P_{9/10}$, Fp_z and O_z, for patients 1 and 3) gold electrodes glued to the scalp with colodium. The sampling rate was 256 Hz and a band pass of 0.1-70 Hz was used. Electrode positions were measured using the method of De Munck et al (1991) for patients 1 and 3 and were obtained from standard positions for the 10-20 system for patients 2 and 4.

The MRIs were obtained using clinical protocols that included in all cases T1 volumetric sequences allowing reconstruction of the brain anatomy and co-registration with the electrodes in the scalp.

The interictal spikes were divided in topographical classes using visual inspection by an experienced clinical neurophysiologist (AL). For each topography a representative spike was selected and used to perform a template based automatic search for similar spikes using the BESA 5.1 software (MEGIS, Graefelfing, Germany). The detected spikes were averaged (N=15 to 40) and submitted to source analysis.

The ictal recordings were processed (three per patient) using the EEGLAB toolbox (Delorme and Makeig, 2004) and methods detailed elsewhere (Leal et al, 2006). Briefly, the EEG was epoched from -20 to 30 s, with zero time at seizure onset. A decomposition in independent components (ICs) using the Infomax algorithm (Bell and Sjenoswsky, 1995; Makeig et al., 1997) was performed and the ICs expressing rhythmical activity after seizure onset, were selected for source analysis of their spatial component.

Source analysis for the averaged interictal spikes and the selected ictal ICA components was done with the sLORETA software package (Pascual-Marqui, 2002), available at *http://www.unizh.ch/keyinst/NewLORETA/LORETA01.htm*.

Clinical data

The patients included in this study have been studied repeatedly at our department with video-EEG to document uncontrollable partial seizures (Table 4.2.1). In all of them we were convinced that a single onset zone for the epileptic fits was present, despite the variable EEG features and clinical manifestations of the seizures along time.

Patient 1 started at an early age (2 months) with motor seizures involving the right face and arm, which lasted 1-3 minutes and on average occurred 15-20 times daily. The early video-EEG study at age 3 months, demonstrated focal interictal spikes with phase reversal on bipolar

montages over C3 (Fig. 4.2.1c, left) and several seizure events with clear onset in the same electrode (Fig. 4.2.1a). Later studies at ages 8 and 10 months confirmed the same ictal onset, despite a more difficult EEG analysis due to increased low frequency activity and decreased amplitude of the epileptic rhythm. Interictal activity demonstrated multifocal spikes (Fig. 4.2.1c, right). The MRI presented a left frontal lesion involving the lower gyrus, which was interpreted as the probable epileptogenic tuber (Fig. 5.2.1e).

Patient 2 also had an early onset of epileptic seizures, which consisted of episodes of interruption of consciousness lasting for several seconds mainly in the morning period. They occurred daily and repeatedly, in burst that could last for 1 to 2 hours and were followed by several hours of confusion. Severe behavioral problems became apparent with attention deficits, lack of social skills and repeated episodes of aggression to his school companions. The repeated evaluation with video-EEG and long-term ambulatory EEG allowed us to identify a consistent ictal rhythm over the right occipital area (Fig. 4.2.2a), while the interictal spikes were multifocal, with a more consistent focus over the right temporal electrodes (Fig. 4.2.2c, left). The comparison of the ictal activity and the MR imaging implied the large dysplastic lesion over the right temporal and occipital cortex as the originator of the seizures (Fig. 4.2.2e).

Patient 3 demonstrated clinical and EEG features very similar to the ones of patient 1, with early onset of partial motor seizures involving the right arm and associated with ictal onset in the C3-F3 electrodes (Fig. 4.2.3a), reproducible in three studies. An associated tuber was found in the lower gyrus of the left frontal lobe (Fig. 4.2.3b). The patient's mother refused surgery.

Patient 4 started with partial motor seizures involving the left arm at the age of 1 year. The episodes occurred 5-10 times daily and were associated with a fast EEG ictal rhythm with onset in the right frontal lobe (Fig. 4.2.4a). The interictal activity was multifocal but more consistent in the frontal lobe electrodes (Fig. 4.2.4c, left). Several small tubers could be identified over the right frontal lobe in the MRI (Fig. 4.2.4e).

Patient 1 was operated at our hospital, while patients 2 and 4 were operated at another institution.

After surgery all patients remain seizure-free. In patient 1 there was a clear improvement in the cognitive development and communication skills. Patient 2 demonstrated a striking reduction in the behavioral disturbances, with improved attention and social integration. In patient 4 no problems in behavior were detected either before or after surgery.

Results

All patients expressed multifocal interictal spikes in the scalp EEG, but a clearly dominant type (the most frequent one) was always present, with consistent morphology and dipolar topography (Figs 4.2.1c, 4.2.2c, 4.2.3c and 4.2.4c, left). For most patients (1, 3 and 4) there was lobar concordance between the most dysplastic brain area and the localization of the phase reversal of the dominant spikes in bipolar montages. The sources obtained from these averaged interictal spikes were localized in the lobe with the largest tuber for all patients with the maximum sLORETA statistic score near the interface between the dysplastic and normal

brain tissue (Figs 4.2.1b, 4.2.2b, 4.2.3b and 4.2.4b). Other spike topographies were associated with very distinct localizations for their generators (Figs 4.2.1b, 4.2.2b, 4.2.3b and 4.2.4b), which overall provide little consistency in defining the epileptic brain area in a given patient from interictal recordings.

The ictal paroxysms showed a very similar topographic pattern to the one of the dominant interictal spikes in patients 3 and 4 (Figs 4.2.3b and 4.2.4b), but a different topography in the remaining patients (Figs 4.2.1b and 4.2.2b). The scalp distribution of seizure activity remained stable in different seizures and the ictal semiology was compatible with the lobar localization of the EEG rhythmic activity (Table 4.2.1).

The decomposition of the ictal EEG by ICA produced one or two rhythmic components synchronous with the raw scalp signal (Figs 4.2.1a, 4.2.2a, 4.2.3a and 4.2.4a). The sources obtained from these ICs demonstrated a close spatial relationship with the largest tubers in all four patients (Figs 4.2.1b-c, 4.2.2b-c, 4.2.3b-c and 4.2.4b-c). These ictal sources showed spatial consistency in different seizure events.

In the three cases successfully submitted to surgery the interictal sources were localized in the neighbourhood but outside the resection volume (Figs 4.2.1d, 4.2.2d and 4.2.4d) and at the interface between the normal and most dysplastic area for the patient not operated. The ictal sources were also predominantly located at the interface between the most dysplastic brain areas and the normal brain. The ECoG performed before cortical resection in patient 1 revealed abundant spikes in the brain surrounding the tuber, but not in the girus containing it. This suggests that the lesion is not an intrinsic generator of interictal spikes, which more likely originate in the adjacent cortex.

Discussion

The main conclusion of our work is that the source analysis of ictal rhythms in patients with epilepsy associated with TS produces consistent results in different seizure events, with a close spatial relationship with the brain area removed in successful surgery for epilepsy. This contrasts with the complex and multifocal interictal spike activity typical of these patients, which makes it very difficult to build a consistent picture of the epileptic activity dynamics from this type of recordings. In some cases, such as in our case 2, there is a significant spatial separation between ictal and interictal sources, which makes it unreliable to extrapolate which brain area is originating the seizures from interictal activity alone.

In clinical neurophysiology the analysis of ictal EEG, which is of fundamental importance for the selection of patients for surgery of epilepsy, has lagged behind the analysis of the interictal spikes (Jansen et al, 2005; Iida et al, 2005; Kamimura et al, 2006; Sperli et al, 2006) mainly due to the poorer signal to noise ratio (SNR). Several aditional factors contribute to this, but the more important ones are the movement and EMG artifacts induced by the ictal behavioral manifestations and also the dynamic character of the epileptic activity which spreads to various brain areas using complex and poorly understood pathways. Furthermore the usual methods of improving the SNR such as averaging and frequency filtering are not very effective in this

setting. The introduction of blind source separation methods such as ICA (Makeig et al, 1997) and spatial filtering offers a much more promising way to improve the SNR, which is a requirement for the use of more advanced methods of analysis.

The power of ICA decomposition of the EEG to identify and remove movement artifacts is well established (Makeig et al, 1997; Urrestarazu et al, 2004) and has been confirmed in our study. The high amplitude and temporal evolution of such components makes their identification easy and their removal allows a more detailed inspection of seizure activity. In our patients the observation of the artifact-free EEG revealed that the rhythmic activity present in the seizure was also present in the remaining ICs. In order to study the ICs specificaly related to the ictal events we selected the rhythmical components demonstrating synchronous activity with the rhythms in the raw EEG (Fig 4.2.1a, 4.2.2a, 4.2.3a and 4.2.4a). This procedure reduced the ictal data to a restricted number of ICs (1 or 2), whose temporal pattern of activation matched the rhythms that in the original EEG were widespread in the scalp, producing a significant convergence of information. The fact that the scalp maps of these ICs have dipolar topography further suggests that focal and fixed sources may be good models for these generators of interest.

The ICA analysis provides a robust method to overcome the two main limitations of ictal analysis: it allows separation and selective elimination of artifacts which in general have very distinct temporal dynamics from the intrinsic epileptic activity; and also separates the contribution of epileptic activity from distinct brain areas which lead to significant volume conductor mixing in the scalp potentials. Previous attempts to do source analysis of ictal events with spatio-temporal dipoles restricted the sudy to seizures with few artifacts and good signal to noise ratio, such as temporal lobe seizures (Assaf and Ebersole, 1997). Lantz et al (2001) attempted to address more representative neocortical epilepsies using microstate segmentation of the EEG to obtain snapshots of the intracranial generators throughout the event. This method does not correct for the problem of volume conductor mixing of concomitant activation of different sources which might be present (such as in the events of figs 4.2.1a and 4.2.4a) and is potentially misleading.

In order to gain insight on the intracranial localization of the generators of the IC patterns seen in the scalp, we adopted the sLORETA algorithm (Pascual-Marqui, 2002), which has good localizing capabilities for focal sources (Wagner et al, 2004). The method provides a smooth distribution of statistical scores in the volume space, with a maximum at the source localization. Anatomical constraints to the volume space can be used, for example restricting the solution space to the cortical volume as in our study, and this further improves the localization of sources while remaining compatible with the physiology.

The interictal spike activity in our patients is multi-focal, but in all a dominant topography could be identified which produced sources in the neighborhood of the epileptogenic lesions. This agrees with the results of Seri et al (1998), which also have been able to recover sources near frontal lobe tubers in cases of TSC and frontal lobe spikes. Nevertheless, in 2 out of 4 patients there was a discrepant topography and corresponding source localization between the two

types of epileptic activity, with results suggesting that the ictal analysis leads to new and spatially more consistent information as compared to the analysis of interictal spikes only.

The surgical results in our cases were good and give support to the suggestion from previous studies implicating the most dysplastic brain areas as the usual area of origin of ictal activity (Bebin et al, 1993). Two major obstacles stand in the way to surgery in these patients: one is the usually complex and variable interictal spike activity that seldom points unambiguously to a particular brain area; the other is the change in the ictal behavioral manifestations along time due not to new epileptic foci but to different propagation patterns of the epileptic activity from the epileptic focus. In our opinion achieving a good case selection for surgery is critically dependent on demonstrating a consistent pattern of ictal activity in the EEG in several seizures and eventually at different ages. Only then can we be confident that a single focus might provide the explanation to the epilepsy of a given patient. In this strategy the convergence of information offered by ICA ictal analysis, complemented with source analysis techniques, seems a promising tool in the pre-surgical study of patients with TS and epilepsy.

Acknowledgements

The authors are grateful to Daniel Borges, Adilia Seabra, Daniel Carvalho, Elisabete Lage and Rita Pinto for technical support and to Dr. Jan the Munck for comments on the manuscript.

Table 4.2.1 - Clinical and neurophysiological data

	Patient 1	Patient 2	Patient 3	Patient 4
Age	23 months	8 years	3 years	3 years
Sex	M	M	M	F
Cog. Develop.	Normal	Delayed	Delayed	Normal
Epilepsy				
Age of onset	2 months	2 months	3 months	1 year
Seizure type	Partial motor (right arm/face)	Partial complex (lasting seconds)	Partial motor (right arm)	Partial motor (left arm clonus)
Seizure freq.	15-20 daily	5-10 daily	10-20 daily	5-10 daily
MRI (largest lesion)	Left inferior frontal gyrus	Right Occipital-Temporal area	Lower left frontal lobe	Right superior frontal lobe
EEG				
Interictal	Multifocal spikes dominant in C3	Multifocal spikes dominant in T4-T6	Multifocal dominant in C3-F3	Multifocal spikes dominant in C4-F4
Ictal	Focal seizures from C3-F3	Rhythmical sharp waves in O2	Rhythmical spike-wave in C3-F3	Rhythmical slow waves in F4-Fp2
Source analysis				
Interictal	Source in left lateral frontal lobe	Source in right temporal lobe	Source in superior left frontal lobe	Source in superior right frontal lobe
Ictal	Sources in left lateral frontal lobe	Source in right parietal lobe	Source in superior left frontal lobe	Source in superior right frontal lobe
Surgery	Frontal lobe lesionectomy	Tempor.+Occip. lesionectomy	Refused	Right frontal lesionectomy
Outcome	Seizure free(6m)	Seizure free(1y)		Seizure free (1y)

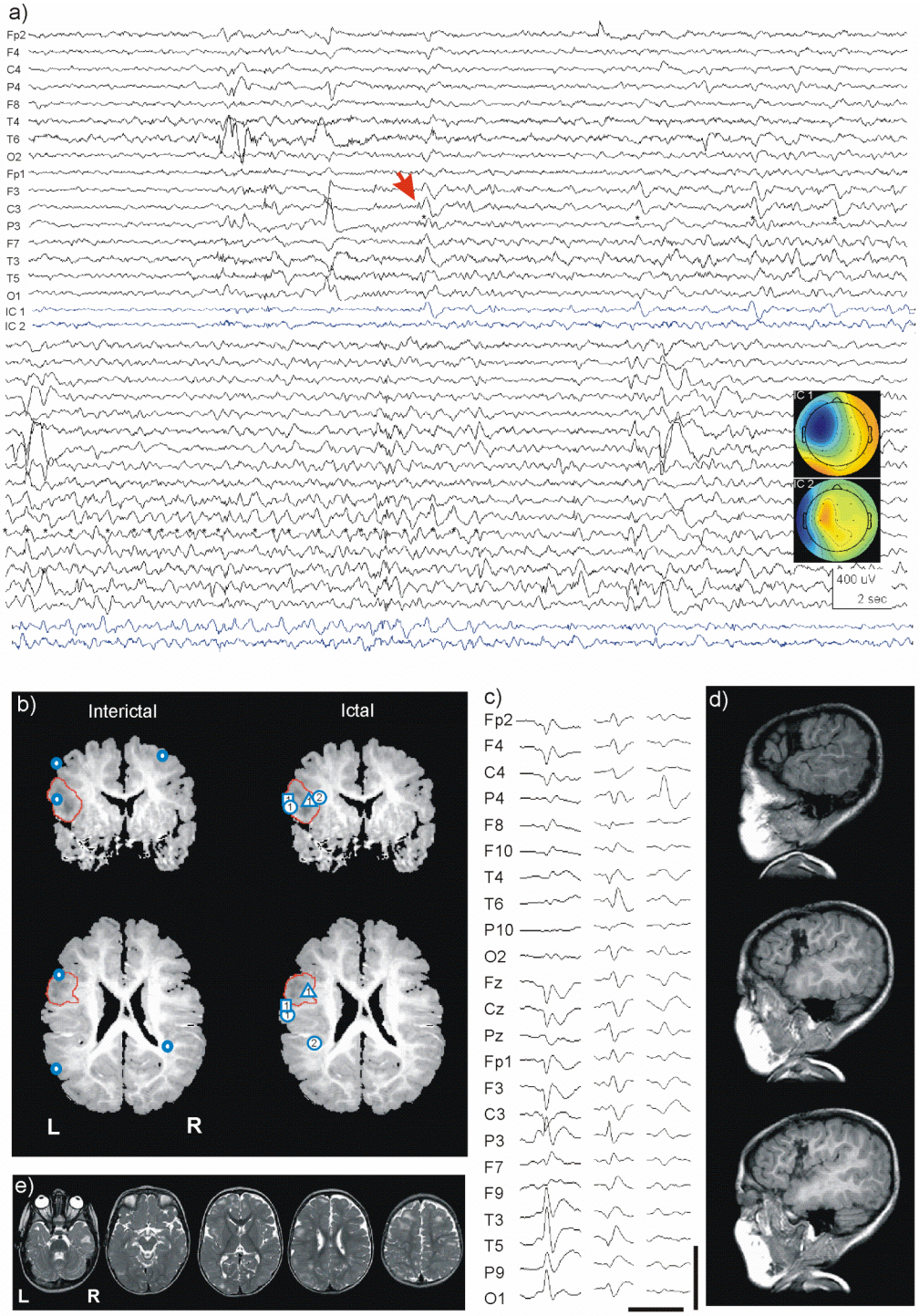

Figure 4.2.1. (a) Seizure event for patient 1, with onset of EEG rhythmical activity in electrodes F3-C3 (arrow and asterisks) and the two ICs demonstrating synchronous activation (IC1 and IC2). In the right is shown the topography of the two ICs, which have a dipolar distribution over the scalp, (vertical scale is 400 μV and the horizontal scale 2 s). (b) Source analysis with the sLORETA method. Projected on the MRI plane with the suspected tuber is represented the interictal maximum for the averaged interictal spikes (circles, left) and for three ictal events (circles, square and triangle on the right). The solutions are localized in the interface between the lesion and normal brain. When more than one IC is present per seizure, they are numbered). (c) Average interictal EEG spikes with the dominant one on the left (horizontal scale 200 ms, vertical scale 100 μV). (d) MRI after successful surgery of epilepsy, demonstrating removal of the tuber. (e) T2 sequence to demonstrate the various tubers in patient 1.

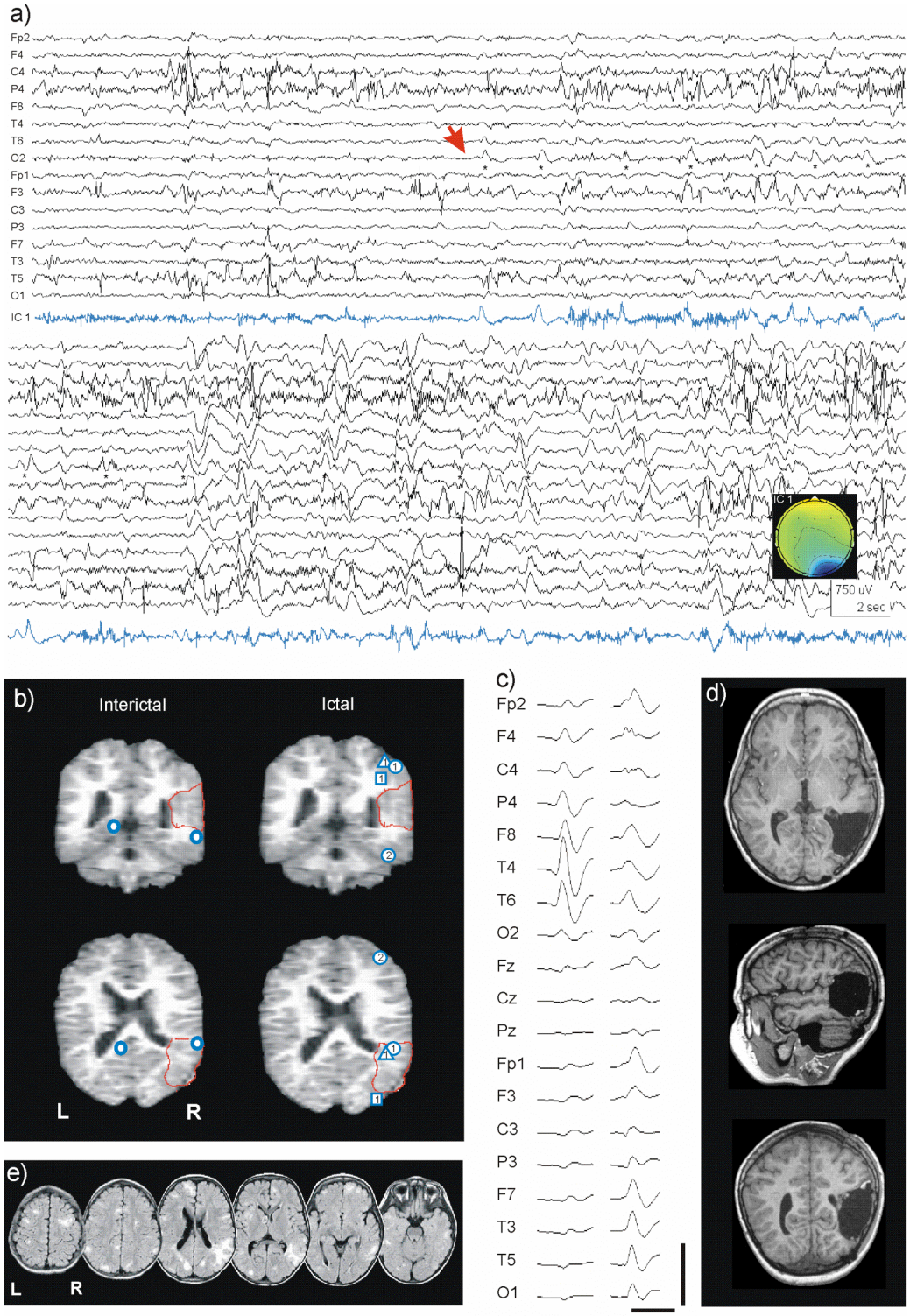

Figure 4.2.2. (a) Seizure event for patient 2, demonstrates onset of rhythmical activity in the electrode O2 (arrow and asterisks). This activity was recovered by a single IC, with maximum over the right posterior areas (below, right), (vertical scale 750 μV and the horizontal scale 2 s). (b) sLORETA results for the averaged interictal spikes (left) and for the ictal events (right). There is a large spatial difference between the two solutions. (c) Average EEG spike (horizontal scale 300 ms, vertical scale 100 μV). (d) MRI after successful surgery for epilepsy. (e) MRI sequence demonstrating the multiple tubers in this patient.

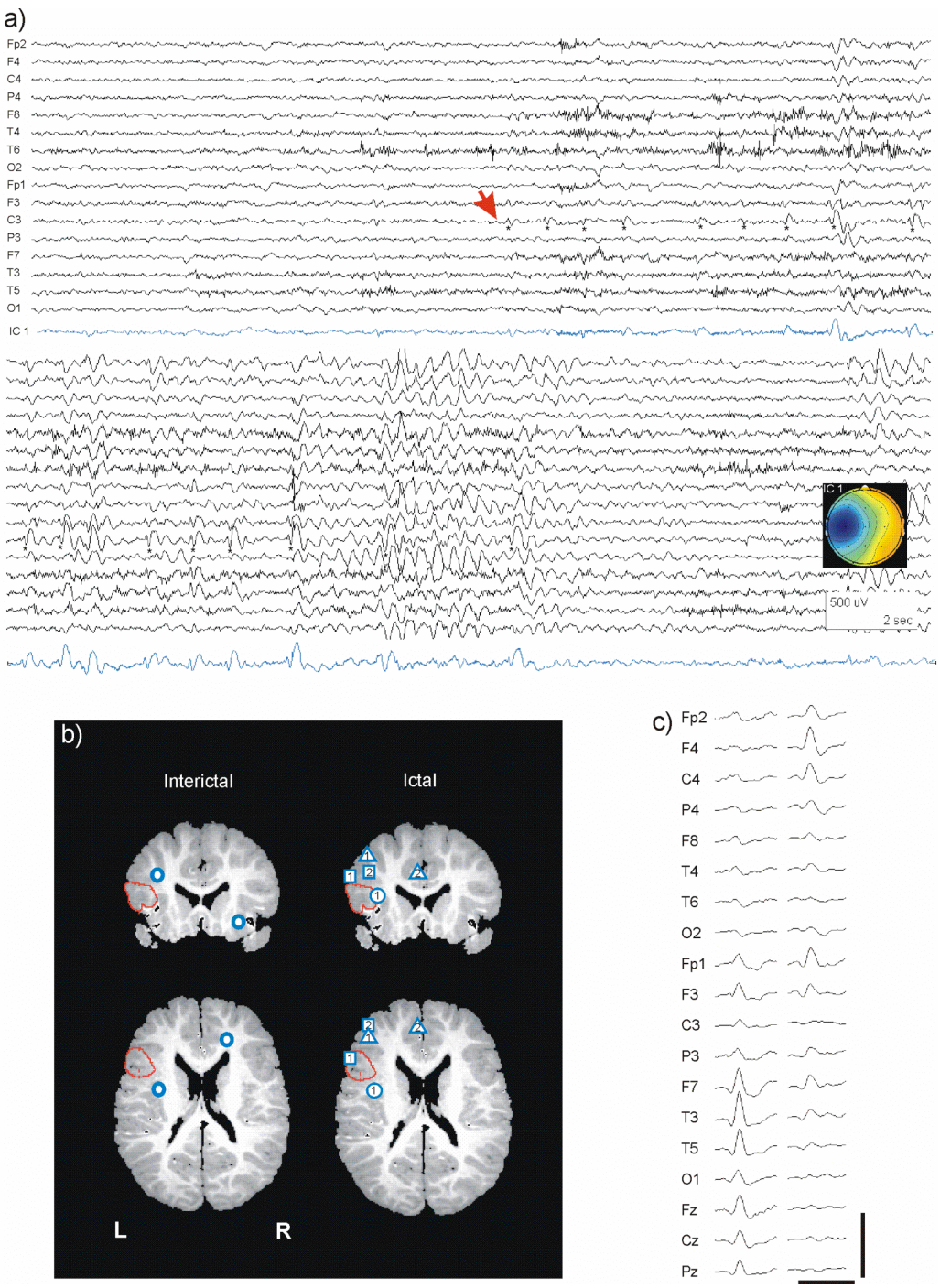

Figure 4.2.3. (a) Seizure event for patient 3, demonstrating onset of rhythmical activity in electrode C3 (arrow). This activity was recovered by a single IC (bellow, right), (vertical scale 500 μV and the horizontal scale 2 s). (b) sLORETA results for the averaged interictal spikes (left) and for the ictal events (right). There is partial spatial overlap of the generators for the two types of epileptic activity. (c) Average EEG spikes (scales as in fig 2).

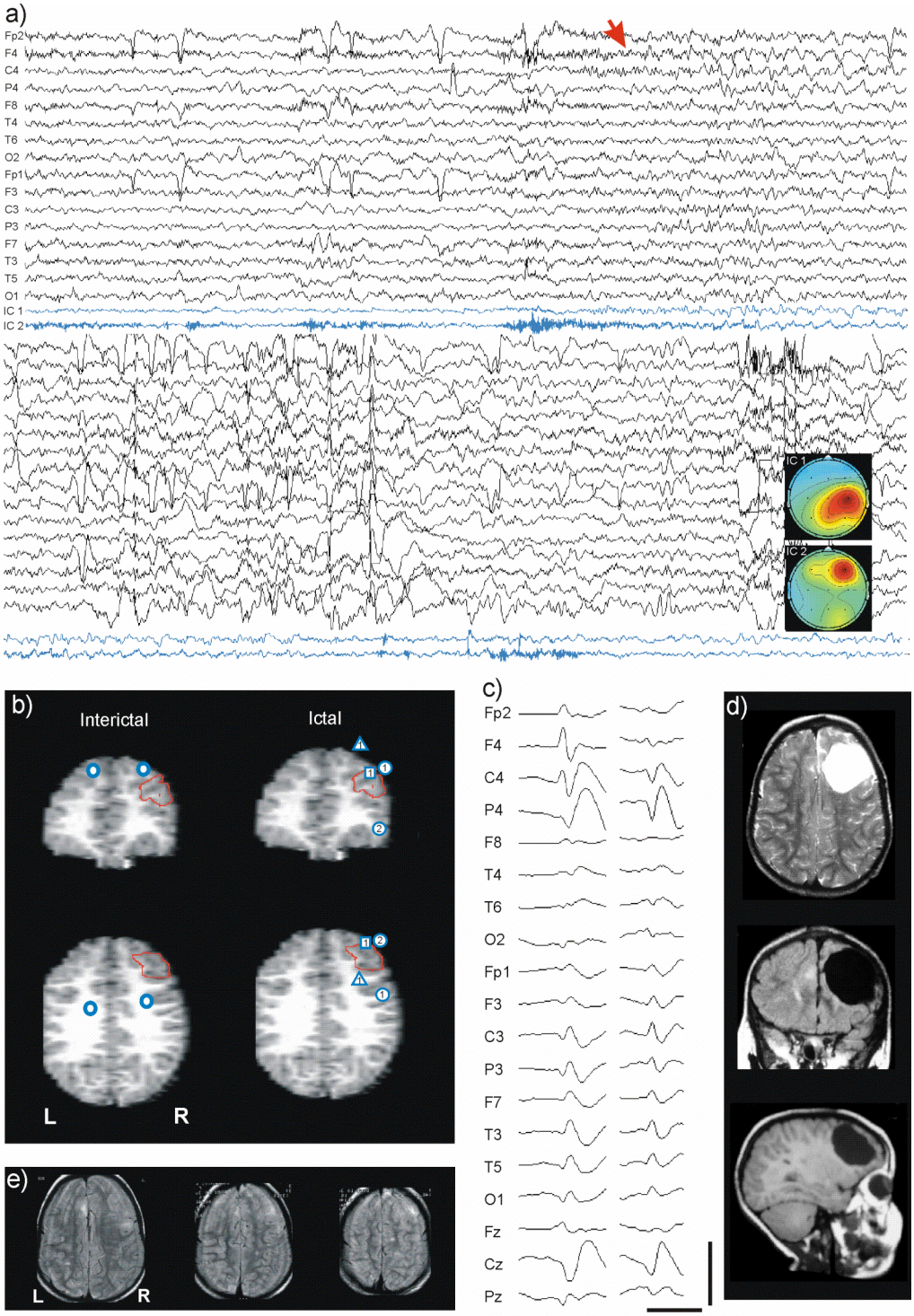

Figure 4.2.4. (a) Seizure event for patient 4, demonstrating onset of rhythmical activity in electrode F4 (arrow). This activity was recovered by two ICs, with maximum over the right frontal lobe (bellow, right), (vertical scale 750 μV and the horizontal scale 2 s). (b) sLORETA results for the averaged interictal spikes (left) and for the ictal events (right). (c) Average EEG spikes (scales as in fig 2). (d) MRI after successful surgery for epilepsy. e) MRI sequence demonstrating the multiple tubers in the frontal lobe of this patient.

4.3. Leal A, Breia P, Dias AI, Canas N, Cabral P, Cabral J, Correia JP, Secca MF, Jordão C. *Comparison of high-resolution EEG and the spike-triggered BOLD activation in focal epilepsy*. 2008d, submitted.

Abstract

Purpose: Integration of EEG and functional Magnetic Resonance Imaging (fMRI) has generated expectations of a major improvement in spatial and temporal resolution of non-invasive functional brain mapping. In epilepsy, several studies have nevertheless demonstrated significant discrepancies between the BOLD activation and the EEG intracranial generators recovered by source analysis.

Methods: The authors use high-resolution EEG (HR-EEG) recordings of interictal spikes in 12 patients with focal epilepsy, processed with an average reference (avg-EEG) and a spline-laplacian algorithm (SL-EEG), and integrate results with the BOLD activation obtained in simultaneous EEG-fMRI.

Results: BOLD activations were obtained in 75% of patients (N=9). In 5 patients activation occurred in the convexity or basal brain areas; in all of these avg-EEG and SL-EEG peaks were in the close neighbourhood (<3 cm). In 4 patients BOLD activations occurred in the inter-hemispheric fissure; in those the SL-EEG failed to show a focal peak, while the avg-EEG showed a nearby maximum in 3.

Each method in isolation had major limitations: widespread maximum in avg-EEG; secondary sources and sinks far from the presumed focus for the SL-EEG; and multiple BOLD clusters for fMRI.

Discussion: There is a close spatial relation between BOLD activation and HR-EEG when the first occur in the brain convexity or basal cortex; BOLD activations in the central fissure do not provide focal sources in the HR-EEG, but in two operated cases removal of a brain area including the BOLD cluster rendered the patient seizure-free.

HR-EEG of interictal spikes demonstrates a close spatial relation with the BOLD activation recorded in simultaneous EEG-fMRI.

Introduction

The localization of the brain structures originating the seizures by non-invasive means is an important goal in the study of focal epilepsies, and it has significant impact on the successful planning of surgical therapy. One strategy to map the epileptogenic areas consists in the study of interictal spikes. The use of a higher number of recording electrodes than the 19 commonly applied for diagnosis (10-20 system) has been associated with improved results (reviewed in Nunez et al, 1994) by allowing the use of advanced analysis methods to improve the spatial resolution of the EEG, such as the laplacian (Law et al, 1993) or deblurring (Gevins et al, 1994). These procedures improve the localization of spikes over the scalp and allow an estimate of their projection on the dura, but do not provide an accurate determination of the number of

generators because they are strongly biased toward superficial cortical generators (Nunez et al, 1994).

The use of source analysis methods to obtain a more accurate localization faces serious problems because the prior assumptions on the properties of the generators that are required to solve the inverse problem in EEG are not widely accepted in the clinical community (reviewed in Plummer et al, 2008) and did not have a significant impact in the evaluation for surgery of epilepsy. The incorporation of additional information on the localization of the sources obtained by a direct physiological measure is expected to bring more consistency to the models and make them less dependent on arbitrary prior conditions.

The BOLD activation associated with the occurrence of interictal spikes is a promising tool, providing localization information by non-invasive means (Krakow et al, 1999; Lazeyras et al, 2000; Al-Asmi et al, 2003; Bonaventura et al, 2006; De Tiège et al, 2007). Some problems must nevertheless be solved before this information can be incorporated in source models (Bagshaw et al, 2006), namely its sensitivity and specificity must be established, as well as the best choice of parameters to obtain a robust map of the epileptic brain structures.

In this study we try to establish the relationship between interictal spikes EEG maps recorded with 64 channels and the BOLD activations obtained in simultaneous EEG/fMRI recordings, from patients with neocortical epilepsies undergoing evaluation for surgery of epilepsy.

Methods

Twelve patients with focal epilepsy undergoing evaluation for Surgery of Epilepsy at the program of the Hospital Centre of West Lisbon were selected for the study. All of them were submitted to a protocol including two experimental sessions, one with recording of high-resolution EEG (HR-EEG) and another with simultaneous recording of EEG and functional Magnetic Resonance Imaging (EEG/fMRI). Informed consent was obtained from all patients or from their parents when appropriate.

The HR-EEG consisted of a 64-channel afternoon recording with 2-hour duration, including a period of sleep. Electrodes were placed using a 10-10 cap (EasyCap, Herrsching-Breitbrunn Germany) and were made of sintered AgCl. Impedances were kept bellow 10 kΩ, a sampling rate of 512 Hz was selected and the high- and low-pass filters were set at 0.5 and 70 Hz. At the end of the session the positions of the electrodes and of the fiducial points (Nasion and pre-auricular points) were determined using an electromagnetic digitizer (Patriot, Polhemus, Colchester, USA).

The EEG/fMRI recordings were performed in a 1.5T GE CVi/NVi scanner, and consisted of several (5 to 10) blocks of continuous and simultaneous acquisition of both modalities, with a short interval between sessions. The EEG was recorded through a special cap of 37 electrodes, made of sintered AgCl and certified for use inside the scanner room (MagLink, Neuroscan, El Paso, USA). The signal was conducted outside the scanner room through a carbon fibre cable and acquired in a DC amplifier (NuAmps, Neuroscan, El Paso, USA). An RF filter was placed at the interface panel of the room. The sampling rate was set at 1000 Hz, the low pass filter was

230 Hz and no high pass filter was used. The EKG was acquired through two electrodes on the chest. The EEG was processed offline with the software Scan 4.3.3 (Neuroscan, El Paso, USA) to remove the echo-planar imaging (EPI) induced artefacts and make visible the epileptic spikes. The balistocardiogram artefact was not corrected for because it was found not to interfere significantly with the spike recognition. The fMRI consisted of EPI sequences with either 16 (patients MC, TF, HC, HS, NF and GM) or 24 (patients IL, LR, FF, JP, JB and AP) slices per brain volume, acquired with a repetition time (TR) of 3.12 and 2.3, respectively. A total of 100 volumes were obtained per session for the patients with 16 slices per volume and 150 volumes per session for the remaining ones. The in-plane resolution of the EPI slices was 3.75x3.75 mm and the slice thickness was 7 and 5 mm for each of the previous protocols.

After acquisition of the fMRI data, a 3D T1 sequence with in plane resolution of 0.86x0.86 mm and slice thickness of 0.60 mm was obtained.

The spikes in the EEG recorded inside the scanner were used to establish the time instants of activation in the even-related analysis protocol of the fMRI data. The software package FSL 4.0 (Smith et al, 2004) was used to perform slice realignment, slice time correction, smoothing with a Gaussian spatial filter with a full-width at half maximum of 5 mm. The first two volumes in each EPI sequence were eliminated. An event-related protocol was established by using the General Linear Model (GLM) to determine the correlation of the BOLD responses with the theoretical curve built by convoluting the time of occurrence of the EEG spikes with a Gamma function with derivatives. The time to peak was tested with values of 3, 6, 8 and 10 seconds and the one producing the best activation selected as the good parameter. The correction for multiple comparisons was done using a cluster-based method with a Z=2.3, corresponding to a confidence value of 95%. The EPI results were registered to the high-resolution 3D T1 sequence to obtain the final anatomical localization of the activations.

The spikes detected in the HR-EEG were averaged, with temporal alignment by the spike peak, and used to map the potential over a realistic scalp obtained from surface rendering of the volumetric T1 sequence and using the individually determined electrode positions. This was done with the ASA 2.2 software package (ANT, Enschede, The Netherlands). The surface rendering of the BOLD activation was represented in the previous maps allowing the final integrated display of both datasets (Figs 4.3.1, 4.3.2 and 4.3.3).

Results

Patients

The patients included in the study had very consistent and focal epileptic activity in the scalp EEG. No structural brain lesion could be found in 6 of the 12 and in the ones with lesions those ranged from large destructive lesions to very small cortical dysplasias (Table 4.3.1). One patient had been previously submitted to surgical removal of a frontal lobe oligodendroglioma (Fig. 4.3.4a).

The epileptic activity in different patients had the maximum amplitude localized in diverse brain areas: the frontal lobes (5 patients); the temporal lobes (2 patients); the parietal lobes (3

patients); and the occipital lobes (2 patients), representing examples of the major types of neocortical epilepsies. The lobar classification of the epilepsies was done not only from the scalp topography of the interictal spikes but also from the clinical and neurophysiological manifestations documented in the long-term video-EEG study performed in the context of the evaluation for surgery of epilepsy (Table 4.3.1). In all cases there was good concordance between the lobe suggested by the interictal spikes and the seizure-onset area in the video-EEG study.

In 9 of the 12 patients (75%) studied, a significant BOLD activation was associated with the occurrence of interictal spikes. Because we are interested in correlating the HR-EEG and EEG/fMRI, the cases with no BOLD activation (one frontal, one parietal and one temporal lobe epilepsy) were excluded from further analysis (Table 4.3.1).

BOLD activation and structural lesions

In 6 of the 9 patients with BOLD activation there was a structural lesion documented in the anatomical MRI (Table 4.3.1). In 4 of these cases there was a cluster of BOLD activation in the neighbourhood (< 2 cm) of the lesion (Figs. 4.3.1b, c and 4.3.3b, c). This activation was not the main BOLD cluster in all cases and in 3 patients there were one or more independent clusters (Figs 4.3.1b, 4.3.3b and c). In two patients (MC and NF) the BOLD activation area was distant from the lesion, but in the same lobe.

One patient (JP) had a BOLD cluster over a sclerotic hippocampus but the seizures documented on video-EEG originated in the parietal lobe of the other hemisphere (Fig 4.3.3b).

Patients IL and FF (Fig. 4.3.4b and c) have been submitted to surgical removal of the presumed epileptogenic lesion and are seizure-free. Patient NF has been submitted to surgical removal guided by ECoG spiking, leaving out the area of BOLD activation (Fig. 4.3.4a), and maintains seizures.

Among cases with no structural lesion, patient GM (Fig. 4.3.2c) has been submitted to invasive monitoring and a highly epileptogenic cortical area in the inferior left occipital lobe was removed, including the BOLD activation cluster, resulting in a seizure-free outcome.

HR-EEG and structural lesions

In 4 patients with structural lesion there was a dipolar topography of the average spike potential in the scalp, with the maximum negativity near (< 4 cm) the scalp projection of the lesion in 2 (Figs 4.3.1b and 4.3.3c). The other patients with lesions (N=3) had a more complex scalp potential topography (Figs 4.3.1a and 4.3.3a,b), with a maximum far from the lesion's scalp projection. The topography of the spikes is therefore not a reliable indicator of the localization of structural lesions, even with the increased number of electrodes used.

The use of the Laplacian montage to increase the spatial resolution of the EEG did not improve the results, as in only 2 of the 6 cases with lesion did this montage produce a focal source or sink of current in the neighbourhood of the structural lesion (Figs 4.3.1b and 4.3.3b). When the evidence for localization was taken from either the average or Laplacian montages, then 4 out

of 6 patients had an EEG maximum near the brain lesion, improving a little the results of each technique in isolation.

HR-EEG and BOLD activations

Seven of the nine patients had a dipolar distribution of the scalp potential in the average reference montage, which was widespread but in all cases pointed to the lobar localization of BOLD activations (Figs 4.3.1, 4.3.2 and 4.3.3c). In four of these patients the increased spatial resolution offered by the Laplacian montage resulted in improvement of the relationship between the electrical and vascular data (Figs 4.3.1a,b and 4.3.2a,c).

In three patients with dipolar potential maps the use of the SL-EEG resulted in clearly discordant data between the BOLD and EEG data (Figs 4.3.1c, 4.3.2b and 4.3.3c), with the appearance of widespread patterns of current sources and sinks far from the BOLD activation areas. In the three cases the BOLD clusters were located in the inter-hemispheric fissure and relatively far from the scalp surface (Table 4.3.2). These cases suggest that for deep generators, the SL-EEG not only does not improve the EEG/BOLD correlation, but it can even make it worse than it is the case for the average reference.

Of the two cases with more complex scalp potential maps, one had skull discontinuities resulting from a previous surgery (Fig 4.3.3a) and the other a complex epilepsy with left parietal ictal onset associated with right hippocampus dysplasia (Fig 4.3.3b) (Table 4.3.1). In the latter case there was good correspondence between SL-EEG maps demonstrating widespread parietal-temporal lobe activity and the BOLD clusters in the parietal and bilateral temporal lobes. The combination of superficial cortical BOLD activations with local SL-EEG sources and sinks seems a combination that helps to select one from several candidate sources present in complex Laplacian patterns (Figs 4.3.2a,c). The absence of a local Laplacian overlying the BOLD activations can be due to a deep localization of fMRI clusters, making more reliable the use of avg-EEG montages in these cases.

Secondary BOLD clusters and focal EEG sources

In five patients multiple BOLD clusters were obtained (Table 4.3.2), which could be quite far apart (Figs 4.3.1b, 4.3.3a,b). In two patients (NF and FF) the secondary clusters were far from the structural lesions and had no apparent local EEG associated with them, suggesting that they correspond to false positive results. For patient TF the secondary cluster was very near the first one, but in the opposite hemisphere. It remains unclear whether it represents a real epileptic involvement of the right hemisphere. The patient JP (Fig. 4.3.3b) has secondary BOLD clusters far away over the scalp but associated with local EEG activity (Fig. 4.3.3b), suggesting that the epileptic area might be widespread. Patient AP had a secondary BOLD activation in the neighbourhood of the main activation (Fig. 4.3.3c).

The spatial association of the brain surface projection of the BOLD clusters and the SL-EEG peaks seems a promising method to improve our capability to determine the value of secondary activations far from the primary candidate area.

The presence of a BOLD activation near a focal configuration of current sources and sinks of the SL-EEG, can help in the selection of one among several such configurations present in the same patient (Fig. 4.3.2a,c).

Discussion

The use of an increased spatial sampling of the scalp EEG in our study allows the use of both average and laplacian maps (Lopes da Silva, 2005), providing a more robust spatial representation of the events of interest than is obtained by the 19 electrodes of the conventional 10-20 system. Despite the use of methods to increase the spatial resolution, this is nevertheless much worse than the one of fMRI and at best, in our dataset, points to a particular brain lobe. The use of source analysis methods offers an increased discrimination at the cost of introducing constrains to the intracranial generators that allow the resolution of the inverse problem in EEG (Bénar et al, 2006). Such “constrained” solutions have had reduced acceptance in clinical epileptology due to the weak justification for such prior postulates (Plummer et al, 2008). In this work we use only methods to improve the spatial resolution of the EEG that do not require such strong assumptions, namely the average reference and the Laplacian montage (Nunez and Srinivasan, 2006).

The patients included in the study represent a large variety of neocortical epilepsies, covering the major brain lobes and diverse ethiologies. They were submitted to simultaneous EEG/fMRI with the expectation that the BOLD activation recovered from such recordings would provide additional information about the characteristics and localization of the underlying sources of scalp epileptic activity (Bénar et al, 2006). We could obtain a significant activation in 75% of the cases (9/12), which is a similar percentage to the one reported for other series (Lazeyras et al, 2000; Bagshaw et al, 2004; Bonaventura et al, 2006).

The overall results of the use of the average and laplacian montages show the complementarities between the two representations, with the SL-EEG demonstrating an increased focalization power in some patients but a complete inability to localize in other patients. The avg-EEG produced more consistent but less focal results. Overall the two techniques complemented each other and their combination produced a modest increase in the spatial correlation with structural lesions and also with the BOLD activations, when compared with the results of each method independently. These results agree well with the known properties of these montages (Nunez and Srinivasan, 2006) and of their application to the mapping of scalp epileptic activity (Nunez and Pilgreen, 1991).

Significant BOLD activations could be recovered near structural brain lesions in 4 out of 6 patients. Because they were either dysplastic or peri-tumoral lesions, with a high epileptogenic potential as determined by the overall neurophysiologial evaluation, such activations are very likely to represent true epileptic-induced BOLD effects. Two out of three operated patients with a brain lesion became seizure-free after a brain resection including the lesion and the BOLD cluster (Fig. 4.3.4b and c), suggesting a good localizing power for this method. One case submitted to resection of the lesion leaving out the BOLD cluster (Fig. 4.3.4a) maintains

seizures, suggesting a more widespread epileptogenic area than demonstrated by intra-operative exploration.

A single case with no structural lesion, submitted to cortical resection including the BOLD cluster, remains seizure-free, supporting good localizing capabilities for the method in this setting.

The lobe implicated by the avg-EEG of interictal spikes had a significant BOLD cluster in 7 out of 9 patients, supporting a local generator for the scalp spikes. In four of these patients the SL-EEG demonstrated a focal configuration of sources and sinks of current, further supporting the case for a localized and superficial cortical generator. The four cases with no local sources or sinks of current had BOLD clusters localized deep in the inter-hemispheric fissure (Figs 4.3.1c, 4.3.2b and 4.3.3c), suggesting deep generators outside the range of the laplacian montage, which is well known to be insensitive to deep sources (Nunez and Srinivasan, 2006).

Half of the patients have more than one BOLD cluster, sometimes in different brain lobes. In some cases these secondary clusters are not associated with structural lesions, with local scalp spikes or with a presumed epileptogenic area from seizure semiology, suggesting that they are false positives. When the BOLD clusters are associated with local scalp spike activity, more evident in the SL-EEG, these cannot be considered false positives. Such is the case for patient JP which showed BOLD clusters in the left parietal lobe (Fig. 4.3.3b) in addition to right BOLD clusters associated to a dysplastic hippocampus. Several seizures were documented in the video-EEG recordings arising from the left parietal lobe. Overall these cases show that the higher spatial resolution provided by the SL-EEG can play an important role in determining the possible clinical significance of multiple BOLD clusters typically found in the simultaneous EEG/fMRI recordings. The association of a BOLD cluster of activation with a focal concentration of sources and sinks of current in the SL-EEG provides the strongest case for a local generator of epileptic activity, but was only found in 5 out of 9 patients.

Acknowledgements

The authors are grateful to Daniel Carvalho, Rita Pinto and Cristina Menezes for technical support in EEG and fMRI acquisition. The study has been supported by grants from Tecnifar SA and from FCT project POSC/EEA-CPS/60977/2004. We confirm that we have read the Journal´s position on issues involved in ethical publication and affirm that this report is consistent with those guidelines.

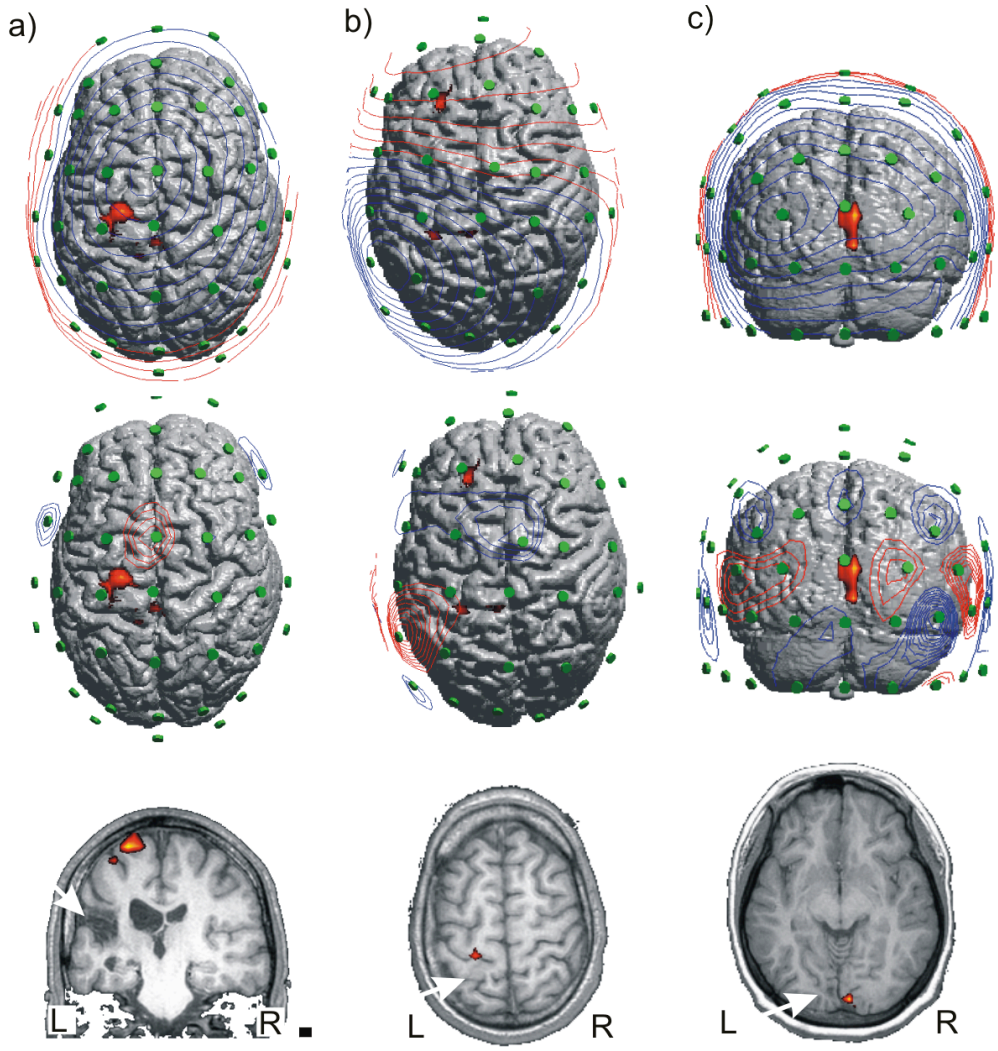

Figure 4.3.1. (a) Scalp potential map of the average interictal spike (N=110) in the average reference (above) and in the spline laplacian montage (middle) for patient MC. The diffuse maximum over the vertex in the average reference is much more focal in the laplacian montage. Both have a close relationship with the main BOLD cluster (in red). EEG electrodes are in green. Bellow, spatial relationship of BOLD activation with the large destructive lesion in the lower left frontal lobe. (b) Average (above) and laplacian (middle) maps for the average interictal spikes for patient FF (N=376). The laplacian improves the spatial resolution as well as the spatial relationship with the BOLD cluster near the structural lesion (white arrow). Bellow, spatial relation of BOLD activation with the small structural lesion over the pre-central girus. (c) The average map (above) for patient IL shows a close spatial relationship between the spike maximal and the main BOLD cluster (N=50). The laplacian map is more complex and with little focal features in the neighbourhood of the BOLD cluster (middle). Bellow, structural lesion over the middle left occipital lobe (white arrow) and BOLD activation cluster.

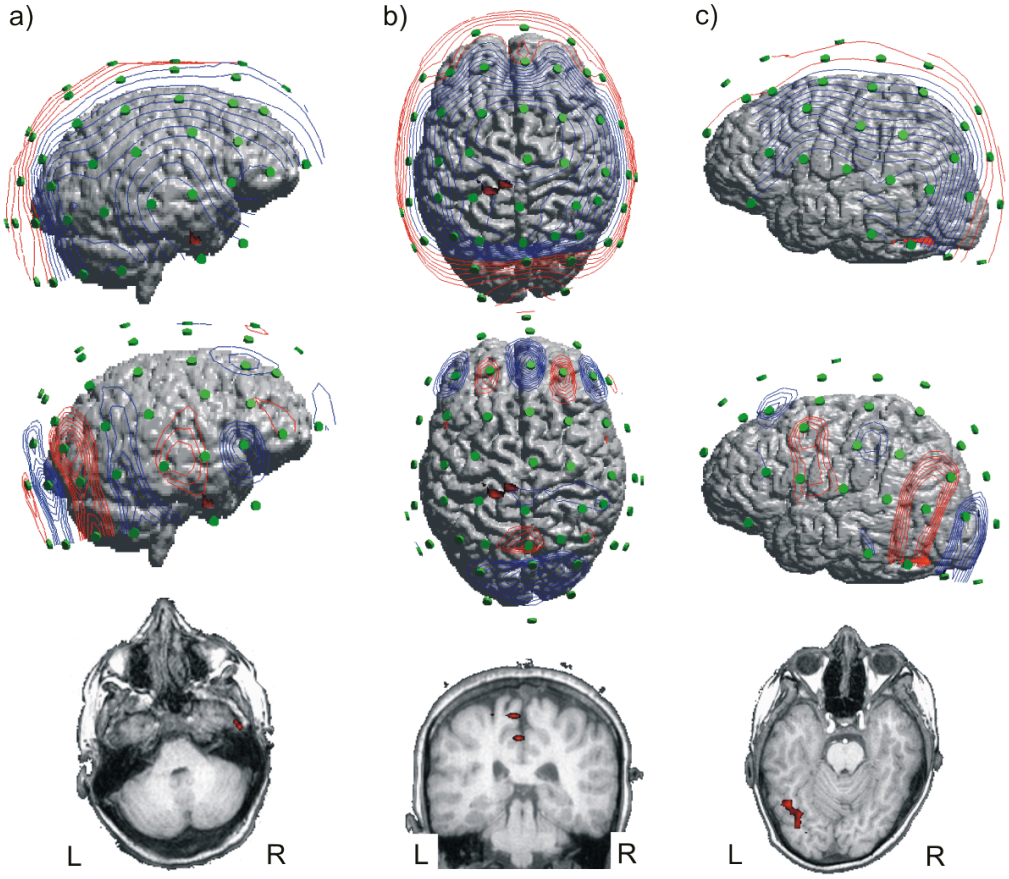

Figure 4.3.2. (a) Average (above) and laplacian (middle) montages for the interictal spikes of patient HS (N=24). Bellow, BOLD activation cluster over an anatomical slice. There is good spatial concordance between the EEG maximum in the average montage and the main BOLD cluster. The laplacian map is more complex but shows a configuration of current sources and sinks compatible with a local source over the BOLD cluster. (b) The average map (above) for patient TF shows a maximum near the surface projection of the main BOLD clusters. The laplacian map (middle) fails to show sources and sinks of current near the BOLD clusters and produces instead complex configurations over the frontal and occipital lobes (middle). Bellow, coronal view of BOLD activations. (c) Average and laplacian montages for patient GM (N=61). No structural lesion was detected, but the laplacian clearly improved the spatial concordance between the BOLD cluster and the scalp EEG.

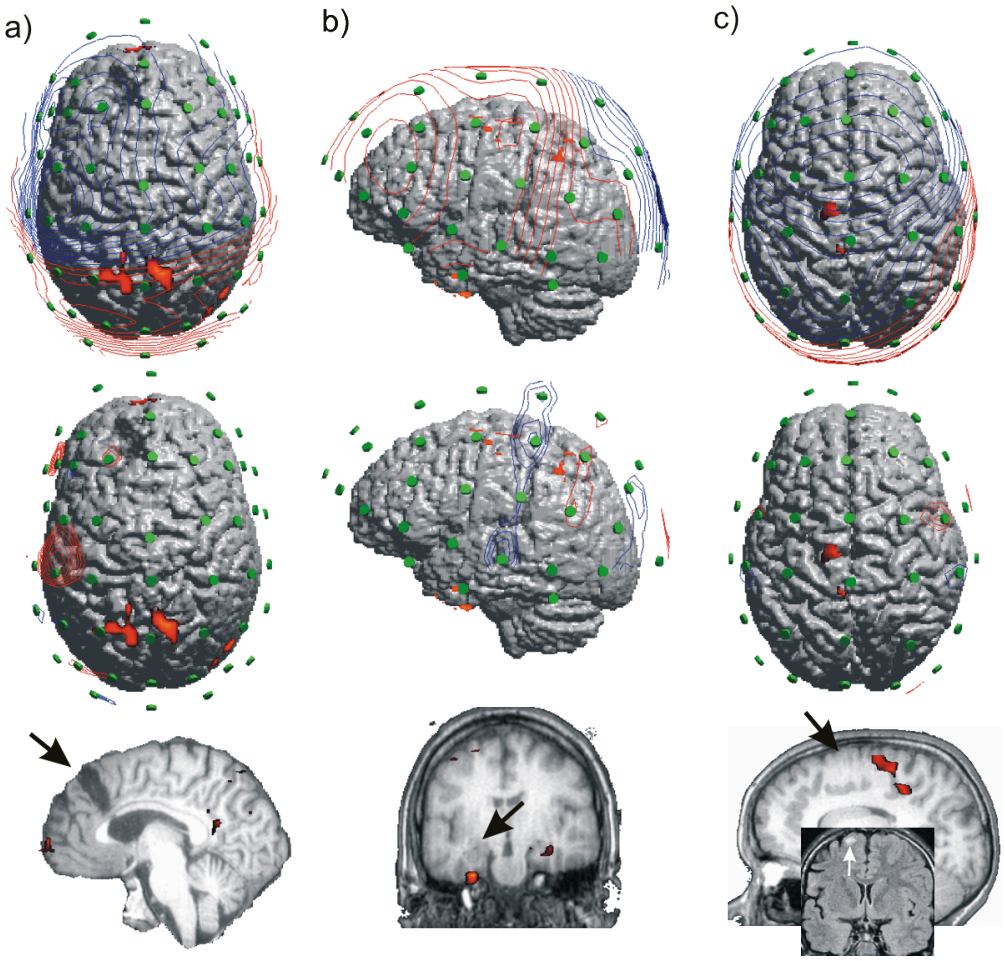

Figure 4.3.3. (a) The average maps for patient NF are complex and with little spatial concordance either with the frontal lobe lesion or with the BOLD clusters (N=220). The structural MRI (bellow) demonstrates the lesion (black arrow) and BOLD activations. (b) The average and laplacian maps for patient JP (N=40), show complex configurations over both temporal lobes and the central area, associated with widespread BOLD activations over the same areas. Bellow, spatial relation of BOLD activations with the right hippocampus structural abnormality (black arrow). (c) Average reference potential map (above) and laplacian (middle) for patient AP (N=50). The cortical lesion consists of a widespread cortical atrophy (black arrow) extending from the sagital plane to the more lateral left frontal lobe. Bellow, BOLD activation in the inter-hemispheric fissure and structural abnormality in the FLAIR coronal slice (inset).

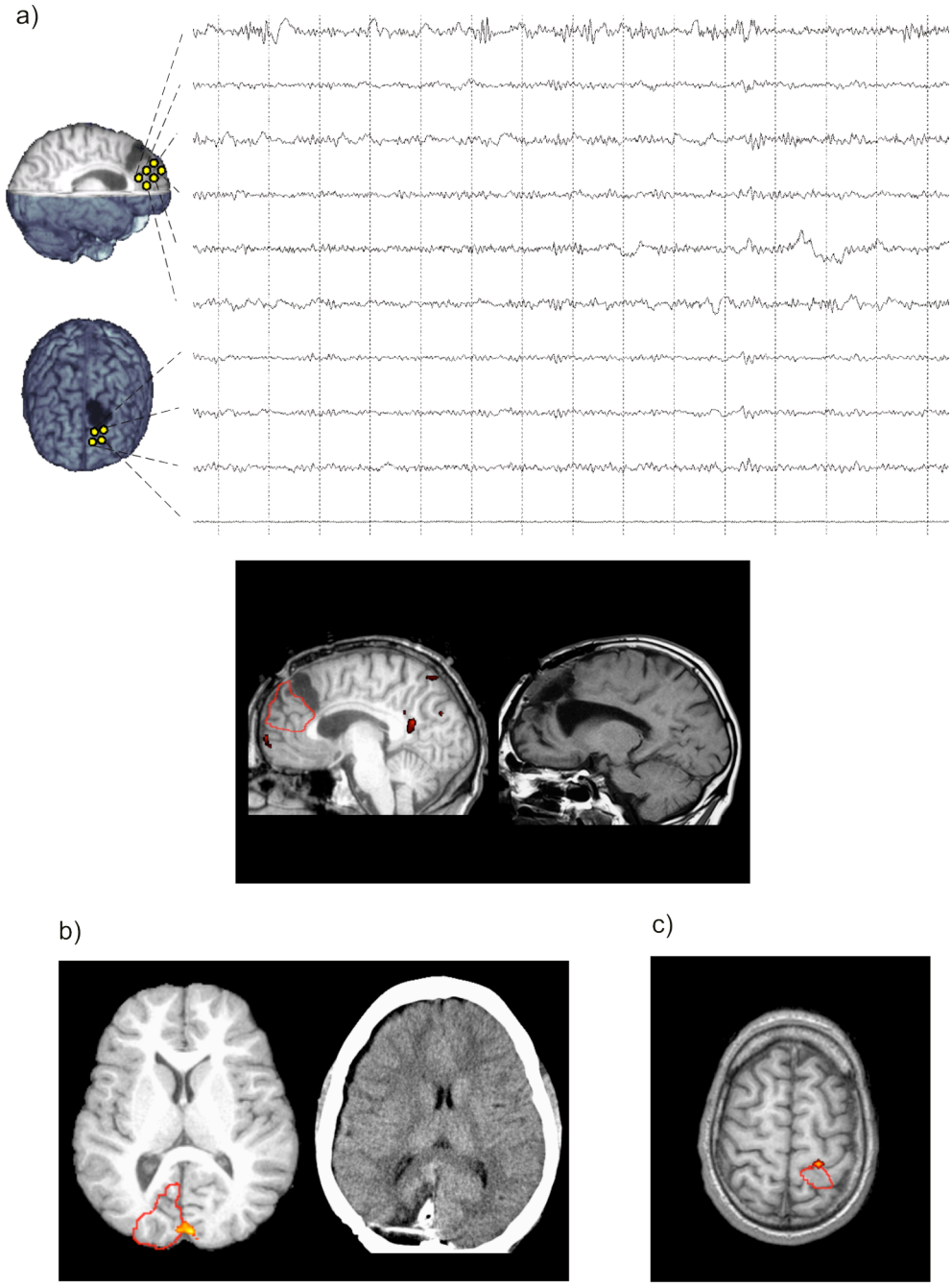

Figure 4.3.4. (a) Electrocorticography for patient NF revealing focal interictal spikes (upper channel) in the anterior border of the old surgical wound. A local resection was performed (outlined in red, below) but the patient is not seizure-free. (b) Pre-surgical (left) MRI for patient IL, demonstrating the relation between the BOLD activation cluster and the resected area (outlined in red). The patient is seizure-free. Post-surgical CT, illustrating the resected area (right). c) BOLD activation and outlined brain lesion removed during surgery for patient FF. The patient is seizure-free.

Table 4.3.1 - Clinical data

Patients	Age(y)	Epilepsy	Seizure type	MRI	Interictal EEG	Ictal EEG
MC	24	Frontal lobe	Mental slowing and right motor activity	Left frontal lobe clastic lesion	Multifocal	Left frontal lobe
TF	12	Frontal lobe	Simple motor seizure in the right hand	N	Multifocal	Not recorded
HC*	30	Temporal lobe	Complex partial seizures	N	Multifocal	Left temporal lobe
HS	34	Temporal lobe	Complex partial seizures	N	Focal	Right temporal lobe
IL	13	Occipital lobe	Complex partial seizures	Displastic medial left occipital lobe	Focal	Left occipital lobe
FF	18	Parietal lobe	Simple motor seizure in the right hand	Pos-central left displastic lesion	Focal	Left rolandic area
LR*	33	Parietal lobe	Umbalance, mental slowing abnormal laughter	N	Focal	Right parietal lobe
NF	31	Frontal lobe	Simple motor seizures in the right limbs	Left frontal lobe pos-surgical lesion	Focal	Left frontal lobe
GM	9	Temporal lobe	Complex partial seizures	N	Multifocal	Left temporal lobe
JP	18	Parietal lobe	Complex partial seizures	Displastic left hippocampus	Multifocal	Central-parietal
JB*	4	Temporal lobe	Complex partial seizures	Displastic lesion in left hippocampus	Multifocal	Bilateral frontal lobes
AP	13	Frontal lobe	Tonic seizure of right limbs, right head rotation.	Atrophy of posterior left frontal lobe.	Focal	Left frontal lobe

* No BOLD activation

Table 4.3.2 - BOLD and EEG data

	BOLD clusters					EEG spikes					Distances		
							Average		Laplacian				
Patients	N	1st	2nd	Depth 1st	Depth 2nd	N	Main	2nd	Main	2nd	BOLD*-lesion	BOLD*-avg	BOLD*-Laplac
MC	2	C1	Cz	15	25	1	FCz		FCz		3,0	2,5	2,5
FF	2	CP3	FC6	23	25	1	CP3-CP1		CP3		0,5	3,5	3,5
IL	1	POz		25		1	PO3		Not focal		0,5	3,5	
HS	1	FT10		20		1	T4-FT8		T8-F8			1,5	2,0
TF	2	C1	Cz	43	60	2	Fpz-Fp1	Cz-CFz	Not focal	Not focal		4,0	
GM	1	P9		32		>5	TP7-P7		P7-PO3			4,5	3,5
NF	4	AFz	CPz	18	22	1	C3-CP3		Not focal		7,1	5,3	6,1
JP	4	FC3-CP3	FT9	20	40	1	Cz		T7-C3-C1		0,5		1,0
AP	2	FCz-Cz	Cz	25	30	2	FCz-C1	F7	Not focal		2,0	2,0	

* nearest cluster

5. General discussion

The experimental studies carried out in this thesis highlight, both the potential and limitations of functional brain mapping using EEG. This is done using clinical neurophysiology techniques in patients with special epilepsy syndromes, chosen in such a way that particular requirements for the EEG mapping are emphasized:

1. One group included patients with distinct syndromes of idiopathic occipital lobe epilepsy as classified by the International League Against Epilepsy based on the age of onset, clinical features of the seizure events and interictal EEG spike features. There are good clinical reasons to assume that the diverse symptomatology in the different syndromes is associated with epileptic activity originating in separate anatomical localizations within the occipital lobes, but the current methods of EEG mapping have not been able to clearly point to the particular brain area involved in each syndrome.
2. Although the precise localization of the epileptic brain areas is unknown in most epileptic patients, in particular cases such as in the epilepsy associated with HH, this localization is very well established (Munari et al, 1995). The origin of the epileptic activity within the HH offers a good experimental test to the localization capabilities of the EEG brain mapping due to the deep brain localization of the source.
3. Patients with refractory focal epilepsy under evaluation for surgery offer an excellent opportunity to push the EEG mapping to its limits and to compare the results with the detailed and multimodal evaluations that these patients undergo in the pre-surgery evaluation process. The results from surgery offer a unique opportunity to validate the results of EEG functional mapping, a fundamental task if such mappings are to be used for understanding brain function.

In the following sections a discussion of our results concerning the topics listed in section 1.1 is done and a comparison with the literature data is performed. In the final section we speculate on future developments which might lead to important advances in the field of functional mapping of the human brain.

5.1. Spatial resolution

The limited capability to distinguish electric potentials originating from distinct brain sources has been a major handicap of the scalp EEG, which cannot be easily solved by simply increasing the electrode sampling, as was demonstrated in the studies of sections 2.5 and 4.3. In them the use of around 3 times as much (64) electrodes as currently used did not result in more detailed scalp potential maps, when the average reference was used. Only with the use of the laplacian algorithm could the spatial detail in the maps be increased.

The issue of the bad spatial resolution in EEG is a complex one and most likely several factors contribute to this:

- Potentials in the scalp result from the synchronous activation of cortical areas of several square centimeters (Cooper et al, 1965) and not from point sources.
- There is a significant overlap at each scalp electrode of locally generated potentials and volume-conducted ones from distant sources, resulting in overlap of scalp maps.
- The skull produces not only a reduction in amplitude, but also a significant blurring of intracranial potentials.
- The reduced number of sampling electrodes in the scalp also contributes to the loss of spatial resolution, at least for less than 128 electrodes (reviewed in Nunez and Srinivasan, 2005).

The first two issues are dealt with in sections 5.5 and 5.6.

The blurring of intracranial focal potentials when seen from the scalp has been the focus of modern techniques of high-resolution EEG such as the spline-laplacian. In our study 4.3 this technique was able to improve spatial focalization of the epileptic sources in 5 out of 9 patients. In the remaining ones the method failed to provide any consistent focalizations; in these cases the simultaneous recording of the BOLD activation suggested the existence of deep sources, providing a consistent explanation for such a failure (Nunez et al, 1994). In the same study the simultaneous use of the average and laplacian montage was found useful as the two methods provide differential but complementary insights into the EEG data. Overall the coexistence of a focal peak in both the average and laplacian maps with a nearby BOLD cluster was found to be the most convincing combination for the existence of a local epileptic source.

The increased resolution offered by the laplacian allows a rough estimate of the surface extent of the EEG sources, as demonstrated in sections 2.4, 2.5 and 4.3. This estimate can be most useful in the appropriate selection of constrains in source analysis (section 2.5).

The number of electrodes that maximizes the spatial resolution in the scalp has not been clearly established. By the Nyquist criterion to avoid aliasing, the sampling frequency should be at least twice the highest spatial frequency of the EEG. But because the latter is dependent on the localization of the EEG sources (unknown in most cases) it is generally a poorly determined quantity. The spatial aliasing problem is nevertheless reduced by the low-pass filtering effect of the skull (Srinivasan, 1999) and of the finite EEG electrode dimensions. Overall it is widely accepted that an electrode to electrode distance of 3 cm (64 electrodes per head) avoids most spatial aliasing (reviewed in Nunez and Srinivasan, 2005) but results seem to improve at least up to 2.5 cm inter electrode distance (Gevins et al, 1991).

5.2. The inverse problem in EEG

A crucial step in the non-invasive mapping of brain physiology is the inverse transformation of the scalp potentials to the brain currents that originate them. The popularity of source analysis methods to perform this step has faced widespread skepticism from the clinical neurophysiology community (Plummer et al, 2008), because of the little justification for constrains put on the

sources that are necessary to solve the inverse problem, in both EEG and MEG. The appropriate constrains to use in a particular type of experimental setting are in general unknown and ultimately they must be validated experimentally.

The case of idiopathic occipital lobe epilepsies is a good demonstration of the inconsistent results provided by source analysis methods when information on the appropriate constrains on the epileptic sources is lacking. In our study of source analysis in two syndromes of IOLE (section 2.2) we found distinct localizations for the sources in patients with similar clinical syndromes and similar source localizations for patients with distinct syndromes. Such inconsistencies extend to the literature data: Van der Meij et al (1997) found dipole generators in superficial localizations near the middle line in patients with IOLE and suggested that superficial sources are a common feature of such cases; Yoshinaga et al (2006) and Kanazawa et al (2006), using EEG and MEG, found deep middle line occipital generators in cases of IOLE (PS type). Our own analysis of a single case of PS syndrome (section 2.5) without the use of source analysis methods, strongly suggests a superficial and lateral origin of the epileptic activity instead of the deep and middle line postulated by the latter two studies.

In general, the “simple” dipolar models commonly used in experimental environments, where hard constrains on the source properties are lacking or poorly justified, give only a rough idea on the localization of the epileptic cortex and none about the surface extension of the source. On the other hand they very easily lead to wrong interpretations and unjustified conclusions about brain physiology.

It is a strong belief of the author that source analysis is useful only when experimentally validated constrains on the sources properties can be used to solve the inverse problem in EEG. Excessive emphasis on the mathematical side of the problem led to the development of a large number of computational algorithms (reviewed in Plummer et al, 2008), while very little efforts have been devoted to experimental determination of the appropriate constrains on the sources and on other important data such as tissue conductances.

We demonstrated that good results can be obtained with source analysis methods for Tuberous Sclerosis seizure events using a combination of ICA and the sLORETA (Pascual-Marqui, 2002) algorithms (section 4.2). A consistent localization was obtained for the sources of ictal rhythmic activity in 4 patients and the comparison of this localization with the brain area removed in successful surgery of epilepsy produced a validation of the models. These results provide a posteriori validation of the anatomical constrains used, in combination with a set of processing algorithms. The same combination did not provide useful or consistent results for the localization of interictal spikes.

In the absence of strong experimental support for the constrains to impose on the source model, the high-resolution methods based on the laplacian algorithms offer a robust procedure to correct for the effects of the different head compartments on the electric and magnetic fields generated by neuronal activity (Nunez and Pilgreen, 1991). Although no generators are obtained, these estimates of the currents and potentials on the cerebral cortex can provide important additional information on the source properties which can be correlated with

information obtained from other brain mapping modalities. We demonstrated that high-resolution EEG and simultaneous EEG-fMRI can be combined in such a way that important clues to the localization and characteristics of the generators of a particular EEG waveform of interest (epileptic spike) can be obtained without the use of source analysis methods (sections 2.4, 2.5 and 4.3).

The combination of source analysis with the BOLD activations obtained through simultaneous EEG-fMRI recording holds important promises of significant advances in the field of functional brain mapping (Gotman et al, 2004). Nevertheless, several studies demonstrated a significant discrepancy between the two methods (Lemieux et al, 2001; Bagshaw et al, 2006). In our own study in IOLE (section 2.2) we also found a significant disagreement between the two methods.

The method of seeding regional dipoles at the BOLD clusters localizations is not a true way of mapping the unknown sources but instead a method of testing the relative contribution of the diverse brain areas producing fMRI activation. This can be useful in some contexts were multiple BOLD clusters are present and no reliable data exists on how to select the meaningful ones (Leal et al, 2007b), but some evidence exists that the BOLD clusters overlap only imprecisely the true area of neuronal activation (Gotman et al, 2004). More experimental work on the degree of concordance of the EEG/fMRI BOLD activation and the epileptogenic areas needs to be done before this data can be reliably used to constrain source analysis methods.

5.3. Reduced sensitivity to subcortical generators

That the scalp EEG has a reduced sensitivity to deep brain sources has been known from the early days of neurophysiology. Nevertheless no simple rule for the relationship between amplitude attenuation and depth has been derived and it is in general very difficult to determine whether a small amplitude waveform on the scalp is due to a weak but superficial source or to a strong but deep one. In the most general case the EEG rhythms will result from the overlap activity from sources at different depths, whose number and localizations are unknown (reviewed in Nunez and Srinivasan, 2005).

In section 3.2 we report a study in patients with known localization of the source of epileptic activity where an attempt was made to recover the dynamics of seizure onset and propagation using modern techniques of blind source decomposition of the EEG activity and source analysis based on surface EEG recordings alone. Although a separation of deep and superficial generators was achieved, the comparison of the localization of the deep sources to the known area of seizure onset (in the HH) demonstrated little precision and a high uncertainty for the localization.

A major improvement in this exercise was obtained in the study detailed in section 3.3, in which a patient with HH was submitted to a high-resolution EEG (64 electrodes) complemented with a simultaneous EEG-fMRI recording of the seizure events. The BOLD effect associated with the occurrence of seizures produced a 3D map of the cortical and subcortical activations, with good spatial resolution. It also allowed the establishment of the origin and early propagation of epileptic activity to the cortex. In conjunction with the temporal dynamics of the cortical activity

provided by the EEG, the combined study allowed a detailed dynamic model of the origin and propagation of the seizure activity.

The imaging of cortical and subcortical sources of epileptic activity in HH has been obtained with SPECT (Arroyo et al, 1997; Kuzniecky et al, 1997; Arzimannoglou et al, 2003) and also with PET (Mullati et al, 2003; Ryvlin et al, 2003). These methods have a reduced temporal resolution and provide very limited information on the dynamics of the epileptic events. The fMRI technique results in relevant improvements in spatial resolution and, when combined with the EEG as in our study, even more significant clarification of the temporal dynamics of the epileptic seizures.

The simultaneous recording of the BOLD effect associated with the neurophysiological events of interest is in our view a powerful method to clarify the spatial and temporal characteristics of the subcortical participation, a traditional weakness of EEG studies.

5.4. Variable sensitivity to sources in sulcus or gyrus

That the EEG potentials on the scalp result mainly from the radial electric field produced on the more superficial girus surface, has been known for a long time (Lorent de No, 1947). Transversal fields produced at the sulci or interhemispheric fissures contribute less to the EEG and in contrast are the main contributors for the magnetic fields recorded in MEG (reviewed in Hari, 2005). These facts, together with the highly convoluted nature of the human neocortex, lead to a variable sensitivity of the scalp EEG to sources along the cortex and in the brain fissures. The combined recording of EEG and MEG seems at the present time the best strategy to overcome the problem of variable sensitivity in the different orientations of the cortical sheet.

In our study detailed in section 4.3, the use of high-resolution EEG and a laplacian derivation resulted in improvement in spatial resolution for cortical superficial sources, but failed for sources near the middle line (3 patients), in which case BOLD activations within the interhemispheric fissure could be found, suggesting deep cortical sources “far” from the scalp surface. In such cases the spatial filtering properties of the laplacian (Srinivasan, 1999) decreased the sensitivity of this montage to the deep sources, and did not produce the expected improvement in spatial resolution. This data suggests that the use of the BOLD activation to complement the EEG localization in sources localized in deep cerebral fissures might be a productive strategy to overcome the previously mentioned limitations of the EEG recording alone.

5.5. Volume conductor mixing at scalp electrodes

A single EEG scalp electrode detects electrical potentials resulting from the summation of nearby and far away sources. In the most general case the researcher plans the study of the brain neurophysiological responses associated with an event of interest by distributing scalp electrodes near the involved brain areas. In this way the potentials of interest are maximized as compared with the ones originating in more distant and less meaningful sources. Nevertheless

an important superposition of potentials, not correlated with the events of interest, always remains and in most cases they are larger in amplitude than the responses of interest. The traditional way to improve this problem consists in the averaging of multiple EEG segments, time locked to the event of interest, exogenous or endogenous. The last procedure is simple but it fails to recover induced but not time-locked activity (Pfurscheller and Lopes da Silva, 2005), and also fails to recover the transient synchronization between distant electrodes (Makeig et al, 2004), which are important and complementary physiological properties of brain networks.

The techniques of blind source separation based on ICA had in recent years a major impact in the field of EEG (Vigário et al, 2000), and promise major contributions to the problem of studying in isolation brain generators which are added at surface electrodes by volume conductor effect. Our papers on occipital lobe spikes (sections 2.3 and 2.4) as well as on ictal EEG analysis (sections 3.2 and 4.2), illustrate the power of such methods for the study of the dynamics and localization of several brain networks. If in the first papers the method has been successful in separating networks with distinct spatial and temporal dynamics, allowing determination of complex patterns of spread of the epileptic activity in the neocortex; in the latte papers ictal rhythms were separated in several spatial components with a time of activation providing information on the dynamics of seizure origin and spread.

5.6. Dependence on synchronization of a large cortical area

In order to be detectable on the scalp the microscopic cortical currents that underlie the EEG must add up synchronously over an area o several square centimeters (Cooper et al, 1965). The experimental determination of the extent of such an area is in general difficult, but it is a useful information on the features of the sources of interest.

The map of the electric potential of features of interest with high-resolution EEG can provide useful details about their intracranial generators. This is illustrated by the study in section 2.5, where the 64 channel EEG of interictal spikes suggested a focal maximum (Fig. 2.5.1b). Such a scalp potential configuration is compatible with the use of a single dipole as an adequate source model; using this strategy Yoshinaga et al (2005) found deep dipoles near the calcarine sulcus. The high resolution map of figure 2.5.1c demonstrates a more complex configuration of sources and sinks of current and suggests that an extended and superficial source more easily fits such data. The widespread BOLD activations in nearby superficial cortex it is a further element favoring such a source configuration instead of the deep focal one.

It is therefore our belief that a high resolution map of scalp potentials can help in the appropriate selection of constrains for the EEG generators when source analysis methods are planned. The BOLD effect associated with the epileptic events is a further element that can help in this selection.

5.7. Fast spread between distant brain areas

The construction of a dynamical model of brain activity must take into account the relative time of activation of distinct networks, in order to establish patterns of connectivity and mutual influence. That the spread of brain activity can be very fast is well illustrated by spike activity in occipital lobe epilepsy where, in less than 50 ms, such an abnormal electric activity can spread from the occipital to the frontal lobe (section 2.4). Failure to determine the precise temporal relationship between the activation of both networks can lead either to the inability to establish the direction of the spread or its very existence.

The main difficulty for the EEG studies in characterization of the fast propagation is to avoid the effects of volume conduction which can produce long distance effects that makes the true determination of the precise timing of activation of a particular part of the brain difficult. The spatial filtering properties of the laplacian represent a major advance in this respect because the brain sources in the close neighborhood of the electrodes are selected and their time of activation can be clearly determined. The fact that such record is reference free is a further advantage for the mapping purposes.

A surface BOLD activation associated with a focal configuration of sources and sinks of current in the laplacian montage gives a particularly powerful support for a local brain generator, as was established in section 4.3. Although the number of patients studied up to now is limited, this association seems more consistent than the combination of EEG source analysis and BOLD activation (section 2.2) and less ambiguous than source analysis alone.

5.8. Future perspectives

The availability of EEG recording devices with large number of electrodes (256 channels or more), together with better electrode technology is an evolving trend that promises to increase the spatial sampling of the scalp EEG to its limits, and therefore improve the spatial resolution of the mapping.

The computing power and software for constructing detailed anatomical models of the head is also evolving fast, providing a better correction for the detrimental effects of the various compartments on the detection of brain currents from the scalp EEG.

Recent efforts have been devoted to a better estimate of the electrical conductances of the different head compartments (Gonçalves et al, 2003), a fundamental information if more advanced models of the volume conductivity properties of the head are to be obtained.

The experimental validation of source analysis models in realistic cases is a necessary step to gain confidence in the models, and a way forward in the appropriate selection of constrains to study the activity of particular brain networks.

An important area of work currently under intense investigation is the connection between the neuronal activity and the vascular response underlying the BOLD effect. Advances in this area promise to lead to a less ambiguous integration of the EEG and fMRI information.

The determination of the hemodynamic response function (HRF) for different brain areas promises to improve the fMRI models and lead to more robust activations than it is currently the case with the use of a single HRF for the all brain.

The development of methods of analysis of the fMRI data not dependent on the previous specification of a model promise to advance our capability to extract useful information on brain physiology in cases where the traditional model-driven approach finds limitations.

The information obtained from simultaneous EEG/fMRI records will have to be validated in order to determine the best strategy to integrate both modalities. The surgery for epilepsy it is a classical and still useful setting in which such validation can take place.

The integration of EEG and BOLD with other functional mapping modalities, such as Transcranial Magnetic Stimulation, is technically feasible and a potential source of useful information.

Overall the best strategy currently available consists in gaining a clear understanding of both the advantages and limitations of each technique of functional brain mapping and to design a strategy to combine them in the most appropriate way to the problem at hand.

6. REFERENCES

Adrian ED. The spread of activity in the cerebral cortex. J Physiol 1936; 88(2): 127-161.

Aghakhani Y, Kobayashi E, Bagshaw AP, Hawco C, Bénar CG, Dubeau F, Gotman J. Cortical and thalamic fMRI responses in partial epilepsy with focal and bilateral synchronous spikes. Clin Neurophysiol 2006; 117: 177-191.

Al-Asmi A, Bénar C, Gross D et al. fMRI activation in continuous and spike-triggered EEG-fMRI studies of epileptic spikes. Epilepsia 44(10): 1328-1339, 2003.

Allen PJ, Polizzi G, Krakow K, Fish DR, Lemieux L. Identification of EEG events in the MR scanner: the problem of pulse artifact and a method for its subtraction. Neuroimage 1998; 8: 229-239.

Allen PJ, Josephs O, Turner R. A method for removing imaging artifact from continuous EEG recorded during functional MRI. Neuroimage 2000; 12: 230-239.

Arroyo S, Lesser RP, Gordon B, Uematsu S, Hart J, Schwerdt P, Andreasson K, Tolosa E. Mirth, laughter and gelastic seizures. Brain 1993; 116: 757-780.

Arroyo S, Santamaria J, Sanmarti F, Lomenã F, Catafau A, Casamitjana R, Setoain J, Tolosa E. Ictal laughter associated with paroxysmal hypothalamopytuitary dysfunction. Epilepsia 1997; 38(1): 114-117.

Arzimannoglou AA, Hirsch E, Aicardi J. Hypothalamic hamartoma and epilepsy in children: illustrative cases of possible evolution. Epileptic Disord 2003; 5: 187-199.

Assaf B, Ebersole J. Continuous source imaging of scalp ictal rhythms in temporal lobe epilepsy. Epilepsia 1997; 38(10): 1114-1123.

Babiloni F, Babiloni C, Carducci F, Fattorini L, Onorati P, Urbano A. Spline laplacian estimate of EEG potentials over a realistic magnetic resonance-constructed scalp surface model. Electroencephal Clin Neurophysiol 1996; 98: 363-373.

Babiloni F, Babiloni C, Carducci F, Angelone L, Del Gratta C, Romani GL, Rossini PM, Cincotti F. Linear inverse estimation of cortical sources by using high resolution EEG and fMRI priors. IJBEM 2001; 3: 1-11.

Bagshaw AP, Aghakhani Y, Bénar CG, Kobayashi E, Hawco C, Dubeau F, Pike GB, Gotman J. EEG-fMRI of focal epileptic spikes: analysis with multiple haemodynamic functions and comparison with gadolinium-enhanced MR angiograms. Hum Brain Map 2004; 22: 179-192.

Bagshaw AP, Kobayashi E, Dubeau F, Pike GB, Gotman J. Correspondence between EEG-fMRI and EEG dipole localisation of interictal discharges in focal epilepsy. Neuroimage 2006; 30(2): 417-425.

Baillet S, Mosher JC, Leahy RM. Electromagnetic brain mapping. IEEE Sign Proc Mag 2001; 18(6): 14-30.

Barlow JS. An electronic method for detecting evoked responses of the brain and for reproducing their average waveforms. Electroencephal Clin Neurophysiol 1957; 9: 340-343.

Bell AJ, Sejnowski TJ. An information-maximization approach to blind separation and blind deconvolution. Neural Computation 1995; 7(6): 1129-1159.

Bebin EM, Kelly PJ, Gomez MR. Surgical treatment for epilepsy in cerebral Tuberosis Sclerosis. Epilepsia 1993, 34(4): 651-657.

Belliveau JW, Kennedy DN, McKinstry RC, Buchbinder BR, Weisskoff RM, Cohen MS, Vevea JM, Brady TJ, Rosen BR. Functional mapping of the human visual cortex by magnetic resonance imaging. Science 1991; 254: 716-719.

Bénar C, Gross D, Wang Y et al. The BOLD response to interictal epileptiform discharges. NeuroImage 17: 1182-1192, 2002.

Bénar CG, Grova C, Kobayashi E, Bagshaw AP, Aghakhani Y, Dubeau F, Gotman J. EEG-fMRI of epileptic spikes: Concordance with EEG source localization and intracranial EEG. Neuroimage 2006; 30: 1161-1170.

Bénar C, Grova C, Kobayashi E, Bagshaw A, Aghakhani Y, Dubeau F, Gotman J. Simultaneous EEG-fMRI of epileptic spikes: concordance with EEG source localization and intracranial EEG. Neuroimage 2006; 30(4): 1161-1170.

Berkovic S, Andermann F, Melanson D, Ethier E, Feindel W, Gloor P. Hypothalamic hamartoma and ictal laughter: evolution of a characteristic epileptic syndrome and diagnostic value of magnetic resonance imaging. Ann Neurol 1998; 23: 429-439.

Blamire AM, Ogawa S, Ugurbil K, Rothman D, McCarthy G, Ellermann JM, Hyder F, Rattner Z, Shulman RG. Dynamic mapping of the human visual cortex by high-speed magnetic resonance imaging. Proc Natl Acad Sci USA 1992; 89: 11069-11073.

Bonaventura C, Vaudano AE, Carni M, Pantano P, NucciarelliV, Garreffa G, Maraviglia B, Prencipe M, Bozzao L, Manfredi M, Giallonardo AT. EEG/fMRI study of ictal and interictal epileptic activity: methodological issues and future prespectives in clinical practice. Epilepsia 2006; 47(Suppl. 5): 52-58.

Boynton GM, Engel SA, Glover GH, Heeger DJ. Linear systems analysis of functional magnetic resonance imaging in human V1. J Neurosci 1996; 16(13): 4207-4221.

Braitenberg V, Schuz A. Anatomy of the cortex: statistics and geometry. Springer-Verlag 1991, New York.

Brazier MAB. Some uses of computers in experimental neurology. Exp Neurol 1960; 2: 123-143.

Buckner RL. Event-related fMRI and the hemodynamic response. Hum Brain Map 1998; 6: 373-377.

Cajal SR. Histologie du systéme nerveux de l´homme et des vertebres, vol II. Maloine 1911.

Carabalo R, Cersósimo R, Fejerman N. Panayiotopoulos syndrome: a prospective study of 192 patients. Epilepsia 2007; 48(6): 1054-1061.

Cascino G, Andermann F, Berkovic S, Kuzniecky R, Sharbrough F, Keen D, Bladin P, Kelly P, Olivier A, Feindel W. Gelastic seizures and hypothalamic hamartomas: evaluation of patients undergoing chronic intracranial EEG monitoring and outcome of surgical treatment. Neurology 1993; 43: 747-750.

Chance B, Leigh JS, Miyake H, Smith DS, Nioka S, Greenfield R, Finander M, Kaufman K, Lery W, Yong M, Cohn P, Yoshioka H, Boretsky R. Comparison of time-resolved and unresolved measurement of deoxy hemoglobin in brain. PNAS 1988; 85: 698-707.

Cherry SR, Phelps ME. Imaging brain function with positron emission tomography. In Toga & Mazziota Eds. Brain Mapping: the methods, 2nd Ed. 2002, Academic Press: 485-511.

Cooper R, Winter AL, Crow HJ, Walter WG. Comparison of subcortical, cortical, and scalp activity using chronic indwelling electrodes in man. Electroencephal Clin Neurophysiol 1965; 18: 217-228.

Covanis A, Ferrie CD, Koutroumanidis M, Oguni H, Panayiotopoulos CP. Panayotopoulos syndrome and Gastaut type idiopathic childhood occipital epilepsy. In Roger J, Bureau M, Dravet Ch, Genton P, Tassinari CA, Wolf P. Epileptic syndromes in infancy, childhood and adolescence. 2005; pages 227-253: 4th ed, John Libbey.

Cuffin BN. Effects of local variations in skull and scalp thickness on EEGs and MEGs. IEEE Trans Biomed Eng 1993; 40(1): 42-48.

Dale AM, Buckner RL. Selective averaging of rapidly presented individual trials using fMRI. Hum Brain Map 1997; 5: 329-340.

Dawson GD. A summation technique for the detection of small evoked potentials. Electroencephal Clin Neurophysiol 1954; 6: 153-154.

Delorme A, Makeig S. EEGLAB: an open source toolbox for analysis of single-trial Eeg dynamics including independent components. J Neurosci Methods 2004; 134(1): 9-21.

Devous MD. SPECT functional brain mapping. In Toga & Mazziota Eds. Brain Mapping: the methods, 2nd Ed. 2002, Academic Press: 513-536.

De Munck JC, Vijn PC, Spekreijse H. A practical method for determining electrode positions on the head. Electroencephalogr Clin Neurophysiol 1991; 78(1): 85-87.

De Munck J, Gonçalves S, Huijboom L, Kuijer JP, Pouwels PJ, Heethaar RM, Lopes da Silva F. The hemodynamic response of the alpha rhythm: an EEG/fMRI study. Neuroimage 2007; 35: 1142-1151.

De Munck J, Gonçalves S, Faes TJ, Kuijer JP, Pouwels PJ, Heethaar RM, Lopes da Silva F. A study of the brain's resting state based on alpha band power, heart rate and fMRI. Neuroimage 2008; 42: 112-121.

De Tiège X, Laufs H, Boyd SG, Harkness W, Allen PJ, Clark CA, Connelly A, Cross JH. EEG-fMRI in children with pharmacoresistant focal epilepsy. Epilepsia 2007; 48(2): 385-389.

De Zwart JA, Gelderen P, Golay X, Ikonomidou VN, Duyn JH. Accelerated parallel imaging for functional imaging of the human brain. NMR Med 2006; 19: 342-351.

Douglas R, Markram H, Martin K. Neocortex. In Shepherd (Ed) The synaptic organization of the brain, 499-558, Oxford University Press 2004.

Douglas RJ, Martin AC. Mapping the matrix: The ways of neocortex. Neuron 2007; 56: 226-238.

Duann JR, Jung TP, Kuo WJ, Yeh TC, Makeig S, Hsieh JC, Sejnowski TJ. Single-trial variability in event-related BOLD signals. Neuroimage 2002; 15: 823-835.

Duong TQ, Kim DS, Ugurbil K, Kim SG. Localized cerebral blood flow response at submillimeter columnar resolution. Proc Natl Acad Sci USA 2001; 98: 60-67.

Engel SA, Glover GH, Wandell BA. Retinotopic organization in human visual cortex and the spatial precision of functional MRI. Cerebral Cortex 1997; 7: 181-192.

Felleman JD, Van Essen CD. Distributed hierarchical processing in the primate cerebral cortex. Cereb Cortex 1991; 1: 1-47.

Fernandes JM, Martins da Silva A, Huiskamp G, Vellis D, Manshanden I, de Munck J, Lopes da Silva F, Cunha JP. What does an epileptiform spike look like in MEG? Comparison between coincident EEG and MEG spikes. J Clin Neurophysiol 2005; 22: 68-73.

Ferrie C, Caraballo R, Covanis A, Demirbilek V, Dervent A, Kivity S, Koutroumanidis M, Martinovic Z, Oguni H, Verroti A, Vigevano F, Watanabe K, Yalcin D, Yoshinaga H. Panayiotopoulos syndrome: a consensus view. Dev Med Child Neurol 2006; 48: 236-240.

Fillard P, Arsigny V, Pennec X, Ayache N. Clinical DT-MRI estimation, smoothing and fiber tracking with Log-Euclidian metrics. IEEE Trans Med Imaging 2007; in press.

Fischl, Bruce, Sereno, M.I., Dale, A.M. Cortical Surface-Based Analysis II: Inflation, Flattening, and a Surface-Based Coordinate System. NeuroImage 1999; 9(2):195-207.

Fohlen M, Lellouch A, Delalande O. Hypothalamic hamartoma with refractory epilepsy: surgical procedures and results in 18 patients. Epileptic Disord 2003; 5: 267-273.

Foldvary N. Ictal electroencephalography in neocortical epilepsy. In Luders and Comair (eds) Epilepsy surgery, 2001 (2nd Ed); 431-439, Lippincot Williams & Wilkins.

Fuchs, M., Wagner, M. & Kastner, J. Confidence limits of dipole source reconstruction results. Clinical Neurophysiology 2004; 115, 1442-1451.

Garreffa G, Carni M, Gualniera G, Ricci GB, Bozzao L, de Carli D, Morasso P, Colonnese C, Roma V, Maraviglia B. Real-time MR artifacts during continuous EEG/fMRI acquisition. Magn Res Imag 2003; 21(10): 1175-1189.

Gastaut H. Benign epilepsy of childhood with occipital paroxysms. In Roger J, Bureau M, Dravet Ch, Dreifuss F, Perret A, Wolf P, (eds) Epileptic syndromes in infancy, childhood and adolescence. 2nd ed, London: John Libbey; 1992: 201-217.

Geller E, Lüders H, Cheek J, Comair Y. Electrical stimulation of the visual cortex. In Lüders H and Noachtar S (ed): Epileptic seizures: pathophysiology and clinical semiology,Churchill Livingstone, 2000: 219-227.

Gevins A, Le J, Brickett P, Reutter B, Desmond J. Seeing through the skull: advanced EEGs use MRIs to accurately measure cortical activity from the scalp. Brain Topogr 1991; 4(2): 125-131.

Gevins A, Le J, Martin N, Brickett P, Desmond J, Reutter B. High resolution EEG: 124-channel recording, spatial deblurring and MRI integration methods. Electroencephal Clin Neurophysiol 1994; 90: 337-358.

Gevins AS, Cutillo B, Desmond J, Ward M, Bressler S, Barbero N, Laxer K. Subdural grid recordings of distributed neocortical networks involved with somatosensory discrimination. Electr Clin Neurophysiol 1994b; 92(4): 282-290.

Gevins A, Le J, Leong H, McEvoy LK, Smith M. Deblurring. J Clin Neurophysiol 1999; 16(3): 204-213.

Gevins A. Electrophysiological imaging of brain function. In Brain Mapping: The Methods, Toga AW & Mazziotta JC Eds, 2nd Ed, pp175-188, 2002.

Goldman RI, Stern JM, Engel J, Cohen MS. Simultaneous EEG and fMRI of the alpha rhythm. Neuroreport 2002; 13(18): 2487-2492.

Gonçalves SI, de Munck J, Verbunt JP, Bijma F, Heethaar RM, Lopes da Silva F. In vivo measurements of the brain and skull resistivities using an EIT-based method and realistic models for the head. IEEE Trans Biomed Eng 2003; 50(6): 754-767.

Gonçalves S, De Munck J, Pouwels PJ, Schoonhoven R, Kuijer JP, Maurits NM, Hoogduin JM, Van Someren EJ, Heethaar RM, Lopes da Silva F. Correlating the alpha rhythm to BOLD using simultaneous EEG/fMRI: inter-subject variability. Neuroimage 2006; 30(1): 203-213.

Gonçalves S, Pouwels PJ, Kuijer JP, Heethaar RM, de Munck JC. Artifact removal in co-registered EEG/fMRI by selective average subtraction. Clin Neurophysiol 2007; 118: 2437-2450.

Gotman J, Bénar cG, Dubeau F. Combining EEG and fMRI in epilepsy: methodological challenges and clinical results. J Clin Neurophysiol 2004; 21(4): 229-240.

Gray CM, Singer W. Stimulus-specific neuronal oscillations in orientation columns of cat visual cortex. PNAS 1989; 86: 1698-1702.

Grova C, Daunizeau J, Kobayashi E, Bagshaw AP, Lina JM, Dubeau F, Gotman J. Concordance between distributed EEG source localization and simultaneous EEG-fMRI studies of epileptic spikes. Neuroimage 2008; 39: 755-774.

Greenberg JH, Reivich M, Alavi A,Hand P, Rosenquist A, Rintelmann W, Stein A, Tusa R, Christman D, Fowler J, MacGregor B, Wolf A. Metabolic mapping of functional activity in human subjects with the [^{18}F]fluorodeoxyglucose technique. Science 1981; 211: 678-680.

Guerrini R, Dravet C, Genton P, Bureau M, Bonanni P, Ferrari A, Roger J. Idiopathic photosensitive occipital lobe epilepsy. Epilepsia 1995; 36: 883-891.

Gurney K. An introduction to neural networks. Taylor & Francis, 1997.

Hamer HM, Morris III HH. Indications for invasive video-electroencephalographic monitoring. In Luders and Comair (eds) Epilepsy surgery, 2001 (2nd Ed); 559-566, Lippincot Williams & Wilkins

Hari R. Magnetoencephalography in clinical neurophysiological assessment of human cortical functions. In Niedermeyer & Lopes da Silva, Eds. Electroencephalography, 5th ed, 2005, Lippincott Williamws & Wilkins.

Harlow JM. Recovery from the passage of an iron bar through the head. Mass Med Soc Publ 1868; 2: 327-347.

Harner RN. Singular value decomposition – a general linear model for analysis of multivariate structure in the electroencephalogram. Brain Topogr 1990; 3(1): 43-47.

Helmholtz H. Ueber einige Gesetze der Vertheilung elektrischer Ströme in körperlichen Leitern, mit Anwendung auf die thierisch-elektrischen Versuche. Ann Phys Chem 1853; 89: 211-233, 353-377.

Hoffman A, Jager L, Werhahn KJ, Jaschke M, Noachtar S, Reiser M. Electroiencephalography during functional echo-planar imaging: detection of epileptic spikes using post-processing methods. Magn Res Med 2000; 44: 791-798.

Holmes GL, Stafstrom CE, The Tuberosis Sclerosis Study Group. Tuberosis Sclerosis Complex and Epilepsy: Recent developments and future challenges. Epilepsia 2007, 48(4): 617-630.

Horsley V. An address on the origin and seat of epileptic disturbance. BMJ 1892; 1: 693-696.

Hoshi Y, Tamura M. Detectionof dynamic changes in cerebral oxygenation coupled to neuronal function during mental work in man. Neurosc Letters 1993; 150: 5-8.

Hubel DH, Wiesel TN. Receptive fields, binocular interaction and functional architecture in the cat´s visual cortex. J Physiol 1962; 160: 106-154.

Huettel SA, McCarthy G. Evidence for a refractory period in the hemodynamic response to visual stimuli as measured by MRI. Neuroimage 2000; 11: 547-553.

Huettel SA, McKeown J, Song A et al. Linking hemodynamic and electrophysiological measures of brain activity: evidence from functional MRI and intracranial field potentials. Cereb Cortex 2004; (4)2: 165-173.

Iriarte J, Urrestarazu E, Valencia M, Alegre M, Malanda A, Viteri C, Artieda J. Independent component analysis as a tool to eliminate artifacts in EEG: a quantitative study. J Clin Neurophysiol 2003; 20(4): 249-257.

Ives JR, Warach S, Schmitt F, Edelman RR, Schomer DL. Monitoring the patient's EEG during echo planar MRI. Electroencephalogr Clin Neurophysiol 1993; 87: 417-420.

Jansen F, Huffelen A, Algra A, Nieuwenhuizen O. Epilepsy surgery in tuberous sclerosis: A systematic review. Epilepsia 2007, Vol 48(8): 1477-1484.

Jansen F, Huiskamp G, Huffelen A, Bourez-Swart M, Boere E, Gebbink, Vincken K, Nieuwenhuizen O. Identification of the epileptogenic tuber in patients with tuberous sclerosis: A comparison of high-resolution EEG and MEG. Epilepsia 2006, 47(1): 108-114.

Jasdzewski G, Strangman G, Wagner J, Kwong K, Poldrack RA, Boas DA. Differences in the hemodynamic response to event-related motor and visual paradigms as measured by near-infrared spectroscopy. Neuroimage 2003; 20: 479-488.

Jaspers HH. Report of the committeee on methods of clinical examination in electroencephalography. Electroencephal Clin Neurophysiol 1958; 10: 370-371.

Jenkinson M, Bannister PR, Brady JM, Smith SM. Improved optimization for the robust and accurate linear registration and motion correction of brain images. Neurimage 2002; 17(2):825-841.

Jobsis FF. Noninvasive, infrared monitoring of cerebral and myocardial oxygen sufficiency and circulatory parameters. Science 1977; 198: 1264-1267.

Kamimura T, Tohyama J, Oishi M, Akasaka N, Kanazawa O, Sasagawa M, Kato M, Ohno K, Masuda H, Kameyama S, Uchiyama M. Magnetoencephalography in patients with tuberous sclerosis and localization-related epilepsy. Epilepsia 2006, 47(6): 991-997.

Kanazawa O, Tohyama J, Akasaka N, Kamimura T. A Magnetoencephalographic study of patients with Panayiotopoulos syndrome. Epilepsia 2006; 46(7): 1106-1113.

Kocsis B, Vertes R. Characterization of neurons of the Supramammillary Nucleus and Mammillary Body that discharge rhythmically with the Hippocampal Theta rhythm in the rat. J Neurosc 1994; 14(11): 7040-7052.

Koutroumanidis M. Panayiotopoulos syndrome: an important electro clinical example of benign childhood system epilepsy. Epilepsia 2007; 48(6): 1044-1053.

Krakow K, Woermann FG, Symms MR, Allen PJ, Lemieux L, Barker BJ, Duncan JS, Fish DR. EEG-triggered functional MRI of interictal epileptiform activity in patients with partial seizures. Brain 1999; 122: 1679-1688.

Krakow K, Allen PJ, Symms MR, Lemieux L, Josephs O, Fish DR. EEG recording during fMRI experiments: image quality. Hum Brain Map 2000; 10: 10-15.

Kuhl DE, Edwards RQ, Ricci AR, Reivich M. Quantitative section scanning using orthogonal tangent correction. J Nucl Med 1973; 14: 196-200.

Kuzniecky R, Guthrie B, Mountz J, Bebin M, Faught E, Gilliam F, Liu H (1997) Intrinsic epileptogenesis of hypothalamic hamartomas in gelastic epilepsy. Ann Neurol; 42: 60-67.

Leal A, Moreira A, Robalo C, Ribeiro C. Different electroclinical manifestations of the epilepsy associated with Hamartomas connecting to the middle or posterior Hypothalamus. Epilepsia 2003; 44(9): 1191-1195.

Kwong KK, Belliveau JW, Chesler DA, Goldberg IE, Weisskof RM, Poncelet BP, Kennedy DN, Hoppel BE, Cohen MS, Turner R, Cheng HM, Brady TJ, Rosen BR. Dynamic magnetic resonance imaging of human brain activity during primary sensory stimulation. Proc Natl Acad Sci USA 1992; 89: 5675-5679.

Lada C, Skiadas K, Theodorou V, Loli N, Covanis A. A study of 43 patients with Panayiotopoulos syndrome, a common and benign childhood seizure susceptibility. Epilepsia 2003; 44(1): 81-88.

Lagerlund TD, Sharbrough FW, Busacker NE. Spatial filtering of multichannel electroencephalographic recordings through principal component analysis by singular value decomposition. J Clin Neurophysiol 1997; 14(1): 73-82.

Lantz G, Michel CM, Seeck M, Blanke O, Spinelli L, Thut G, Landis T, Rosén I. Space-oriented segmentation and 3-dimensional source reconstruction of ictal EEG patterns. Clin Neurophysiol 2001; 112: 688-697.

Law SK, Nunez PL, Wijesinghe RS. High-resolution EEG using spline generated surface laplacians on spherical and ellipsoidal surfaces. IEEE Trans Biomed Eng 1993; 40(2): 145-153.

Lazeyras F, Blanke O, Perrig S et al. EEG-triggered functional MRI in patients with pharmacoresistant epilepsy. J Mag Res Imaging 2000; 12: 177-185.

Lazeyras F, Zimine I, Blanke O, Perrig S, Seeck M. Functional MRI with simultaneous EEG recording: feasibility and application to motor and visual activation. J Mag Res Imag 2001; 13: 943-948.

Leahy RM, Mosher JC, Spencer ME, Huang MX, Lewine JD. A study of dipole localization accuracy for MEG and EEG using a human skull phantom. Electroencephal Clin Neurophysiol 1998; 107(2): 159-173.

Leal AJR, Passão V, Calado E, Vieira JP, Cunha JP. Interictal spike EEG source analysis in hypothalamic hamartoma epilepsy. Clin Neurophysiol 2002; 113: 1961-9.

Leal AJR, Moreira A, Robalo C, Ribeiro C. Different electroclinical manifestations of the epilepsy associated with hamartomas connecting to the middle or posterior hypothalamus. Epilepsia 2003; 44(9): 1191-1195.

Leal AJR, Dias AI, Vieira JP, Secca MF, Jordão C. The BOLD effect of interictal spike activity in childhood occipital lobe epilepsy. Epilepsia 2006a; 47(9): 1536-1542.

Leal AJR, Dias AI, Vieira JP. Analysis of the EEG dynamics of epileptic activity in gelastic seizures using decomposition in independent components. Clin Neurophysiol 2006b; 117: 1595-1601.

Leal AJR, Nunes S, Dias AI, Vieira JP, Moreira A, Calado E. Analysis of the generators of epileptic activity in early-onset childhood benign occipital lobe epilepsy. Clin Neurophysiol 2007a; 118: 1341-1347.

Leal AJR, Nunes S, Martins A, Secca MF, Jordão C. Brain mapping of epileptic activity in a case of idiopathic occipital lobe epilepsy (Panayiotopoulos syndrome). Epilepsia 2007b; 48(6): 1179-1183.

Leal AJR, Dias AI, Vieira JP, Moreira A, Távora L, Calado E. Analysis of the dynamics and origin of epileptic activity in patients with Tuberous Sclerosis evaluated for surgery of epilepsy. Clin Neurophysiol 2008a; 119: 853-861.

Lemieux L, Allen PJ, Krakow K, Fish DR. Methodological issues in EEG-correlated functional MRI experiments. IJBEM 1999; 1(1): 87-95.

Lemieux L, Haddadi AS, Josephs O, Allen P, Toms N, Scott C, Krakow K, Turner R, Fish DR. Event-related fMRI with simultaneous and continuous EEG: description of the method and initial case report. Neuroimage 2001; 14: 780-787.

Lemieux L, Krakow K, Fish D. Comparison of spike-triggered functional MRI BOLD activation and EEG dipole model localization. Neuroimage 2001; 14: 1097-1104.

Iida K, Otsubo H, Mohamed I, Okuda C, Ochi A, Weiss S, Chuang S, Snead III O. Characterizing magnetoencephalographic spike sources in children with tuberous sclerosis complex. Epilepsia 2005, Vol 46(9): 1510-1517.

List CF, Dowman CE, Bagahi BK, Bebin J. Posterior hypothalamic hamartomas and gangliomas causing precocious puberty. Neurology 1958; 8: 164-174.

Liston AD, De Munck JC, Hamandi K, Laufs H, Ossenblok P, Duncan JS, Lemieux L. Analysis of EEG-fMRI data in focal epilepsy based on automated spike classification and signal space projection. Neuroimage 2006; 31: 1015-1024.

Liu Z, He B. fMRI-EEG integrated cortical source imaging by use of time-variant spatial constraints. Neuroimage 2008; 39: 1198-1214.

Logothetis NK, Pauls J, Augath M, TrinathT, Oeltermann A. Neurophysiological investigationof the basis of the fMRI signal. Nature 2001; 412: 150-157.

Logothetis NK. The neural basis of the blood-oxygen-level-dependent functional magnetic resonance imaging signal. In Parker, Derrington and Balkmore (Eds) The physiology of cognitive processes. (2003); 62-116.

Logothetis NK. The underpinnings of the BOLD functional magnetic resonance imaging signal. J Neurosci 2003; 23(10): 3963-3971.

Logothetis NK, Wandell BA. Interpreting the BOLD signal. Annu Rev Physiol 2004; 66: 735-769.

Lopes da Silva F, Storm van Leeuwen W. The cortical alpha rhythm in dog: the depth and surface profile of phase. In Brazier & Petsche (Eds.) Architectonics of the cerebral cortex. 1978, Raven Press: 319-333.

Lopes da Silva F. Dynamics of EEGs as signals of neuronal populations: models and theoretical considerations. In Electroencephalography. Niedermeyer & Lopes da Silva (Eds), 2005a: 85-105, Lippincott Williams & Wilkins.

Lopes da Silva F. Event-related potentials: methodology and quantification. In Electroencephalography, Niedermeyer & Lopes da Silva (Eds), 2005b: 991-1001, Lippincott Williams & Wilkins.

Lopes da Silva F. Computer-assisted EEG diagnosis: pattern recognition and brain mapping. In Niedermeyer and Lopes da Silva (Eds.), Electroencephalography, 5th ed, 2005, Lippincott Williams & Wilkins: 1233-1263.

Lorent de No R. Action potential of the motoneurons of the hypoglossus nucleus. J Cell Comp Physiol 1947; 29: 207-287.

Makeig S. Auditory event-related dynamics of the EEG spectrum and effects of exposure to tones. Electroencephal Clin Neurophysiol 1993; 86: 283-293.

Makeig S, Bell A, Jung TP, Sejnowski TJ. Independent component analusis of electroencephalographic data. Adv Neur Inf Proc Syst 1996; 8: 145-151.

Makeig S, Jung TP, Bell AJ, Ghahremani D, Sejnowski TJ. Blind separation of auditory event-related brain responses into independent components. Proc Natl Acad Sci USA 1997; 94: 10979-10984.

Makeig S, Westerfield M, Jung TP, Enghoff S, Townsend J, Courchesne E, Sejnowski TJ. Dynamic brain sources of visual evoked responses. Science 2002; 295: 690-694.

Makeig S, Jung TP, Sejnowsky T. Having your voxels and timing them to? In: Sommer & Wichert Eds, Exploratory analysis and data modeling in functional neurimaging. MIT Press, 2003, p. 195-207.

Makeig S, Debener S, Onton J, Delorme A. Mining event-related brain dynamics. Trends Cogn Sci 2004; 8(5): 204-210.

Mantini D, Perrucci MG, Cugini S, Ferretti A, Romani GL, Del Gratta C. Complete artifact removal for EEG recorded during continuous fMRI using independent compoonent analysis. Neuroimage 2007; 34: 598-607.

Marco-Pallarés J, Grau C, Ruffini G. Combined ICA-LORETA analysis of mismatch negativity. Neuroimage 2005; 25: 471-477.

Mazziotta JC, Phelps ME, Carson RE, Kuhl DE. Tomographic mapping of human cerebral metabolism: auditory stimulation. Neurology 1982; 32: 921-937.

McCormick DA. Membrane properties and neurotransmitter actions. In Shepherd (Ed) The synaptic organization of the brain. 5th ed, Oxford University Press, 2004.

McKeown MJ, Makeig S, Brown GG, Jung TP, Kindermann SS, Bell AJ, Sejnowski TJ. Analysis of fMRI data by blind separation into independent components. Hum Brain Map 1998; 6: 160-188.

Menon RS, Ogawa S, Hu X, Strupp JP, Anderson P, Ugurbil K. BOLD-based functional MRI at 4 tesla includes a capillary bed contribution: echo-planar imaging correlates with previous optical imaging using intrinsic signals. Mag Reson Med 1995; 33: 453-459.

Mountcastle V. Modality and topographic properties of single neurons of cat somatosensory cortex. J Neurophysiol 1957; 20: 408-434.

Mullati N, Selway R, Nashef L, Elwes R, Honovar M, Chandler C, Morris R, Jarosz J, Buchanan S, Polkey S. The clinical spectrum of epilepsy in children and adults with Hypothalamic Hamartomas. Epilepsia 2003; 44(10): 1310-1319.

Munari C, Kahane P, Francione S, Hoffmann D, Tassi L, Cusmai R, Vigevano F, Pasquier B, Betti O. Role of the hypothalamic hamartoma in the genesis of gelastic fits (a video-stereo-EEG study). Electroenceph Clin Neurophysiol 1995; 95: 154-160.

Munari C, Quarato P, Kahane P et al. Gelastic and Dacrystic seizures. In Lüders and Noachtar eds. Epileptic seizures: pathophysiology and clinical semiology. Churchill Livingstone 2000.

Negishi M, Abildgaard M, Nixon T, Constable RT. Removal of time-varying gradient artifacts during continuous fMRI. Clin Neurophysiol 2004; 115: 2181-2192.

Niedermeyer E. Epileptic seizure disorders. In Electroencephalography. Niedermeyer & Lopes da Silva (Eds), 2005: 505-619, Lippincott Williams & Wilkins.

Nguyen D, Singh S, Zaatreh M, Novotny E, Levy S, Testa F, Spencer S. Hypothalamic Hamartomas : seven cases and review of the literature. Epilepsy & Behavior 2003; 4: 246-258.

Niazy RK, Beckmann CF, Iannetti GD, Brady JM, Smith SM. Removal of fMRI environment artifacts from EEG data using optimal basis sets. Neuroimage 2005; 28: 720-737.

Nishio S, Fukui M, Goto Y. Surgical treatment of intractable seizures due to hypothalamic hamartoma. Epilepsia 1994; 35(3): 514-519.

Nunez P, Pilgreen KL. The spline-laplacian in clinical neurophysiology: a method to improve EEG spatial resolution. J Clin Neurophysiol 1991; 8(4): 391-413.

Nunez PL, Silberstein RB, Cadiush PJ, Wijesinghe J, Westdorp AF, Srinivasan R. A theoretical and experimental study of high resolution EEG based on surface Laplacians and cortical imaging. Electroenceph Clin Neurophysiol 1994; 90: 40-57.

Nunez PL, Silberstien RB. On the relationship of synaptic activity to macroscopic measurements: Does co-registration of EEG with fMRI make sense? Brain Topogr 2000; 13: 79-96.

Nunez PL, Srinivasan R. Electric Fields of the Brain. 2nd Ed, Oxford University Press 2005.

Nybakken GE, Quigley MA, Cordes D, Haughton VM, Meyereand ME. Test-retest precision of functional magnetic resonance imaging processed with independent component analysis. Neuroradiol 2002; 44: 403-406.

Ogawa S, Lee TM, Kay AR, Tank DW. Brain magnetic resonance imaging with contrast dependent on blood oxygenation. Proc Natl Acad Sci USA 1990; 87: 9868-9872.

Ogawa S, Tank DW, Menon R, Ellermann JM, Kim SG, Merkle H, Ugurbil K. Intrinsic signal changes accompanying sensory stimulation: functional brain mapping with magnetic resonance imaging. Proc Natl Acad Sci USA 1992; 89: 5951-5955.

Ohtsu M, Oguni H, Hayashi K, Funatsuka M, Imai K, Osawa M. EEG in children with early-onset benign occipital seizure susceptibility syndrome: Panayiotopoulos syndrome. Epilepsia 2003; 44(3): 435-442.

Palmini A, Chandler C, Andermann F, Costa da Costa J, Paglioli-Neto E, Polkey C, Rosenblatt B, Montes J, Martinez JV, Farmer JP, Sinclair B, Aronyk K, Paglioli E, Coutinho L, Raupp S, Portuguez M. Resection of the lesion in patients with hypothalamic hamartomas and catastrophic epilepsy. Neurology 2002; 58(9): 1338-1347.

Palmini A, Paesschen W, Dupont P, Laere K, Driel G. Status gelasticus after temporal lobectomy: ictal FDG-PET findings and the question of dual pathology involving hypothalamic hamartomas. Epilepsia 2005; 46(8): 1313-1316.

Panayiotopoulos CP. Benign childhood epilepsy with occipital paroxysms: a 15-year prospective study. Ann Neurol 1989; 26: 51-56.

Panayiotopoulos CP. Panayiotopoulos syndrome: A common and benign childhood epileptic syndrome. London: John Libbey, 2002.

Papez J. A proposed mechanism of Emotion. Arch Neurol Psychiatry 1937; 38(4): 725-743.

Pascual-Marqui RD, Esslen M, Kochi K, Lehmann D. Functional imaging with low resolution brain electromagnetic tomography (LORETA): a review. Meth Find Exp Clin Pharmac 2002, 24C:91-95.

Pascual-Marqui RD. Review of methods for solving the EEG inverse problem. Int J Bioelectromag 1999; 1: 75-86.

Pascual-Marqui RD. Standardized low-resolution brain electromagnetic tomography (sLORETA): technical details. Methods & Findings in Experimental & Clinical Pharmacology 2002, 24D: 5-12.

Pauling L, Coryell CD. The magnetic properties and structure of hemoglobin, oxygenated hemoglobin, and carbonmonoxygenated hemoglobin. PNAS 1936; 22(4): 210-236.

Perot P, Weir B. Tubeorus sclerosis: surgical therapy for seizures. Arch Neurol 1966; 15: 498-506.

Perrin F, Bertrand O, Pernier J. Scalp current density mapping: Value and estimation from potential data. IEEE Trans Biomed Eng 1987; 34(4): 283-288.

Perrin F, Pernier J, Bertrand O, Echalier JF. Spherical splines for scalp potential and current density mapping. Electroenceph Clin Neurophysiol 1989; 72: 184-187.

Petit L, Haxby JV. Functional anatomy of pursuit eye movements in humans as revealed by fMRI. J Neurophysiol 1999; 82: 463-471.

Pfurscheller G, Lopes da Silva F. EEG event-related desynchronization (ERD) and event-related synchronization (ERS). In Niedermeyer & Lopes da Silva Eds, Electroencephalography. 5th ed, Lippincot Williams & Wilkins, 2005.

Phelps ME, Hoffmen EJ, Mullani NA, Ter-Pogossian M. Application of annihilation coincidence detection to transaxial reconstruction tomography. J Nucl Med 1975; 16: 210-224.

Phelps ME, Khul DE, Mazziotta JC. Metabolic mapping of the brain's response to visual stimulation: studies in humans. Science 1981; 211: 1445-1448.

Plummer C, Harvey A, Cook M. EEG source localization in focal epilepsy: where are we now? Epilepsia 2008; 49(2): 201-218.

Quigley MA, Haughton VM, Carew J, Cordes D, Moritz CH, Meyerand ME. Comparison of independent component analysis and conventional hypothesis-driven analysis for clinical functional MR image processing. AJNR 2002; 23: 49-58.

Raftopoulos C, Rijckevorsel K, Serieh B, Tourtchaninoff M, Ivanoiu A, Mary G, Grandin C, Duprez T. Epileptic discharges in a Mammillary Body of a patient with refractory epilepsy. Neuromodulation 2005; 8(4): 236-240.

Rall W. Electrophysiology of a dendritic neuron model. Biophys J 1962 ; 2 : 145-167.

Richer F, Martinez M, Cohen H et al. Visual motion perception from stimulation of the human medial parieto-occipital cortex. Exp Brain Res 1991; 87: 649.

Rijckevorsel K, Serieh B, Tourtchaninoff M, Raftopoulos C. Deep EEG recordings of the Mammillary Body in epilepsy patients. Epilepsia 2005; 46(5): 781-785.

Ritter P, Villringer A. Simultaneous EEG-fMRI. Neurosc Biobehav Rev 2006; 30: 823-838.

Rosenfeld J, Feiz-Erfan I. Hypothalamic Hamartoma treatment: surgical resection with the transcallosal approach. Sem Ped Neurol 2007; 14: 88-98.

Roy CS, Sherrington CS. On the regulation of the blood-supply of the brain. J Physiol 1890; 11: 85-158.

Ryvlin P, Ravier C, Bouvard S, Mauguiere F, Bars D, Arzimanoglou A, Petit J, Kahane P. Positron emission tomography in epileptogenic hypothalamic hamartomas. Epileptic Disord 2003; 5: 219-227.

Salanova V, Andermann F, Olivier A et al. Occipital lobe epilepsy: Electroclinical manifestations, electrocorticography, cortical stimulation and outcome in 42 patients treated between 1930 and 1991. Brain 1992; 115: 1655.

Saitoh M, Kubota M, Kimura I, Mizuguchi M, Igarashi T. A case of Panayiotopoulos syndrome showing an atypical course. Seizure 2006; 15: 643-648.

Sayers P, Beagley HA, Hanshall WR. The mechanisms of auditory evoked EEG responses. Nature 1974; 247: 481-483.

Schneider MR. A multistage process for computing virtual dipolar sources of EEG discharges from surface information. IEEE Trans Biomed Eng 1972; 19(1): 1-12.

Scott A. Stairways to the mind. Springer-Verlag, 1995.

Scoville WB, Milner B. Loss of recent memory after bilateral hippocampal lesions. J Neurol Neurosurg Psychiat 1957; 20: 11-21.

Seri S, Cerquiglini A, Pisani F, Michel C, Pascual-Marqui R, Curatolo P. Frontal lobe epilepsy associated with tuberous sclerosis: Electroencephalographic-Magnetic Resonance imaging fusioning. J Child Neurol 1998; 13(1): 33-38.

Shepherd G. Introduction to synaptic circuits. In Shepherd (Ed) The synaptic organization of the brain. 1-38, Oxford University Press, 2004.

Sherg M Von Cramon D. Two bilateral sources of the late AEP as identified by a spatio-temporal dipole model. Electroencephal Clin Neurophysiol 1985 ; 62 : 32-44.

Sherwin RP, Grassi JE, Sommers SC. Hamartomatous malformations of the posterolateral hypothalamus. Lab Investigation 1962; 11: 89-97.

Shibasaki H. Human brain mapping: hemodynamic response and electrophysiology. Clin Neurophysiol 2008; 119(4): 731-743.

Sidman RD. A method for simulating intracerebral potential fields: the cortical imaging method. J Clin Neurophysiol 1991; 8: 432-441.

Singer W. Synchronization of cortical activity and its putative role in information processing and learning. Ann Rev Physiol 1993 ; 55 : 349-374.

Sloper J, Hiorns R, Powell T. A qualitative and quantitative electron microscope study of the neurons in the primate motor and somatic sensory cortices. Phil Trans R Soc Lond 1979; B285: 141-171.

Smith S, Jenkinson M, Woolrich M et al. Advances in functional and structural MR image analysis and implementation as FSL. Neuroimage 2004; 23(S1): 208-219.

Smith SM, Beckmann CF, Ramnani N, Woolrich MW, Bannister PR, Jenkinson M, Matthews PM, McGonigle DJ. Variability in FMRI: A re-examination of intersession differences. Human Brain Mapping 2005; 24:248-257.

Sommer M, Meinhardt J, Volz HP. Combined measurement of event-related potentials (ERPs) and fMRI. Acta Neurobiol Exp 2003; 63: 49-53.

Speckmann EJ, Elger CE. Introduction to the neurophysiological basis of the EEG and DC potentials. In Niedermeyer and Lopes da Silva (eds) Electroencephalography, 5th ed 2005; 17-29, Lippincot Williams & Wilkins.

Sperli F, Spinelli L, Seeck M, Kurian M, Michel C, Lantz G. EEG source imaging in pediatric epilepsy surgery: A new perspective in presurgical workup. Epilepsia 2006, 47(6): 981-990.

Srinivasan R. Methods to improve the spatial resolution of EEG. Int J Bioelectromag 1999; 1(1): 102-111.

Steriade M. Cellular substrates of brain rhythms. In Niedermeyer & Lopes da Silva, eds Electroencephalography, 5th ed, pages 33-83, Lippincott Williams & Wilkins 2005.

Stock CJ. The influence of model parameters on EEG/MEG single dipole source estimation. IEEE Trans Biomed Eng 1987; 34(4): 289-296.

Striano S, Meo R, Bilo L, Cirillo S, Nocerino C, Ruosi P, Striano P, Estreano A. Gelastic epilepsy: symptomatic and cryptogenic cases. Epilepsia 1999; 40(3): 294-302.

Striano S, Striano P, Cirillo S, Nocerino C, Bilo L, Meo R, Ruosi P, Boccela P, Briganti F. Small hypothalamic hamartomas and gelastic seizures. Epileptic Disor 2002; 4: 129-133.

Taylor I, Scheffer I, Berkovic S. Occipital epilepsies: identification of specific and newly recognized syndromes. Brain 2003; 126: 753-769.

Thulborn KR, Waterton JC, Matthews PM, Radda GK. Oxygenation dependence of the transverse relaxation time of water protons in whole blood at high fields. Biochim Biophys Acta 1982; 714(2): 265-270.

Urrestarazu E, Iriarte J, Alegre M, Valencia M, Viteri C, Artieda J. Independent component analysis artifacts in ictal recordings. Epilepsia 2004; 45(9): 1071-1078.

Van der Meij W, Van der Dussen, Huffelen V et al. Dipole source analysis may differenciate benign focal epilepsy of childhood with occipital paroxysms from symptomatic occipital lobe epilepsy. Brain Topogr 1997; 10: 115-120.

Vigário R, Särelä J, Jousmäki V, Hämäläinen M, Oja E. Independent component approach to the analysis of EEG and MEG recordings. IEEE Trans Biomed Eng 2000; 47(5): 589-593.

Vijn PCM, Van Dijk BW, Spekreije H. Visual stimulation reduces EEG activity in man. Brain Res 1991; 550: 49-53.

Villringer A, Planck J, Hock C, Schleinkofer L, Dirnagl U. Near infrared spectroscopy (nirs): a new tool to study hemodynamic changes during activation of brain function in human adults. Neurosc Letters 1993; 154: 101-104.

Villringer A, Obrig H. Near-infrared spectroscopy and imaging. In Brain Mapping: the methods. Toga & Mazziotta (Eds.), 2nd ed, 2002, Academic Press.

Wagner M, Fuchs, M. Integration of functional MRI, structural MRI, EEG and MEG. IJBEM 2001; 3(1):

Wagner M, Fuchs M, Kastner J. Evaluation of sLORETA in the presence of noise and multiple sources. Brain Topogr 2004; 16(4): 277-280.

Wolff M, Weiskopf N, Serra E, Preissl H, Birbaumer N, Kraegeloh-Mann. Benign partial epilepsy in childhood: selective cognitive deficits are related to the location of focal spikes determined by combined EEG/MEG. Epilepsia 2005: 46(10): 1661-1667.

Wood CC, McCarthy G. Principal component analysis of event-related potentials: simulation studies demonstrate misallocation of variance across components. Electroencephal Clin Neurophysiol 1984; 59: 249-260.

Worsley KJ, Evans AC, Marrett S, Neelin P. A three-dimensional statistical analysis for CBF activation studies in human brain. J Cerebr Blood Flow and Metabolism 1992; 12: 900-918.

Yao D. The theoretical relation of scalp Laplacian and scalp current density of a spherical shell head model. Phys Med Biol 2002; 47: 2179-2185.

Yoshinaga H, Koutroumanidis M, Shirasawa A, Kikumoto K, Ohtsuja Y, Oka E. Dipole analysis in panayiotopoulos syndrome. Brain Dev 2005; 27: 46-52.

Yoshinaga H, Koutroumanidis M, Kobayashi K, Shirasawa A, Kikumoto K, Inoue T, Oka M, Ohtsuka Y. EEG dipole characteristics in Panayotopoulos syndrome. Epilepsia 2006; 47(4): 781-787.